

**Coat to Constrict: Silicon carbide coatings on alumina membranes by low-pressure chemical vapor deposition to enhance durability and performance**

Jan, A.

**DOI**

[10.4233/uuid:ef71a53a-9af9-4809-a921-1bcc623ace5f](https://doi.org/10.4233/uuid:ef71a53a-9af9-4809-a921-1bcc623ace5f)

**Publication date**

2025

**Document Version**

Final published version

**Citation (APA)**

Jan, A. (2025). *Coat to Constrict: Silicon carbide coatings on alumina membranes by low-pressure chemical vapor deposition to enhance durability and performance*. [Dissertation (TU Delft), Delft University of Technology]. <https://doi.org/10.4233/uuid:ef71a53a-9af9-4809-a921-1bcc623ace5f>

**Important note**

To cite this publication, please use the final published version (if applicable).  
Please check the document version above.

**Copyright**

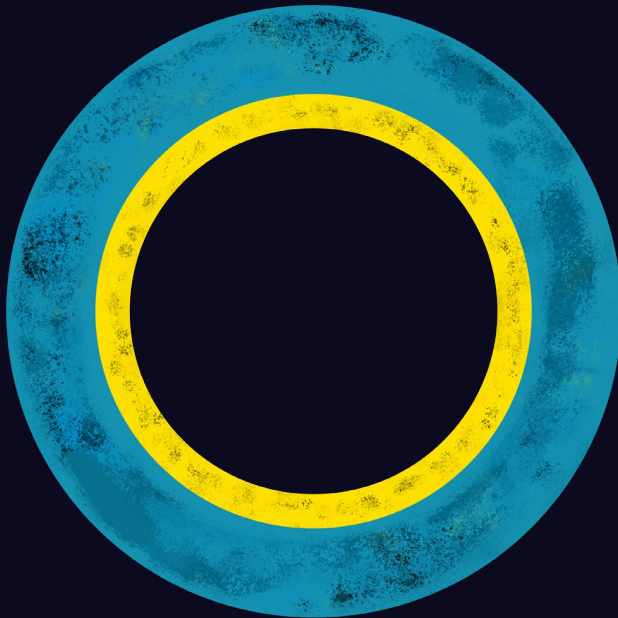
Other than for strictly personal use, it is not permitted to download, forward or distribute the text or part of it, without the consent of the author(s) and/or copyright holder(s), unless the work is under an open content license such as Creative Commons.

**Takedown policy**

Please contact us and provide details if you believe this document breaches copyrights.  
We will remove access to the work immediately and investigate your claim.

# Coat to Constrict

Silicon carbide coatings on alumina membranes by low-pressure chemical vapor deposition to enhance durability and performance



Asif Jan



## Propositions accompanying the dissertation

Coat to Constrict: Silicon carbide coatings on alumina membranes by low-pressure chemical vapor deposition to enhance durability and performance

Asif Jan

1. Low-pressure chemical vapor deposition (LP-CVD) provides a controllable method to deposit thin functional coatings on selective layers of ceramic supports, offering a compelling alternative to high-temperature multi-step sol-gel fabrication of full selective layers (this thesis).
2. LP-CVD at temperatures of 860°C yields robust silicon carbide (SiC) coatings on alumina (Al<sub>2</sub>O<sub>3</sub>) supports that retain their pore structure and permeance after 200 hour of sodium hypochlorite exposure (this thesis).
3. The chemical robustness of SiC coated membranes facilitate their applications in oxidative and corrosive water treatment scenarios where polymeric membranes fail (this thesis).
4. Combining LP-CVD and atomic layer deposition can potentially offer next-generation ceramic membranes with physical chemical stability and sub-nanometer precision in pore structure with uniform pore size distribution (this thesis).
5. Ceramic membranes that combine size exclusion and electrostatic mechanisms are essential to treat complex wastewater streams.
6. Achieving circularity is central to sustainable wastewater treatment technologies.
7. Industrial wastewater streams represent an under-utilized resource for water reclamation and resource recovery.
8. The intersection of materials science and environmental engineering drives the development of robust separation technologies.
9. Like a membrane that undergoes periodic backwash to shed fouling layers and restore flux, life demands retrospection to clear obstructions of past and regain clarity.
10. Being a Pakistani in the West often feels like a sealed novel with a striking cover - judged by its appearance before anyone reads the first page.

*These propositions are regarded as opposable and defensible, and have been approved as such by the promotors Prof.dr.ir. L.C. Rietveld and Dr.ir. S.G.J. Heijman.*

**Coat to Constrict:**  
**Silicon carbide coatings on alumina membranes by**  
**low-pressure chemical vapor deposition to enhance**  
**durability and performance**

**Dissertation**

for the purpose of obtaining the degree of doctor  
at Delft University of Technology  
by the authority of the Rector Magnificus Prof.dr.ir. T.H.J.J. van der Hagen  
Chair of the Board of Doctorates  
to be defended publicly on  
Thursday 9 October 2025 at 12:30 o'clock

By

Asif JAN

Master of Engineering in Nanomaterials Science and Engineering, University of Science and  
Technology, South Korea  
Born in Gilgit, Pakistan

This dissertation has been approved by the promotors.

Composition of the doctoral committee:

Rector Magnificus,	chairperson
Prof.dr.ir. L.C. Rietveld	Delft University of Technology, promotor
Dr.ir. S.G.J. Heijman	Delft University of Technology, promotor

Independent members:

Dr. H. Bazyar	Delft University of Technology
Prof.dr.ir. J.A.M.H. Hofman	University of BATH, UK
Prof.dr. M.D. Kennedy	Delft University of Technology
Prof.dr.ir. A. Nijmeijer	University of Twente / Shell, NL

Reserve member:

Prof.dr.ir. J.B. van Lier	Delft University of Technology
---------------------------	--------------------------------

Other member:

Dr.ing. M.W.J. Luiten-Olieman	University of Twente
-------------------------------	----------------------

The research presented in this thesis is performed at the Sanitary Engineering Section, Department of Water Management, Faculty of Civil Engineering, Delft University of Technology, The Netherlands.

## Table of contents

<b>Chapter 1 Introduction.....</b>	<b>10</b>
1.1 Research problem from a global perspective.....	11
1.2 Ceramic membranes.....	11
1.3 A negatively charged ceramic membrane: Silicon Carbide .....	12
1.4 Limitations in preparing SiC ceramic membranes.....	13
1.5 Research questions: Rethinking the preparation of SiC membranes .....	14
1.6 How to read this thesis.....	14
References.....	17
<b>Chapter 2 Literature review of chemical vapor deposition for ceramic membranes.....</b>	<b>22</b>
2.1 Introduction.....	23
2.2 Key steps in a CVD process: Target material selection and reaction dynamics .....	24
2.3 Critical parameters influencing the CVD process for membrane coating .....	27
2.4 Polymeric membrane modification by CVD .....	30
2.5 Ceramic membrane modification by CVD .....	33
2.6 Conclusions and future outlook .....	35
References.....	36
<b>Chapter 3 Effect of long-term sodium hypochlorite cleaning on silicon carbide ultrafiltration membranes prepared by low-pressure chemical vapor deposition .....</b>	<b>42</b>
3.1 Introduction.....	43
3.2 Materials and Methods.....	45
3.3 Results and Discussion .....	49
3.4 Conclusion .....	59
3.5 Supplementary information .....	60
References.....	61
<b>Chapter 4 Single-step modification of tubular alumina membrane to silicon carbide tight-ultrafiltration membrane by low-pressure chemical vapor deposition for sulphate ion retention.....</b>	<b>66</b>
4.1 Introduction.....	68
4.2 Materials and Methods.....	70

4.3 Results and Discussion .....	73
4.4 Conclusions.....	84
4.5 Supplementary information .....	86
References.....	88
<b>Chapter 5 A review on atomically modified materials by atomic layer deposition for wastewater treatment .....</b>	<b>94</b>
5.1 Introduction.....	95
5.2 Historical perspective and fundamentals of ALD.....	98
5.3 Atomically Engineered Materials by ALD for Wastewater Treatment .....	103
5.4 Challenges and Opportunities .....	124
5.5 Conclusions.....	126
References.....	128
<b>Chapter 6 Conclusions and future research directions .....</b>	<b>138</b>
6.1 Conclusions.....	138
6.2 Future research directions .....	141
References.....	144

## Summary

Stringent industrial wastewater discharge regulations and rising energy costs demand industries to shift to sustainable water treatment technologies. The conventional physical-chemical wastewater treatment processes struggle to separate inorganic ions and emulsions. While polymeric membranes have limited mechanical, thermal and chemical stability. Ceramic membranes, and in particular silicon carbide (SiC) membranes, have emerged as promising alternatives due to their mechanical strength, thermal resilience, resistance to fouling, low isoelectric point, and super hydrophilicity. However, fabricating both SiC membrane supports and the selective layers require sintering temperatures of ca. 2100°C, with consequent high energy consumption. Additionally, preparing a SiC selective layer requires multiple coating and sintering cycles, which hinder precise pore size control and economic feasibility.

To address these limitations, this thesis explores low-pressure chemical vapor deposition (LP-CVD) as a route to coat commercially available alumina ( $\text{Al}_2\text{O}_3$ ) supports by SiC at moderate temperatures to replace full SiC membranes.

Through a comprehensive review of CVD for membrane surface engineering the importance of operational conditions to produce highly conformal and adhesive coatings has been emphasized. Knowledge gaps in exploring the full potential of CVD to tailor pore size and surface functionality of membranes have been identified, such as, unavailability of deposition reactors compatible with tubular and flat-sheet membranes, lack of in-situ diagnostic tools to monitor pore size evolution, and limited exploration of coating conditions and materials.

Then the fabrication of SiC coated  $\text{Al}_2\text{O}_3$  ultrafiltration (UF) membranes in two different LP-CVD operational conditions, 750°C and 600 mTorr for 60 min (SiC-7), 860°C and 100 mTorr for 30 min (SiC-8), respectively, have been presented to assess the influence of temperature and pressure on coating quality and stability. By adjusting the deposition time, comparable SiC coating thicknesses (ca. 9  $\mu\text{m}$ ) were achieved, enabling a systematic evaluation of membrane characteristics. Following a 200 hour exposure to sodium hypochlorite, SiC-8 retained its initial permeance and pore structure, whereas SiC-7 coatings deteriorated and lost permeance entirely. These results demonstrate that higher deposition temperatures produce highly adhesive and robust SiC coatings that can undergo multiple harsh oxidative cleaning cycles.

In the following the optimized deposition conditions to a nominally 20 nm (actual ca. 13 nm)  $\text{Al}_2\text{O}_3$  UF support have been applied to test the limits of LP-CVD. A 38 minute deposition narrowed the mean pore diameter to ca. 7 nm. However, longer deposition times resulted in pore clogging. This highlights the limitation of LP-CVD in fabricating nanofiltration (NF) membranes. Filtration experiments with sodium sulphate ( $\text{Na}_2\text{SO}_4$ ) feeds revealed that at low

ionic strength of 2mM, the strongly negative SiC coated Al<sub>2</sub>O<sub>3</sub> membrane (zeta potential ca. -67 mV at pH 7) achieved ca. 79% sulphate ion (SO<sub>4</sub><sup>2-</sup>) rejection via Donnan exclusion and electrical double layer overlap within the membrane pores. At higher ionic strength of 20mM, contraction of the electrical double layer within in the membrane pores led to a significant decrease of SO<sub>4</sub><sup>2-</sup> rejection underscoring the interplay between pore size, surface charge, and feed chemistry in anion separation.

As an alternative to transcend LP-CVD's pore narrowing limits to achieve NF membranes, therefore, atomic layer deposition (ALD) as a complementary technique has been introduced. ALD's sequential, self-saturating surface reactions deposit one monolayer per cycle with atomic-scale thickness control and exceptional conformality on any support (ceramics, polymers, or powders). The applications of ALD over the past decade have been reviewed, demonstrating how ultrathin coatings can refine the pore size without sacrificing permeance while also enabling surface functionalization and catalytic integration in adsorbents, ceramic and polymeric membranes.

The thesis thus demonstrates the feasibility of LP-CVD as a scalable and moderate temperature method for fabricating durable SiC coated Al<sub>2</sub>O<sub>3</sub> UF membranes. The as-prepared membranes show promising SO<sub>4</sub><sup>2-</sup> retention and exceptional stability in oxidative cleaning solutions. Moreover, by integrating ALD for preparing NF membranes, groundwork has been provided for next generation ceramic membranes that can meet stringent wastewater treatment needs.







# Chapter 1

Introduction



## Chapter 1 Introduction

### Abstract

Industrial expansion and population growth have led to complex wastewater streams that conventional treatment processes often fail to adequately treat. Ceramic membranes have emerged as a promising solution due to their superior mechanical strength, thermal stability, and chemical resistance. Among these, silicon carbide (SiC) membranes offer exceptional thermal stability, super-hydrophilicity, and low isoelectric point, leading to high permeability and reduced fouling. Despite these advantages, traditional routes for fabricating SiC membranes present challenges, including high sintering temperatures, multiple deposition steps, and environmental concerns related to toxic solvent use. This chapter introduces low-pressure chemical vapor deposition (LP-CVD) as a promising technique for coating ceramic membrane supports, e.g. alumina ( $\text{Al}_2\text{O}_3$ ), with SiC. The motivations for exploring LP-CVD along with broader objectives of achieving robust and high-performing membranes for wastewater treatment are outlined. Furthermore, the chapter briefly situates atomic layer deposition (ALD) as a complementary method for fine-tuning membrane properties to the nanofiltration (NF) range. Through a clear outline of the thesis organization, this introduction establishes the groundwork for subsequent chapters that explore material synthesis, membrane performance, and future advancements in SiC-based membrane technologies for wastewater treatment.

## 1.1 Research problem from a global perspective

The industrial revolution has been marked by rapid industrial and population growth. All the industrial processes use water as a raw material which is then ultimately discarded as wastewater. Furthermore, the population boom has resulted in increased water demand. According to the United Nations World Water Development report, the global freshwater usage has been increased by six-fold over the past century [1]. Therefore, sustainable treatment of wastewater is imperative.

The conventional physical-chemical wastewater treatment processes, such as coagulation, flocculation, and sand filtration, are often ineffective in removing dissolved heavy metals (e.g.,  $\text{Pb}^{2+}$ ,  $\text{Cd}^{2+}$ ,  $\text{As}^{3+}$ ), emerging micropollutants (e.g., pharmaceuticals, pesticides), viruses, and oil water emulsions [2-4]. The complex nature of wastewater, therefore, requires improved processes with high efficiency and low energy inputs.

## 1.2 Ceramic membranes

A ceramic membrane is a porous physical barrier between two phases, i.e. the feed stream and the permeate stream, respectively, through which one type of a substance can pass more readily than the others [5]. A driving force, such as pressure difference, induces a water flux from the feed stream to the permeate stream, separating the target substances (Fig. 1.1). The performance of a ceramic membrane is gauged by permeability and selectivity. Permeability determines the volume of permeate stream passing through the membrane as a function of applied pressure, and selectivity determines the rejection percentage of a target substance by membrane. An ideal ceramic membrane would have both a high permeability and selectivity. However, in practice ceramic membranes exhibit a trade-off between the two variables.

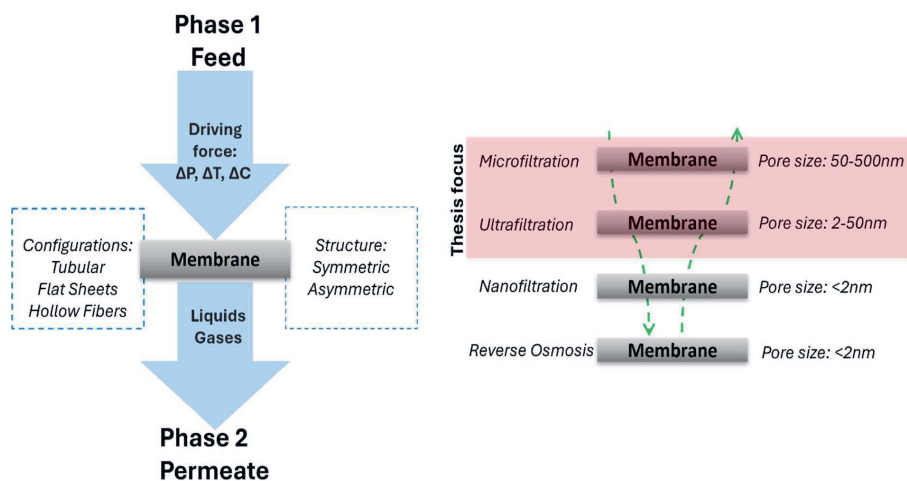


Figure 1.1. Schematic representation of a ceramic membrane and membrane types.

Polymeric membranes are the competitors of ceramic membranes. They have currently the highest market share due to low manufacturing costs, and various polymeric membranes are available for a variety of separation applications [6]. However, some advantages, such as high mechanical strength, high thermal stability, narrow pore size distribution, long service life, higher hydrophilicity, and the potential to be recycled as a raw ceramic material [7-11], provided by ceramic membranes over polymeric membranes can outweigh the upfront high manufacturing costs. In addition, ceramic membranes have a low propensity towards reversible and irreversible fouling [12]. Furthermore, ceramic membranes can be cleaned with harsh chemicals and backwashed at higher pressures during cleaning of the membrane [13], which could guarantee a service life of approximately 15 years or more. Thus, leading to lesser downtime and lower operational costs due to less frequent membrane replacements.

### 1.3 A negatively charged ceramic membrane: Silicon Carbide

SiC membranes offer even better thermal, chemical, and mechanical properties for wastewater treatment applications than the more conventional  $\text{Al}_2\text{O}_3$  ceramic membranes [14].

Furthermore, in comparison with conventional ceramic membranes, SiC membranes are super-hydrophilic and possess a low isoelectric point (in pH range of 2.3-3.5 with the presence of thin silica layer at the surface of SiC) [15, 16]. These characteristics of the SiC membranes could lead to a high permeability and low fouling susceptibility [17]. Therefore, they have the potential for a range of applications in treatment of wastewater with varying temperature, pressure, and pH gradients.

#### 1.4 Limitations in preparing SiC ceramic membranes

SiC membranes comprise of a SiC layer (selective layer) deposited on a porous support. The porous support gives mechanical integrity to the membrane layer, and the selective layer is responsible for sieving properties of the membrane [18]. Although efforts have been made to develop fully SiC-based membranes, challenges such as higher production costs and limited control over pore size control remain significant limitations [19, 20].

Usually the SiC selective layer is prepared by sol-gel methods. These methods involve: (i) a sol-step in which a liquid precursor solution, containing dispersed nanoparticles/molecular precursors, forms a stable colloidal suspension; and (ii) a gel-step in which the suspension undergoes gelation due to sintering/pyrolysis to form a solid structure. The most commonly reported methods in literature are deposition of colloidal suspensions and deposition of pre-ceramic polymeric precursors [15]. These methods, however, have the following limitations:

- The covalent nature of bond between silicon (Si) and carbon (C) requires high sintering temperatures of ca. 2100°C [21].
- To prepare a SiC selective layer with a small pore size, several layers of the solution need to be coated with individual sintering step, thus driving the production costs up and decreasing water permeability [22].
- It is difficult to prepare SiC membranes with a high porosity and narrow pore size

distribution for ultrafiltration (UF) and NF applications due to the difficulties in preparing homogeneous suspensions of SiC powder [23].

- There is shrinkage of structure during repetitive sintering/pyrolysis, thus making it difficult to produce defect-free selective layer with controlled thickness [24].
- Organic solvents utilized in preparation of suspensions can cause environmental issues due to toxicity [25].

### **1.5 Research questions: Rethinking the preparation of SiC membranes**

In order to tackle the limitations of the aforementioned sol-gel deposition of SiC on ceramic support membranes the overall objective of this thesis is to explore LP-CVD to prepare SiC coated membranes. Al<sub>2</sub>O<sub>3</sub> supports were used and the deposition conditions were varied to obtain robust SiC coated Al<sub>2</sub>O<sub>3</sub> membranes. Subsequently, the performance of the SiC coated Al<sub>2</sub>O<sub>3</sub> membranes was tested for sulphate ion (SO<sub>4</sub><sup>2-</sup>) retention.

To achieve this objective the following research questions were formulated:

- What are key findings in literature regarding LP-CVD modification of ceramic membranes for wastewater treatment?
- How to prepare chemically robust SiC coated Al<sub>2</sub>O<sub>3</sub> membranes using the available LP-CVD setup?
- What is the smallest pore size achievable for SiC coated Al<sub>2</sub>O<sub>3</sub> membranes by LP-CVD, and what is the SO<sub>4</sub><sup>2-</sup> retention?
- How can the limitations of LP-CVD in preparing ceramic nanofiltration membranes be overcome by ALD?

### **1.6 How to read this thesis**

The outline of the thesis is shown in Fig. 1.2.

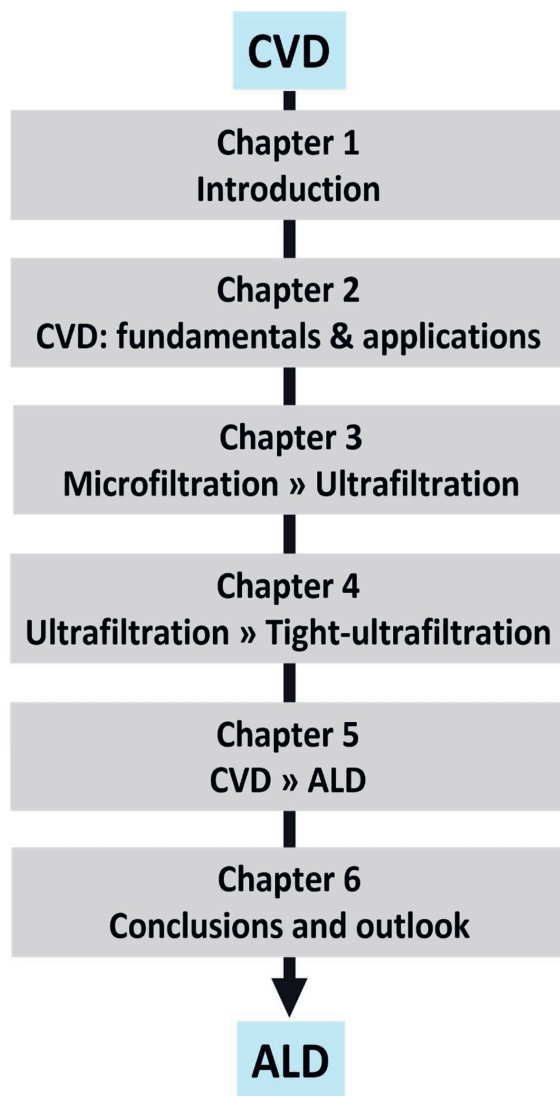


Figure 1.2. Layout of the thesis.

LP-CVD could facilitate the deposition of SiC on membranes. **Chapter 2** discusses: (i) fundamentals of CVD; (ii) key parameters influencing a CVD process; and (iii) the literature available for the pore size and surface charge modification of various supports by CVD.

In **chapter 3**, SiC was coated on an Al<sub>2</sub>O<sub>3</sub> microfiltration (MF) membrane to obtain SiC UF membrane. SiC was coated at two distinct regimes of temperatures and pressures to investigate



the physical and chemical properties of the deposit. Deposition times were varied in both regimes to achieve a similar thickness of the coating for comparison purposes. Subsequently, the chemical stability of the resultant SiC coated UF membrane was evaluated in a membrane cleaning medium, for example, sodium hypochlorite (NaClO).

In **Chapter 4**, the limits of LP-CVD for membrane modification are discussed. The ideal deposition conditions were chosen from chapter 3, and SiC was coated on an Al<sub>2</sub>O<sub>3</sub> UF membrane to achieve the smallest pore size. The performance of the as-prepared SiC coated tight-UF membrane was tested by measuring SO<sub>4</sub><sup>2-</sup> rejection.

**Chapter 5** presents a sister technology of LP-CVD, i.e. ALD, that can be used to narrow down pore sizes to NF range. The fundamentals and application of ALD for modification of ceramic membranes, as well as polymeric membranes and adsorbents for wastewater treatment applications are discussed.

**Chapter 6** critically assesses the materials and methods developed in chapter 2-5. A perspective has been provided on the work performed in this thesis, and potential research directions are identified and discussed.

## References

- [1] W.W.A.P. UNESCO, The United Nations world water development report 2021: valuing water WWDR 2021, UNESCO, 2021.
- [2] A. Alshameri, A. Ibrahim, A.M. Assabri, X. Lei, H. Wang, C. Yan, The investigation into the ammonium removal performance of Yemeni natural zeolite: Modification, ion exchange mechanism, and thermodynamics, *Powder Technology* 258 (2014) 20-31.
- [3] M. Kang, H. Chen, Y. Sato, T. Kamei, Y. Magara, Rapid and economical indicator for evaluating arsenic removal with minimum aluminum residual during coagulation process, *Water Research* 37(19) (2003) 4599-4604.
- [4] J. Zhong, X. Sun, C. Wang, Treatment of oily wastewater produced from refinery processes using flocculation and ceramic membrane filtration, *Separation and Purification Technology* 32(1) (2003) 93-98.
- [5] M. Mulder, *Basic principles of membrane technology*, Springer science & business media 2012.
- [6] D.M. Warsinger, S. Chakraborty, E.W. Tow, M.H. Plumlee, C. Bellona, S. Loutatidou, L. Karimi, A.M. Mikelonis, A. Achilli, A. Ghassemi, L.P. Padhye, S.A. Snyder, S. Curcio, C.D. Vecitis, H.A. Arafat, J.H. Lienhard, A review of polymeric membranes and processes for potable water reuse, *Progress in Polymer Science* 81 (2018) 209-237.
- [7] M. Cifuentes-Cabezas, M.C. Vincent-Vela, J.A. Mendoza-Roca, S. Álvarez-Blanco, Use of ultrafiltration ceramic membranes as a first step treatment for olive oil washing wastewater, *Food and Bioproducts Processing* 135 (2022) 60-73.
- [8] Q. Gu, T.C.A. Ng, Y. Bao, H.Y. Ng, S.C. Tan, J. Wang, Developing better ceramic membranes for water and wastewater Treatment: Where microstructure integrates with chemistry and functionalities, *Chemical Engineering Journal* 428 (2022) 130456.
- [9] M. Lee, Z. Wu, K. Li, 2 - Advances in ceramic membranes for water treatment, in: A. Basile, A. Cassano, N.K. Rastogi (Eds.), *Advances in Membrane Technologies for Water Treatment*, Woodhead Publishing, Oxford, 2015, pp. 43-82.
- [10] C. Li, W. Sun, Z. Lu, X. Ao, S. Li, Ceramic nanocomposite membranes and membrane fouling: A review, *Water Research* 175 (2020) 115674.
- [11] X. Wang, K. Sun, G. Zhang, F. Yang, S. Lin, Y. Dong, Robust zirconia ceramic membrane with exceptional performance for purifying nano-emulsion oily wastewater, *Water Research* 208 (2022) 117859.
- [12] Q. Gu, T.C.A. Ng, L. Zhang, Z. Lyu, Z. Zhang, H.Y. Ng, J. Wang, Interfacial diffusion assisted chemical deposition (ID-CD) for confined surface modification of alumina microfiltration membranes toward high-flux and anti-fouling, *Separation and Purification Technology* 235 (2020) 116177.
- [13] S.-J. Lee, J.-H. Kim, Differential natural organic matter fouling of ceramic versus polymeric ultrafiltration membranes, *Water Research* 48 (2014) 43-51.
- [14] E. Eray, V.M. Candelario, V. Boffa, H. Safafar, D.N. Østedgaard-Munck, N. Zahrtmann, H. Kadrispahic, M.K. Jørgensen, A roadmap for the development and applications of silicon carbide membranes for liquid filtration: Recent advancements, challenges, and perspectives, *Chemical Engineering Journal* 414 (2021) 128826.
- [15] E. Eray, V. Boffa, M.K. Jørgensen, G. Magnacca, V.M. Candelario, Enhanced fabrication of silicon carbide membranes for wastewater treatment: From laboratory to industrial scale, *Journal of Membrane Science* 606 (2020) 118080.
- [16] M. Xu, C. Xu, K. Rakesh, Y. Cui, J. Yin, C. Chen, S. Wang, B. Chen, L. Zhu, Hydrophilic SiC hollow fiber membranes for low fouling separation of oil-in-water emulsions with high flux, *RSC advances* 10(8) (2020) 4832-4839.

- [17] B. Hofs, J. Ogier, D. Vries, E.F. Beerendonk, E.R. Cornelissen, Comparison of ceramic and polymeric membrane permeability and fouling using surface water, *Separation and Purification Technology* 79(3) (2011) 365-374.
- [18] M. Chen, R. Shang, P.M. Sberna, M.W.J. Luiten-Olieman, L.C. Rietveld, S.G.J. Heijman, Highly permeable silicon carbide-alumina ultrafiltration membranes for oil-in-water filtration produced with low-pressure chemical vapor deposition, *Separation and Purification Technology* 253 (2020) 117496.
- [19] Y. Wang, Y. Liu, Z. Chen, Y. Liu, J. Guo, W. Zhang, P. Rao, G. Li, Recent progress in the pore size control of silicon carbide ceramic membranes, *Ceramics International* 48(7) (2022) 8960-8971.
- [20] Y. Zhou, M. Fukushima, H. Miyazaki, Y.-i. Yoshizawa, K. Hirao, Y. Iwamoto, K. Sato, Preparation and characterization of tubular porous silicon carbide membrane supports, *Journal of Membrane Science* 369(1) (2011) 112-118.
- [21] G. Magnani, G. Sico, A. Brentari, P. Fabbri, Solid-state pressureless sintering of silicon carbide below 2000°C, *Journal of the European Ceramic Society* 34(15) (2014) 4095-4098.
- [22] A.R. Jamaludin, S.R. Kasim, M.Z. Abdullah, Z.A. Ahmad, Physical, mechanical, and thermal properties improvement of porous alumina substrate through dip-coating and re-sintering procedures, *Ceramics International* 42(6) (2016) 7717-7729.
- [23] Q. Wang, R. Zhou, T. Tsuru, *Recent Progress in Silicon Carbide-Based Membranes for Gas Separation, Membranes*, 2022.
- [24] V. Suwanmethanond, E. Goo, P.K.T. Liu, G. Johnston, M. Sahimi, T.T. Tsotsis, Porous Silicon Carbide Sintered Substrates for High-Temperature Membranes, *Industrial & Engineering Chemistry Research* 39(9) (2000) 3264-3271.
- [25] C.M. Teaf, Properties and Effects of Organic Solvents, *Principles of Toxicology* 2000, pp. 367-408.





# Chapter 2

Literature review of chemical vapor deposition for ceramic membranes



## **Chapter 2 Literature review of chemical vapor deposition for ceramic membranes**

### **Abstract**

Chemical vapor deposition (CVD) has the capability to modify membranes for wastewater treatment applications. This chapter reviews the fundamental principles and recent advances in CVD for polymeric and ceramic membranes modification. It discusses how process parameters, such as temperature, pressure, and deposition time, influence morphology and adhesion of the coating. This chapter also introduces initiated CVD (iCVD) as a low-temperature alternative for modifying polymeric membranes. By evaluating current literature, this chapter underscores the need for optimized CVD conditions to tailor membrane properties for enhanced operational performance in wastewater treatment applications.

## 2.1 Introduction

CVD is a versatile and widely used technique for the synthesis and deposition of materials in various forms, including coatings (thin films), powders, and single crystals [1]. This process involves the deposition of a solid material from vapor-phase reactants onto a heated substrate, where chemical reactions either occur near the substrate or directly on its surface, depending on the reaction conditions [2]. The adaptability of CVD enables its application across a broad range of materials and substrates, from simple flat surfaces to complex geometries, making it indispensable in many fields of application, including electronics, optics, and membrane technology [3].

One of the key advantages of CVD over physical vapor deposition (PVD) techniques lies in its ability to achieve conformal coatings on substrates with intricate geometries and high aspect ratios. PVD methods, such as sputtering, evaporation, and ion plating, operate based on three principal steps: (1) vaporization of a solid or liquid source to create vapor phase species, (2) transport of the vapor species to the substrate via line-of-sight, and (3) condensation and growth of the film on the substrate surface [4]. The reliance on line-of-sight transport makes PVD less effective for coating substrates with complex shapes. Additionally, PVD processes typically require high vacuum environments to maintain uninterrupted transport of vapor phase species, as collisions between these species in the gas phase can lead to ionization and the formation of plasma, altering the deposition dynamics.

In contrast, CVD offers significant flexibility, as it is not restricted by line-of-sight requirements and can be performed under high vacuum to atmospheric pressure. This allows for the uniform deposition of high-quality films on complex geometries and porous structures. CVD's ability to achieve highly conformal coatings, even on substrates with intricate porosities, makes it



particularly suitable for applications such as membrane modification for water treatment, where the performance of the membrane is dependent on the precise control of surface properties [5].

CVD has a rich historical background, with its first known application dating back to the 1880s, when it was used to deposit carbon coatings to strengthen the filaments of incandescent lamps. Since then, its applications have expanded to include a wide range of coatings for corrosion resistance, thermal protection, electrical conductivity, diffusion barriers, and microelectronic device fabrication. The breadth of CVD applications is largely attributable to its capacity to deposit materials from nearly all elements of the periodic table, either in their elemental form or as complex compounds [6]. This versatility underpins CVD's widespread use across numerous industries, from microelectronics and aerospace to energy and environmental technologies [7].

This chapter focuses on the fundamental principles of CVD, outlining the working mechanism, process parameters, and various CVD techniques used for the modification of membranes. Emphasis will be placed on the role of CVD in tailoring membrane surfaces and pore structures to optimize filtration performance for (waste)water treatment applications. The chapter will also explore the specific advantages of CVD in creating selective layers on ceramic membranes, enhancing their permeability, selectivity, and long-term stability in challenging operating environments.

## **2.2 Key steps in a CVD process: Target material selection and reaction dynamics**

The CVD process begins with the identification of the material to be deposited, known as the target material. The next critical step is to determine the chemical reaction responsible for synthesizing the target material. In CVD, these reactions are inherently heterogeneous, involving a phase transition from gaseous precursors to a solid product [8]. Common reactions facilitating this phase change include thermal decomposition, reduction, oxidation, nitridation, carburization, and

hydrolysis. Each reaction must be carefully selected based on the chemical nature of the target material and the desired properties of the deposited film. Once the appropriate reaction pathway is identified, the precursors and deposition conditions (such as temperature and pressure) are selected to deposit the target material [9]. CVD relies on the precise control of these parameters to ensure film formation, uniformity, and adhesion to the substrate.

The deposition process takes place within a CVD chamber, typically a high-temperature furnace where temperature and pressure are meticulously regulated. High-purity precursors, often in liquid or solid form, are stored in containers outside the chamber. Prior to deposition, these precursors are volatilized and introduced into the chamber through a system of gas lines, with gas flow rates carefully controlled to maintain optimal reaction conditions [2]. The sequence of events completing a CVD reaction are summarized as follows (see also Fig. 2.1):

1. Forced flow of reactant gases into the chamber.
2. Mass transport of reactant species to the vicinity of the substrate.
3. Diffusion of reactant species through boundary layer to substrate surface.
4. Adsorption of species on the surface of substrate.
5. Heterogeneous reaction to form the target material and by-products.
6. Desorption and diffusion of by-products through boundary layer into the bulk gas;
7. Removal of by-products from the chamber via exhaust.

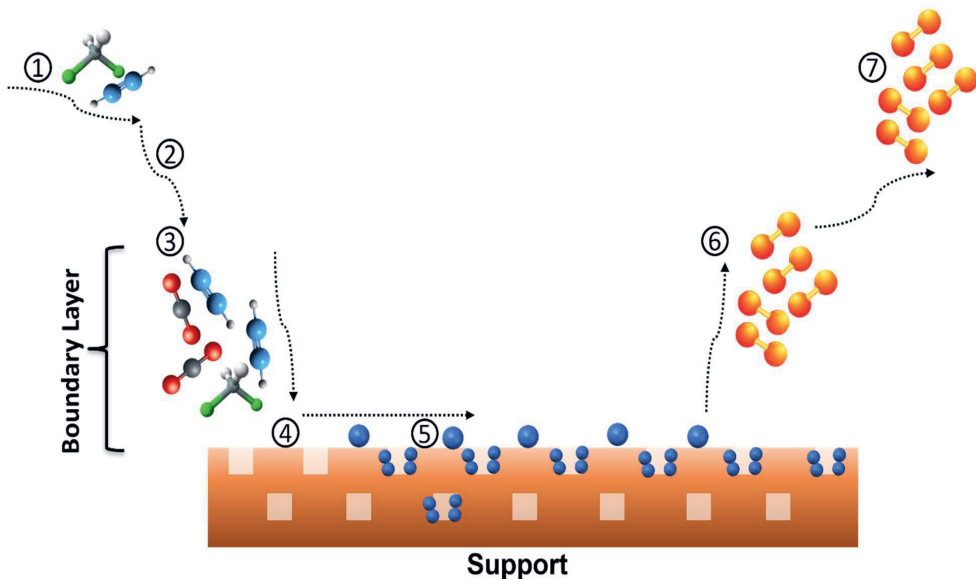


Figure 2.1. Schematic representation of CVD sequence of events.

The deposition conditions, particularly temperature and pressure, play a critical role in determining the structural, morphological, and adhesive properties of the deposited material [1]. These parameters influence the growth rate, crystallinity, and density of the deposited film [10]. Moreover, the rate at which deposition occurs can be limited by one of two factors: surface-reaction kinetics or mass transport. At relatively low temperatures (e.g. 650-850°C) and sub-atmospheric pressures, the deposition rate is predominantly controlled by surface-reaction kinetics. In contrast, when temperature exceeds approximately 900°C and process operates at atmospheric pressure, mass transport of reactant species across a thick boundary layer becomes the limiting factor [11]. The transition between these two regimes, kinetically-limited and mass-transport-limited, occurs gradually through a transition zone where both mechanisms may exert influence [12]. Careful optimization of the deposition parameters (temperature and pressure) is essential to maximize film uniformity, adhesion, and overall material properties, especially in applications

where membrane performance is critical for selective filtration of target substances in membrane systems.

### **2.3 Critical parameters influencing the CVD process for membrane coating**

The CVD process is highly dependent on key operational parameters, such as deposition time, reactor temperature, and total pressure. These factors collectively influence the morphology, chemical composition, and mechanical properties of the coated material [13]. Furthermore, the deposition mechanism in CVD can involve either surface reactions, gas-phase reactions, or a combination of both. To limit the extent of gas-phase reactions, and thus reduce undesirable particle formation or non-uniform coatings, strategies such as lowering the precursor partial pressures, optimizing reactor temperature, and controlling flow rates are often employed [14]. These adjustments which relate directly to key operational parameters help ensure more uniform surface-controlled deposition.

Effective regulation of aforementioned process parameters enables the fine-tuning of deposition mechanisms, allowing for the synthesis of materials with specific properties tailored to the application. Optimizing these parameters is particularly critical when depositing thin films on porous ceramic membranes, where achieving uniform and conformal coatings is a key requirement for enhancing membrane performance [3].

In this section, the most important parameters that govern the CVD process are defined and their impact on the deposition mechanism is discussed.

#### **2.3.1 Influence of deposition time on film growth and membrane properties**

Deposition time plays a pivotal role in determining the final thickness of the coating, particularly when dealing with porous substrates as membranes [10]. As the deposition progresses, the thickness of the coating increases, and the effective pore size of the membrane decreases. Selecting

an appropriate deposition time is thus critical for achieving uniform growth, while preventing excessive pore clogging, which can significantly impair membrane performance [15, 16].

In the case of porous substrates as membranes, controlling the deposition time becomes even more complex due to the inherent difficulties in accurately measuring the thickness of coatings on irregular surfaces. To circumvent this challenge, Si wafers are often placed alongside porous substrates during the CVD process. Si wafers provide a flat and uniform reference surface, allowing for precise measurement of coating thickness using techniques such as ellipsometry or X-ray reflectometry (XRR) [5]. These measurements serve as an approximation for the deposition on the membranes, offering valuable insights into the rate of film growth and ensuring that the deposition conditions are as optimal as possible for the desired membrane properties.

### **2.3.2 Impact of deposition temperature on membrane structure and performance**

Deposition temperature is also a key determinant in controlling the structural and morphological characteristics of coatings produced by CVD. The temperature governs critical attributes of the coated layer, including crystallinity, microstructure, adhesion strength, and surface morphology [17, 18].

Higher deposition temperatures (above 900°C) facilitate the formation of crystalline phases [19, 20]. The resultant crystalline coatings exhibit a high mechanical strength and chemical durability, traits that are essential for the operational robustness of membranes in harsh filtration environments. In contrast, lower deposition temperatures (650-850°C) often lead to the formation of amorphous coatings with a rough surface morphology [21]. Such increased roughness results in a large surface area, and it may create additional sites for particle adhesion, potentially leading to fouling and affecting membrane's performance.

Additionally, the adhesion strength of the coating is also temperature-dependent. Elevated temperatures can enhance interfacial bonding between the coated layer and the substrate, leading to improved coating adhesion [22]. Conversely, deposition at suboptimal temperatures may result in poor coating-support interactions, which can lead to delamination or mechanical failure under mechanical or chemical stress during filtration [23]. Although elevated temperatures (above 900°C) generally produce crystalline and adhesive coatings, excessively high temperatures may induce thermal stresses or increase the likelihood of microcracking. Therefore, achieving an optimal balance between deposition temperature and coating adhesion is crucial for ensuring the long-term stability of membranes under varying filtration conditions.

### **2.3.3 Role of deposition pressure in controlling pore structure and film density**

Deposition pressure during the coating process by CVD significantly influences the mass transport of reactant species, the pore structure of the membrane, and the density of the resulting coating [24]. Pressure controls the mean free path of the gas-phase reactants and the thickness of the boundary layer that forms at the support surface during deposition, both of which are key factors in determining coating morphology and uniformity. However, this parameter has not been explored in the literature.

At elevated atmospheric pressures, the mean free path of the reactant molecules is reduced, leading to increased gas-phase collisions and the formation of a thicker boundary layer at the support surface. This thicker boundary layer hinders the diffusion of reactant species to the support, resulting in lower film growth rates [12]. Consequently, high-pressure CVD tends to produce dense coatings, which may be advantageous for applications requiring impermeable or highly selective membranes.

Conversely, operating at lower deposition pressures (below atmospheric pressure) increases the mean free path of the reactant molecules, thereby enhancing the diffusion of these species through the gas phase and into the support's pore network. In the context of porous substrates as membranes, low-pressure CVD is thus particularly beneficial, as it promotes deeper penetration of the reactants into the pore structure, leading to more uniform coating of the internal surfaces [25]. This improves the overall membrane functionality by minimizing the risk of pore blockage and ensuring that the coating retains sufficient permeability while maintaining structural integrity. However, a delicate balance must be achieved between pressure, pore accessibility, and coating density. Excessively low pressures may result in non-uniform coatings with poor adhesion, compromising the membrane's mechanical properties and long-term stability. Therefore, optimizing deposition pressure is essential for controlling the interplay between pore structure and coating density.

#### **2.4 Polymeric membrane modification by CVD**

Polymeric membranes, due to their sensitivity to elevated temperatures and pressures, present unique challenges in surface modification. Their thermal and mechanical fragility limits the applicability of conventional high-temperature CVD processes. To address these challenges, initiated chemical vapor deposition (iCVD) has been developed as a solvent-free polymerization method that operates at lower temperatures (20-80°C), thereby enabling surface modifications without compromising the integrity of polymeric membranes [26]. iCVD is a low-temperature, solvent-free method for the deposition of polymeric coatings. In this process, a free-radical polymerization reaction is initiated by radicals formed through the thermal decomposition of an initiator. The sequence of events in the iCVD process are as follows:

1. Forced flow of precursors (initiators and monomers) into the chamber.

2. Decomposition of initiators by a heated filament to form radicals.
3. Adsorption of monomers onto a cooled substrate surface.
4. Mass transport of free radicals to react with monomers on the cooled substrate surface.
5. Surface polymerization to form a polymeric coating.

The iCVD process is distinct from other CVD methods due to its low filament temperature (typically between 150–300°C), which prevents the fragmentation of monomers [27, 28]. Furthermore, the support temperature during iCVD remains within a low range of 20–80°C, using water as a coolant, making it particularly suitable for the deposition of coatings on thermally sensitive polymeric membranes [29-31]. This low-temperature operation ensures the preservation of polymeric membrane properties, while allowing for precise control over the thickness and uniformity of the deposited coating.

The application of iCVD for polymeric membrane modification has demonstrated promise in enhancing the performance and durability of membranes, particularly for water treatment applications. In recent years, iCVD has been leveraged to create selective layers on polymeric membranes, improving their fouling resistance, permeability, and surface properties without altering their inherent structure [32].

Yang et al. pioneered this approach by depositing a 600 nm coating of Poly(DMAEMA-co-SPMA-co-EGDMA) onto a reverse osmosis membrane [33]. The coating was conformally deposited on the membrane surface without penetration into the membrane's pores. This surface modification endowed the membrane with high fouling resistance, effectively mitigating the adverse effects of organic foulants, such as humic acid, sodium alginate, and bovine serum albumin. It is important to note that the inherent solute rejection performance of the membrane is determined by its original



selective layer. The polymer coating, whereas, functions solely to reduce fouling and thereby maintain operational efficiency over time.

Building on this foundation, Matin et al. explored the iCVD modification of thin-film composite polyamide reverse osmosis membranes by coating a copolymer film of 2-hydroxyethyl methacrylate and perfluorodecyl acrylate [34]. The modified membranes also exhibited an enhanced fouling resistance towards sodium alginate. The polymeric coatings created by iCVD are highly uniform, ensuring that the intrinsic permeability of the membrane is not compromised while introducing fouling-resistant properties.

The versatility of iCVD in modifying both organic and inorganic substrates is further highlighted by the work of Cong et al., where poly(1H,1H,2H,2H-PFDA) was coated onto Al<sub>2</sub>O<sub>3</sub> membranes [35]. This iCVD modification converted the hydrophilic Al<sub>2</sub>O<sub>3</sub> surface into hydrophobic. Interestingly, while the deposition process improved permeate flux and salt rejection (99%) in desalination applications, it was challenging to determine whether the polymeric coating was deposited solely on the surface or had penetrated the membrane's pores. Despite this ambiguity, the Al<sub>2</sub>O<sub>3</sub> membranes exhibited an increase in the permeate flux as a function of feed temperature, and showed salt rejection rates of 99% over continuous operation of 16 hours. This illustrates the potential of iCVD for creating highly selective and durable filtration systems.

Collectively, these studies demonstrate the transformative potential of iCVD in membrane modification. By enabling the coating of thin polymeric films at low temperatures, iCVD addresses critical challenges in polymeric membrane technology, particularly for applications requiring delicate balancing between permeability, fouling resistance, and mechanical stability. Additionally, it offers a route to prepare solvent-free polymeric coatings. As research continues to advance, the

scalability of iCVD and its long-term performance in industrial settings will determine its broader applicability in membrane-based filtration technologies.

## 2.5 Ceramic membrane modification by CVD

While the application of CVD in gas separation ceramic membranes has extensively been studied, its use in the modification of ceramic membranes for (waste)water treatment remains relatively underexplored. However, recent pioneering studies highlight the promising potential of CVD techniques for this purpose [36]. Ceramic membranes, due to their inherent high-temperature stability and chemical resistance, provide an ideal support for CVD-based surface modification, with materials such as alumina ( $\text{Al}_2\text{O}_3$ ), titanium dioxide ( $\text{TiO}_2$ ), and zirconium oxide ( $\text{ZrO}_2$ ) being the most frequently utilized. These materials allow for the deposition of a coating layer on membrane's selective layer, thus transforming the membrane's surface characteristics to enhance performance in filtration processes.

Lin et al. (1993) initiated one of the earliest studies focusing on pore size modification of ceramic membranes using CVD [37]. Their theoretical and experimental analysis demonstrated that pore size reduction could effectively be achieved by tailoring the CVD process parameters, specifically by aligning the deposition rate with the membrane's pore volume. Although this study has not directly assessed changes in permeance, it has laid foundational guidelines for optimizing CVD processes to coat the selective layer of ceramic supports. Their work has also highlighted the importance of selecting ceramic membrane supports with uniform pore size distributions to ensure uniform pore size reduction. In addition, they have found that the process conditions have to be adjusted in such a way that the pore narrowing rate should be proportional to the pore size of the membrane to ensure homogeneous pore narrowing across the membrane surface.

Athanasekou et al. have made progress by coating  $\text{TiO}_2$  onto  $\gamma\text{-Al}_2\text{O}_3$  UF tubular membranes, thereby creating photocatalytic NF membranes [38]. By carefully modulating the deposition conditions, they ensured a uniform  $\text{TiO}_2$  layer that coated both the surface and the pores of the membrane. The resulting membranes, in comparison with uncoated membranes, exhibited a 1.3 times greater rejection efficiency for methyl orange while maintaining a stable permeance. Chen et al. have extended these findings by preparing SiC UF membranes through LP-CVD deposition onto  $\text{Al}_2\text{O}_3$  MF membranes [5]. Their results have revealed a clear trend: both pore size and permeance decreased as deposition time increased, underscoring the importance of deposition time as a critical parameter in controlling the thickness of the coating, and thus, the filtration performance of CVD-modified membranes.

Miao et al. have taken a different approach by employing ion impregnation and CVD to deposit carbon nanotubes on flat  $\text{Al}_2\text{O}_3$  membranes [39]. This modification altered the membrane's surface characteristics, converting it into a highly hydrophobic material with a reduced pore size. The introduction of carbon nanotubes via CVD not only minimized pore dimensions but also imparted hydrophobicity to the membrane, severely restricting permeance under certain operating conditions (e.g., nitrogen pressure at 0.5 bar). The study demonstrated the ability of CVD to drastically alter the wettability of ceramic membranes, though the results indicated that fine-tuning the deposition parameters is crucial to balance hydrophobicity with permeance.

These early studies, though relatively limited in scope, reveal the versatility and transformative potential of CVD in ceramic membrane modification. The ability to impart specific properties, such as photocatalytic activity, hydrophobicity, and pore size reduction, through coating of selective layer paves the way for future innovations in (waste)water treatment technologies. As research progresses, optimizing CVD techniques for ceramic membranes is likely to become a key

focus, enabling the development of more efficient and robust filtration systems tailored to complex industrial water treatment challenges.

## **2.6 Conclusions and future outlook**

In this chapter CVD techniques were reviewed for modifying polymeric and ceramic membranes for water treatment applications. For ceramic membranes, low-pressure CVD variants have demonstrated capacity to uniformly coat the selective layer that, consequentially improves selective layer's performance while maintaining a proper permeance of the membrane. However, the ability of iCVD to operate at low temperatures has shown significant promise for polymeric membranes, particularly in enhancing fouling resistance and surface properties without compromising structural integrity.

Despite these advancements, further work is needed to optimize deposition parameters and fully realize the potential of CVD in commercial-scale water filtration processes. The future of CVD-modified membranes lies in fine-tuning these deposition techniques to address scalability, long-term durability and performance consistency under diverse operational conditions.

## References

- [1] J.-O. Carlsson, P.M. Martin, Chapter 7 - Chemical Vapor Deposition, in: P.M. Martin (Ed.), Handbook of Deposition Technologies for Films and Coatings (Third Edition), William Andrew Publishing, Boston, 2010, pp. 314-363.
- [2] H. Pierson, Handbook of Chemical Vapor Deposition: Principles, Technology, and Applications, Noyes Publications/William Andrew Publishing 1999.
- [3] G. Vignoles, Chemical vapor deposition/infiltration processes for ceramic composites, Advances in Composites Manufacturing and Process Design, Elsevier 2015, pp. 147-176.
- [4] S.I. Shah, G.H. Jaffari, E. Yassitepe, B. Ali, Evaporation: Processes, bulk microstructures, and mechanical properties, Handbook of Deposition Technologies for Films and Coatings (2010) 135-252.
- [5] M. Chen, R. Shang, P.M. Sberna, M.W.J. Luiten-Olieman, L.C. Rietveld, S.G.J. Heijman, Highly permeable silicon carbide-alumina ultrafiltration membranes for oil-in-water filtration produced with low-pressure chemical vapor deposition, Separation and Purification Technology 253 (2020) 117496.
- [6] J. Creighton, P. Ho, Introduction to chemical vapor deposition (CVD), ASM International 407 (2001).
- [7] M. Fraga, R. Pessoa, Progresses in Synthesis and Application of SiC Films: From CVD to ALD and from MEMS to NEMS, Micromachines 11(9) (2020) 799.
- [8] L.-S. Hong, Z.-L. Liu, Gas-to-particle conversion mechanism in chemical vapor deposition of silicon carbide by SiH<sub>4</sub> and C<sub>2</sub>H<sub>2</sub>, Industrial & engineering chemistry research 37(9) (1998) 3602-3609.
- [9] K.L. Choy, Chemical vapour deposition of coatings, Progress in Materials Science 48(2) (2003) 57-170.
- [10] S. Nishino, Y. Hazuki, H. Matsunami, T. Tanaka, Chemical Vapor Deposition of Single Crystalline  $\beta$ -SiC Films on Silicon Substrate with Sputtered SiC Intermediate Layer, Journal of the Electrochemical Society 127(12) (1980) 2674.
- [11] E. Kinsbron, M. Sternheim, R. Knoell, Crystallization of amorphous silicon films during low pressure chemical vapor deposition, Applied Physics Letters 42(9) (1983) 835-837.
- [12] L. Wang, S. Dimitrijević, J. Han, F. Iacopi, J. Zou, Transition between amorphous and crystalline phases of SiC deposited on Si substrate using H<sub>3</sub>SiCH<sub>3</sub>, Journal of crystal growth 311(19) (2009) 4442-4446.
- [13] A.I. Labropoulos, C.P. Athanasekou, N.K. Kakizis, A.A. Sapalidis, G.I. Pilatos, G.E. Romanos, N.K. Kanellopoulos, Experimental investigation of the transport mechanism of several gases during the CVD post-treatment of nanoporous membranes, Chemical Engineering Journal 255 (2014) 377-393.
- [14] C.-F. Wang, D.-S. Tsai, Low pressure chemical vapor deposition of silicon carbide from dichlorosilane and acetylene, Materials chemistry and physics 63(3) (2000) 196-201.
- [15] N. Said, Y.S. Khoo, W.J. Lau, M. Gürsoy, M. Karaman, T.M. Ting, E. Abouzari-Lotf, A.F. Ismail, Rapid surface modification of ultrafiltration membranes for enhanced antifouling properties, Membranes 10(12) (2020) 401.
- [16] S. Wilski, M. Jaritz, L. Kleines, R. Dahlmann, C. Hopmann, Quantification of dominant diffusion processes through plasma enhanced chemical vapor deposition-coated plastics by combining two complementary methods for porosity analysis, Journal of Physics D: Applied Physics 53(32) (2020) 325305.

- [17] H. Nagasawa, Y. Yamaguchi, T. Izumi, K. Tonosaki, Heteroepitaxial growth and ESR evaluation of 3C-SiC, *Applied surface science* 70 (1993) 542-545.
- [18] H. Nagasawa, Y.-i. Yamaguchi, Atomic level epitaxy of 3C-SiC by low pressure vapour deposition with alternating gas supply, *Thin Solid Films* 225(1-2) (1993) 230-234.
- [19] L. Calcagno, P. Musumeci, F. Roccaforte, C. Bongiorno, G. Foti, Crystallisation mechanism of amorphous silicon carbide, *Applied surface science* 184(1-4) (2001) 123-127.
- [20] H. Nagasawa, Y.-i. Yamaguchi, Mechanisms of SiC growth by alternate supply of SiH<sub>2</sub>Cl<sub>2</sub> and C<sub>2</sub>H<sub>2</sub>, *Applied surface science* 82 (1994) 405-409.
- [21] G. Qin, A. Jan, Q. An, H. Zhou, L.C. Rietveld, S.G.J. Heijman, Chemical vapor deposition of silicon carbide on alumina ultrafiltration membranes for filtration of microemulsions, *Desalination* 582 (2024) 117655.
- [22] N. Li, K. Wang, T. Xu, J. Gao, Y. Wang, W. Wang, H. Sun, Effect of rapid thermal annealing on microstructure, mechanical and tribological properties of amorphous SiC hard coatings, *Journal of Non-Crystalline Solids* 632 (2024) 122939.
- [23] M. Ignat, J. Park, T. Sudarshan, Stresses and mechanical stability of CVD thin films, Chapter 3 (2001) 45-80.
- [24] G.P. Gakis, E.N. Skountzos, I.G. Aviziotis, C.A. Charitidis, Multi-parametric analysis of the CVD of CNTs: Effect of reaction temperature, pressure and acetylene flow rate, *Chemical Engineering Science* 267 (2023) 118374.
- [25] T. Nagano, K. Sato, K. Kawahara, Gas permeation property of silicon carbide membranes synthesized by counter-diffusion chemical vapor deposition, *Membranes* 10(1) (2020) 11.
- [26] K.K. Gleason, Nanoscale control by chemically vapour-deposited polymers, *Nature Reviews Physics* 2(7) (2020) 347-364.
- [27] T.P. Martin, K.K.S. Lau, K. Chan, Y. Mao, M. Gupta, W. Shannan O'Shaughnessy, K.K. Gleason, Initiated chemical vapor deposition (iCVD) of polymeric nanocoatings, *Surface and Coatings Technology* 201(22) (2007) 9400-9405.
- [28] H. Yang, H. Wang, J. Feng, Y. Ye, W. Liu, Solventless Synthesis and Patterning of UV-Responsive Poly(allyl methacrylate) Film, *Macromolecular Chemistry and Physics* 220(18) (2019) 1900299.
- [29] C. Cheng, M. Gupta, Surface functionalization of 3D-printed plastics via initiated chemical vapor deposition, *Beilstein Journal of Nanotechnology* 8 (2017) 1629-1636.
- [30] C. Cheng, M. Gupta, Roll-to-Roll Surface Modification of Cellulose Paper via Initiated Chemical Vapor Deposition, *Industrial & Engineering Chemistry Research* 57(34) (2018) 11675-11680.
- [31] D. Soto, A. Ugur, T.A. Farnham, K.K. Gleason, K.K. Varanasi, Short-Fluorinated iCVD Coatings for Nonwetting Fabrics, *Advanced Functional Materials* 28(33) (2018) 1707355.
- [32] Q. Song, M. Zhu, X. Chen, T. Liu, M. Xie, Y. Mao, Flexible membranes fabricated by initiated chemical vapor deposition for water treatment, battery, and drug delivery, *Chemical Engineering Journal* 477 (2023) 146911.
- [33] R. Yang, K.K. Gleason, Ultrathin antifouling coatings with stable surface zwitterionic functionality by initiated chemical vapor deposition (iCVD), *Langmuir* 28(33) (2012) 12266-12274.
- [34] A. Matin, H. Shafi, M. Wang, Z. Khan, K. Gleason, F. Rahman, Reverse osmosis membranes surface-modified using an initiated chemical vapor deposition technique show resistance to alginate fouling under cross-flow conditions: filtration & subsequent characterization, *Desalination* 379 (2016) 108-117.

- [35] S. Cong, X. Liu, F. Guo, Membrane distillation using surface modified multi-layer porous ceramics, *International Journal of Heat and Mass Transfer* 129 (2019) 764-772.
- [36] M. Sabzi, S. Mousavi Anijdan, M. Shamsodin, M. Farzam, A. Hojjati-Najafabadi, P. Feng, N. Park, U. Lee, A review on sustainable manufacturing of ceramic-based thin films by chemical vapor deposition (CVD): reactions kinetics and the deposition mechanisms, *Coatings* 13(1) (2023) 188.
- [37] Y. Lin, A. Burggraaf, Experimental studies on pore size change of porous ceramic membranes after modification, *Journal of membrane science* 79(1) (1993) 65-82.
- [38] C.P. Athanasekou, G.E. Romanos, F.K. Katsaros, K. Kordatos, V. Likodimos, P. Falaras, Very efficient composite titania membranes in hybrid ultrafiltration/photocatalysis water treatment processes, *Journal of Membrane Science* 392-393 (2012) 192-203.
- [39] M. Miao, T. Liu, J. Bai, Y. Wang, Engineering the wetting behavior of ceramic membrane by carbon nanotubes via a chemical vapor deposition technique, *Journal of Membrane Science* 648 (2022) 120357.







# Chapter 3

## Effect of long-term sodium hypochlorite cleaning on silicon carbide ultrafiltration membranes prepared by low-pressure chemical vapor deposition

This chapter is based on:

Jan, A.; Chen, M.; Nijboer, M.; Luiten-Olieman, M.W.J.; Rietveld, L.C.; Heijman, S.G.J. Effect of Long-Term Sodium Hypochlorite Cleaning on Silicon Carbide Ultrafiltration Membranes Prepared via Low-Pressure Chemical Vapor Deposition. *Membranes* 2024, 14, 22.



## **Chapter 3 Effect of long-term sodium hypochlorite cleaning on silicon carbide ultrafiltration membranes prepared by low-pressure chemical vapor deposition**

### **Abstract**

Sodium hypochlorite (NaClO) is widely used for chemical cleaning of fouled UF membranes. Various studies performed on polymeric membranes demonstrate that long-term (>100hrs) exposure to NaClO deteriorates the physicochemical properties of the membranes, leading to reduced performance and service life. However, the effect of NaClO cleaning on ceramic membranes, particularly the number of cleaning cycles they can undergo to alleviate irreversible fouling, remains poorly understood. SiC membranes have garnered widespread attention for water and (waste)water treatment, but their chemical stability in NaClO has not been studied. In this work, SiC coated UF membranes were prepared by LP-CVD at two different deposition temperatures and pressures, and their chemical stability in NaClO was investigated over 200 hours of ageing. LP-CVD facilitates preparation of SiC coated membranes at much lower temperatures (700-900°C) than sol-gel methods (ca. 2000°C). Subsequently, the properties and performance of the as-prepared SiC coated UF membranes were evaluated before and after ageing to determine the optimal deposition conditions. Our results indicate that SiC coated UF membrane prepared by LP-CVD at 860°C and 100mTorr exhibit excellent resistance to NaClO ageing, while the membrane prepared at 750°C and 600mTorr significantly deteriorated. These findings highlight the importance of careful selection of LP-CVD conditions for SiC coated membranes to ensure their robustness and long-term performance under harsh chemical cleaning conditions.

### 3.1 Introduction

SiC UF membranes have found widespread applications for industrial (waste)water [1-3], produced water [4], grey water [5], and surface water treatment [6]. In addition, they are employed as a pre-treatment step prior to reverse osmosis [7] and for pool water filtration in public swimming pools [8]. The popularity of SiC UF membranes stem from their ability to provide: (i) high permeate fluxes due to their hydrophilic nature; (ii) a high-quality permeate irrespective of variation in feed quality; (iii) an excellent hydrothermal stability; (iv) a good stability against pressure and pH gradients; and (v) a high porosity and uniform pore size distribution [9-11].

Wastewaters consist of a complex mixture of contaminants, including organic matter and colloidal particles [12, 13]. These contaminants are susceptible to attach to the membranes' surface via physisorption or chemisorption. In both cases, a significant decline in flux and an increase in trans-membrane pressure (TMP) has been observed [14-16]. If the physisorption of the contaminants can be alleviated by back-washing the membrane, the fouling is called reversible. However, if the contaminants are chemisorbed on the membranes' surface, the fouling is irreversible and chemical cleaning must be performed to remove the contaminants and restore membrane flux. Chemical cleaning is performed by an aggressive oxidizing chemical, e.g. NaClO, and repetitive chemical cleaning results in the degradation of membranes of both organic and inorganic nature [17-19]. Consequentially, the permeability and selectivity of the membrane are compromised.

From the perspective of organic membranes, various studies have been performed on different polymeric membranes (polyethersulphone, polyvinylpyrrolidone, polyvinylchloride) to study the degradation of membrane properties upon NaClO exposure and the underlying mechanisms responsible for degradation. Susanto et al. observed an increase in pure water flux (PWF) of polyethersulphone (PES) membranes after exposure to NaClO [20]. Mechanistic analysis of the

degradation of PES membranes has also been reported in various studies, and it is concluded that the chain scission of PES is responsible for altering membrane properties [21, 22]. In comparison, from the perspective of inorganic membranes, the studies on the effect of membrane properties by NaClO exposure are scarce. Kramer et al. tested the chemical stability of ceramic ultrafiltration and nanofiltration membranes by exposing them to 1% NaClO solution for 100 hours. It was observed that the NaClO deteriorated the glass seal at the edges of the membrane and an increase in water permeability and molecular-weight cut-off was observed. However, mechanistic insights were not provided [18].

NaClO is commonly employed for the chemical cleaning of membranes. The highly oxidative nature of NaClO can selectively leach out organic, inorganic, and biological fouling and restore the primary properties of the membrane [23]. The active species, present in NaClO solution depend on the pH of the solution. NaClO dissociates into hypochlorous acid (HOCl) and hypochlorite ion ( $\text{OCl}^-$ ) depending on the pH. HOCl is the active species in germicidal activity, and the concentration of  $\text{OCl}^-$  determines the cleaning efficiency [24]. The concentration of  $\text{OCl}^-$  is highest in the pH range of 10-12 [25]. Therefore, chemical cleaning is usually performed in aforementioned pH range. However, these active species can also deteriorate the physicochemical properties of the selective layer of the membrane and the service life of a membrane is then subject to the total hours of chemical cleaning with NaClO. In this regard, various studies on polymeric membranes have been performed to show that the long-term effects of NaClO cleaning on the membrane properties are detrimental [26-28]. However, to the authors' knowledge, studies on the impact of long-term NaClO ageing on SiC UF membranes still lack.

Therefore in the present work, SiC coated UF membranes were prepared by LP-CVD under two different deposition conditions. Subsequently, the effects of accelerated NaClO ageing on the

physiochemical properties and performance of SiC coated UF membranes were studied to determine the suitable LP-CVD deposition conditions. The chemical robustness of the SiC coated UF membranes was investigated by exposing tubular SiC coated UF membranes to 5% NaClO for 200 hours to simulate long-term ageing. Surface chemical composition, surface morphology, pore size, and PWP of the pristine and aged SiC coated UF membranes were scrutinized to gauge the chemical robustness of the as-prepared SiC coated UF membranes.

## 3.2 Materials and Methods

### 3.2.1 Materials & Chemical Agents

Commercial tubular Al<sub>2</sub>O<sub>3</sub> membranes, obtained from CoorsTek, the Netherlands, were used as supports for coating of SiC by LP-CVD. The membranes had an inner diameter of 7 mm, an outer diameter of 10 mm, and were 10 cm long (Fig. 3.1). As per suppliers' specifications, the membranes consisted of a 100 nm Al<sub>2</sub>O<sub>3</sub> selective layer on a 600 nm macroporous Al<sub>2</sub>O<sub>3</sub> support. Great variations were observed for the PWP of the membranes. Therefore, membranes with a PWP of ca. 350 L.m<sup>-2</sup>.h<sup>-1</sup>.bar<sup>-1</sup> were selected for LP-CVD of SiC.

Commercially available 12.5% NaClO was purchased from Sigma-Aldrich Chemicals (The Netherlands). 5% NaClO was prepared by diluting the 12.5% stock solution, and the pH was maintained at 12. Deionized water was used to prepare all the solutions.

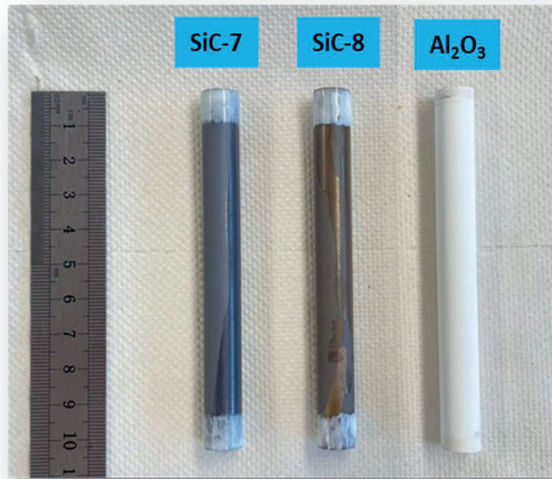


Figure 3.1. Sealed pristine Alumina and SiC coated membranes.

### 3.2.2 Low-Pressure Chemical Vapor Deposition

A hot-wall LP-CVD furnace (Tempress Systems BV, The Netherlands) was used for the coating of SiC. The construction of the LP-CVD system is given elsewhere [29]. Precursors used were Dichlorosilane ( $\text{SiH}_2\text{Cl}_2$ ) and 5% acetylene ( $\text{C}_2\text{H}_2$ ) in hydrogen ( $\text{H}_2$ ) balance for the Si and C sources respectively. Ultrapure nitrogen ( $\text{N}_2$ ) from a liquid  $\text{N}_2$  source was employed as purging gas in the system. During SiC coating, the membranes were placed longitudinally to the flow of precursor gases.

Deposition conditions were adapted from the study of Morana et al. to obtain a thin amorphous SiC coating on and in membranes' surface [30] and the SiC coating was performed at two different temperatures and pressures. Due to difficulties in directly measuring growth rate of SiC coating in the pores of the membrane, the SiC growth rate at both conditions was measured on Si wafers with ellipsometry. Low-temperature SiC coating (SiC-7) was carried out at a temperature of  $750^\circ\text{C}$ ,

pressure of 600 mTorr, and deposition time of 60 min. High-temperature SiC coating (SiC-8) was carried out at a temperature of 860°C, pressure of 100 mTorr, and deposition time of 30 min. Both deposition conditions led to same thickness of SiC coating on Si wafers (Table S3.1). Temperature, pressure, and deposition time were selected so that a SiC coating of the same thickness was obtained for membranes.

### 3.2.3 Membranes Accelerated Ageing Procedure

Before the ageing experiments, the SiC-7 and SiC-8 membranes were soaked in ultrapure water for 24 h, and, afterwards, their PWP was measured. For the membrane ageing procedure, dried membrane samples were soaked in a 5% NaClO solution in an air-tight container at ambient temperature ( $25\pm 3^\circ\text{C}$ ) in the dark for 200 h. This corresponds to an exposure dose of 10000 g.hr/L. The ageing solutions were replaced every 24 h to avoid variation of concentration and pH with time. The aged SiC-7 and SiC-8 membrane are referred to as SiC-7-2A and SiC-8-2A, respectively. After 200 h, SiC-7-2A and SiC-8-2A were removed from the 5% NaClO solution, rinsed with ultrapure water, and soaked in ultrapure water overnight to remove residual NaClO species before characterization and performance analysis.

### 3.2.4 Membrane Characterization and Performance Evaluation

The morphology of the pristine  $\text{Al}_2\text{O}_3$ , the SiC-7/SiC-8, and the SiC-7-2A/SiC-8-2A membranes was observed by scanning electron microscopy (SEM, FEI Nova NanoSEM 450, USA). An energy dispersive x-ray (EDX) analyzer coupled with SEM was used to determine the Si atomic percentage. Sample preparation for SEM involved breaking the membranes with a hammer to obtain a flat specimen which was afterwards sputter coated with gold to increase sample conductivity to achieve clear images.



The surface chemical composition of the SiC-7/SiC-8 and SiC-7-2A/SiC-8-2A membranes was evaluated by X-ray photoelectron spectroscopy (XPS). XPS spectra were obtained using a ThermoFisher K-alpha XPS system. Further processing of the XPS spectra was done using CasaXPS software.

The average pore size of the membranes was measured by capillary flow porometry (Porolux 500, IBFT GmbH, Germany). FC43 (Benelux Scientific B.V., the Netherlands) was used as wetting agent for porometry measurements, and flow and feed pressure were recorded in time. Pore size was then calculated using Young-Laplace equation [31]:

$$D = (4\gamma \cdot \cos \theta \cdot SF) / P$$

where  $D$  is the pore diameter of the membrane (m),  $\gamma$  is the surface tension of the wetting liquid (N/m),  $\theta$  is the contact angle of the liquid on the membrane surface ( $0^\circ$ ),  $P$  is the used pressure (bar), and  $SF$  is the shape factor (SF is 1 based on the assumption that all pores have an exact cylindrical shape).

The PWP of the membranes was measured under constant flux in an in-house built cross-flow filtration setup for tubular membranes using deionized water (Fig. 3.2).

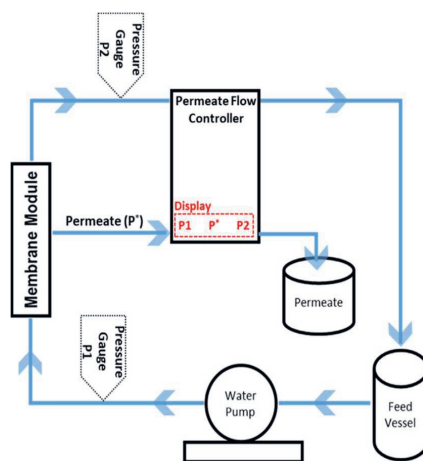


Figure 3.2. Cross-flow filtration setup.

### 3.3 Results and Discussion

#### 3.3.1 Microstructure and Surface Composition of the SiC Coated Membranes

Surface morphologies of the  $\text{Al}_2\text{O}_3$  and SiC coated membranes (SiC-7, SiC-8) were analyzed by SEM as shown in Fig. 3.3. The macroporous  $\text{Al}_2\text{O}_3$  membrane comprised of randomly oriented fine and coarse particles (Fig. 3.3a-b). The discrepancy in shape and size of  $\text{Al}_2\text{O}_3$  particles resulted in a non-homogeneous surface. The surface of SiC-7 membrane comprised of amorphous SiC nodules, and a decrease in porosity was observed in comparison with  $\text{Al}_2\text{O}_3$  membrane (Fig. 3.3c-d). The SiC deposition at  $860^\circ\text{C}$  resulted in a continuous dense SiC coating [32], and the decrease in porosity was larger than that observed for SiC-7 (Fig. 3.3e-f). Our observations are consistent with the LP-CVD growth mechanisms reported previously, i.e. when SiC is deposited on a foreign substrate (which in this case is  $\text{Al}_2\text{O}_3$ ), the growth proceeds via the three-dimensional Volmer-Weber island growth mechanism [33]. At the low-deposition temperature of  $750^\circ\text{C}$ , the growth kinetics were slow leading to the formation of distinct SiC islands, which subsequently grow into SiC nodules, as suggested by Greene [33]. However, at high-deposition temperature of  $860^\circ\text{C}$ , fast growth kinetics led to coalescing and growth of SiC nodules to form a homogeneous and continuous coating [34, 35]. The intrinsic stress, introduced due to either deposition conditions or mismatch in thermal coefficients between support and coating, is greatly reduced by the transition in morphology of SiC from nodules to a continuous coating [36]. Consequentially, the growth of continuous SiC coating will properly shield the  $\text{Al}_2\text{O}_3$  particles and hence the interfacial energy between  $\text{Al}_2\text{O}_3$  substrate and SiC coating will be minimized [37], leading to the enhancement of adhesion strength between the SiC coating and the  $\text{Al}_2\text{O}_3$  support.

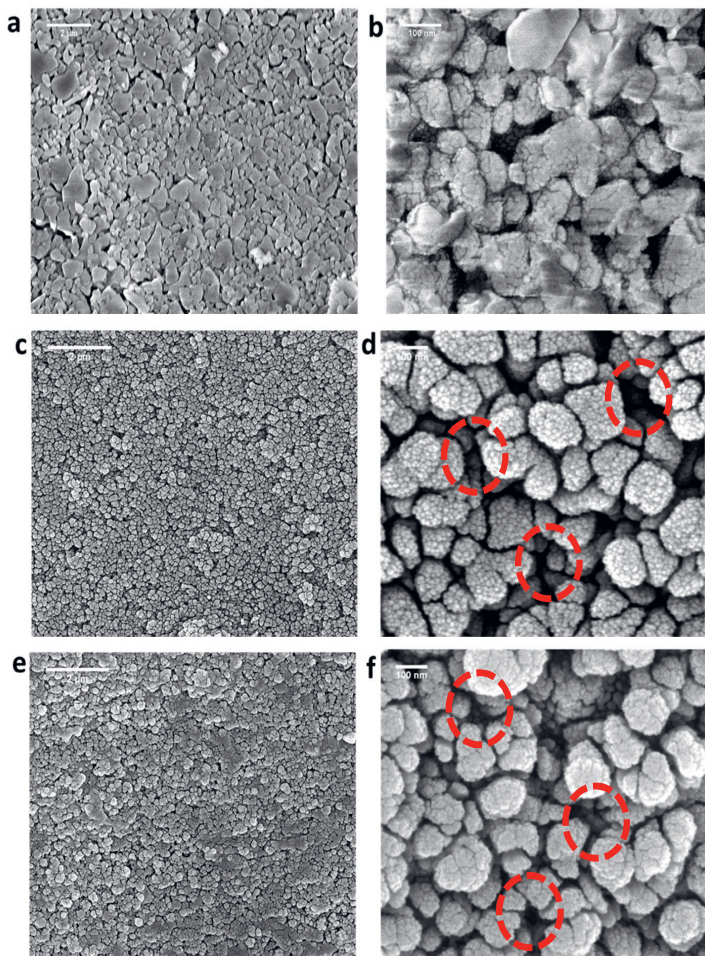


Figure 3.3. Surface morphology analysis by SEM of (a-b) pristine alumina membrane; (c-d) SiC-7 membrane; and (e-f) SiC-8 membrane. Red circles highlight the difference in porosities.

XPS was performed to study the elemental makeup of the SiC coated membranes' surface. Fig. 3.4a-b presents the Si  $2p$  XPS spectra of the SiC-7 and SiC-8 membranes. In both cases, the Si  $2p$  peaks were deconvoluted into four peaks, confirming the presence of Si both in the form of oxides ( $\text{SiO}_x$ ) and carbides ( $\text{SiC}_x$ ) [38, 39]. The presence of the Si-C4 peak at a binding energy of  $\sim 99.5$  in Fig. 3.4a, and the presence of the Si-C4 peak at binding energy of  $\sim 99.6$  in Fig. 3.4b confirm

the coating of SiC by LP-CVD [40]. The presence of Si-C3-O, Si-C2-O2/Si-C-O3, and Si-O4 suggest that the SiC is of amorphous nature.

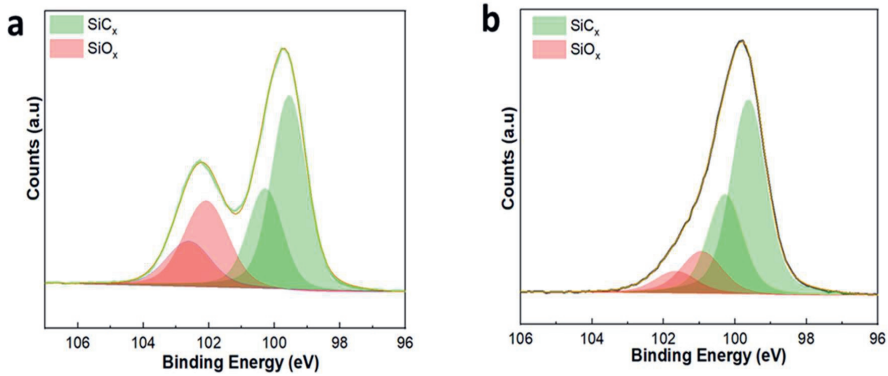


Figure 3.4. XP-spectra of (a) SiC-7 membrane; (b) SiC-8 membrane.

The morphological transformation of the cross-section of the membranes after SiC coating by LP-CVD was further studied by SEM-EDX. The pristine  $\text{Al}_2\text{O}_3$  membrane had an  $\text{Al}_2\text{O}_3$  separation layer of ca.  $15\mu\text{m}$  in thickness, and it had a granular appearance (Fig. 3.5a). After the coating of SiC at  $750^\circ\text{C}$ , huge deposits of nodular SiC can be observed on the surface of the membrane (Fig. 3.5b). Additionally, random deposits of SiC were also observed along the cross-section of the membrane. Since ceramic material has two types of pores: (i) open pores, which are accessible to precursors; and (ii) closed pores, which are not accessible to precursors [41], the occurrence of haphazard deposits of SiC along the cross-section of the membrane, deposited at  $750^\circ\text{C}$ , can be explained. However, as shown in Fig. 3.5c, the coating of SiC at  $860^\circ\text{C}$  resulted in the formation of a thin SiC coating at the surface of the membrane, and deposits of SiC were also observed at the sub-surface ( $3\text{-}6\mu\text{m}$ ) of the membrane. Furthermore, Si deposits were observed by EDX only until the cross-sectional depth of  $9\mu\text{m}$  for both SiC-7 and SiC-8 (Fig. 3.5d). So, it is concluded that the SiC coating did not completely coat the previous  $\text{Al}_2\text{O}_3$  selective layer of ca.  $15\mu\text{m}$  in thickness.

In fact, the effective thickness of SiC coated Al<sub>2</sub>O<sub>3</sub> selective layer in both cases is ca. 9 μm. Additionally, the difference in cross-sectional morphology of SiC-7 and SiC-8 membranes can be explained by the difference in deposition conditions. At 750°C, the high pressure and high concentration of the precursor gases probably led to a decrease of the mean free path of the precursor gases [42]. Therefore, the deposition proceeded via both gas phase reactions of the precursors; and reactions of the adsorbed precursors at the surface of the membrane [43], which is confirmed by the high atomic percentage of Si on the surface of the membrane in the Fig. 3.5d. At 860°C, the pressure and concentration of precursor gases was relatively low, which only led to the deposition of a dense SiC via reactions of adsorbed precursors on the surface of the membrane. Different pressures were chosen at the two respective coating temperatures in order to elucidate the effect of pressure on the penetration depth of precursors. However, it can be seen in Fig. 3.5d that the chamber pressure did not affect the penetration depth of precursors.

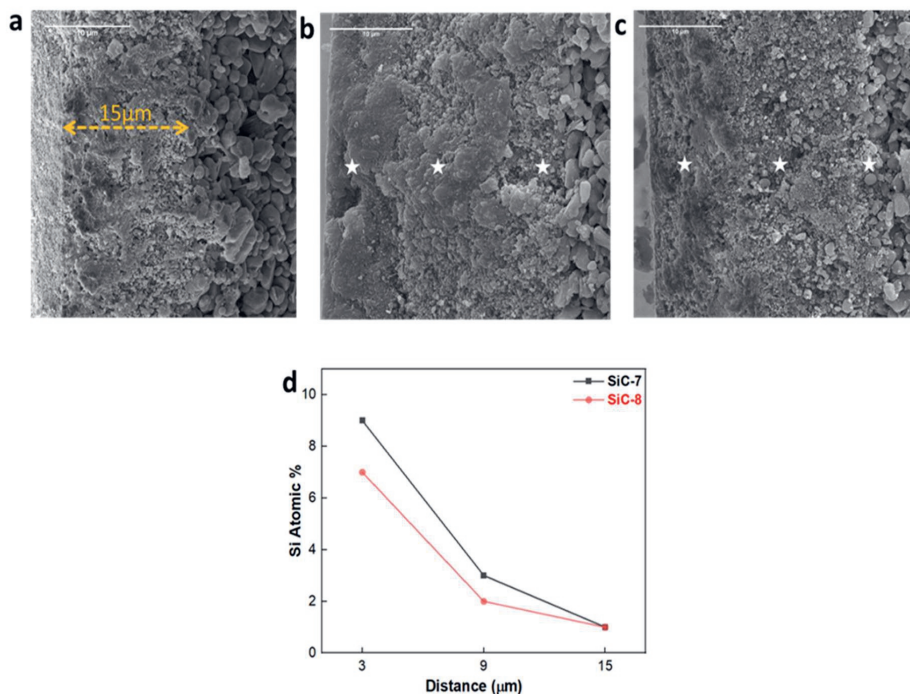


Figure 3.5. SEM cross-sectional images of (a) pristine membrane; (b) SiC-7 membrane; (c) SiC-8 membrane; and (d) EDX spectra. Stars represent the points where EDX spectra was taken.

### 3.3.2 Effect of SiC LP-CVD & NaClO Ageing on Membrane Permeability and Pore Size

PWP of the pristine, SiC-7/SiC-7-2A, and SiC-8/SiC-8-2A was measured and the results are shown in Fig. 3.6. The PWP of the pristine alumina membranes was ca.  $350 \text{ L.m}^{-2}.\text{h}^{-1}.\text{bar}^{-1}$ , while for the SiC-7 membrane, it dropped to  $200 \text{ L.m}^{-2}.\text{h}^{-1}.\text{bar}^{-1}$ . Increasing the SiC coating temperature to  $860^\circ\text{C}$  led to a significant reduction of the PWP of the SiC-8 membrane to  $128 \text{ L.m}^{-2}.\text{h}^{-1}.\text{bar}^{-1}$ . The difference between SiC-7 and SiC-8 membranes can be explained by the difference in morphology of the SiC, as described earlier.

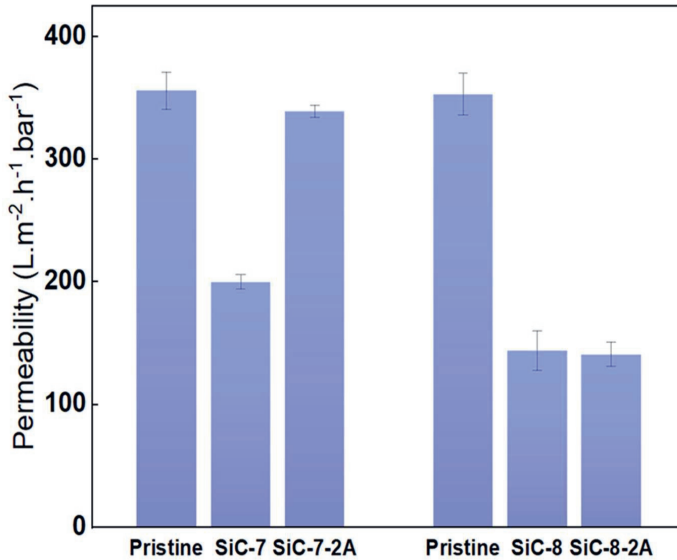


Figure 3.6. Pure water permeability of Pristine; SiC-7; SiC-8; SiC-7-2A; and SiC-8-2A membranes.

Alam et al. concluded in their study that in contrast to a smooth surface, a rough surface has a higher specific surface area. As a consequence, more surface sites will be available for the water molecules and thus PWP will be higher [44], which is consistent with our findings. Ageing in 5% NaClO for 200h had different effects on the PWP of both membranes. The PWP of SiC-7-2A membrane increased to ca. 339 L.m<sup>-2</sup>.h<sup>-1</sup>.bar<sup>-1</sup>, and the membrane changed its appearance from black to off-white after ageing, indicating that the SiC was deteriorated (Fig. S3.1). In contrast, the PWP of the SiC-8-2A membrane was unaffected by NaClO ageing.

Pore size measurements were conducted to obtain insights in the pore size distribution of the membranes after SiC coating and NaClO ageing (Fig. 3.7). The actual mean pore size of the pristine membrane was determined to be 42 nm, which differed greatly from the suppliers' claimed pore size of 100 nm. The pristine membrane had a broad pore size distribution with the smallest

pores of ca. 26nm and the largest pores of ca. 98 nm. The mean pore size dropped to ca. 30 nm for the SiC-7 membrane, and it was reduced to ca. 27 nm for the SiC-8 membrane. The difference in pore size confirms the difference in PWP. After ageing, the mean pore size of SiC-7-2A membrane increased to ca. 37 nm, which is in accordance with the SEM images, showing the deterioration of the SiC coating. In contrast, the mean pore size of SiC-8-2A membrane was unaffected by ageing, confirming the chemical robustness of the SiC-8 membrane in NaClO.

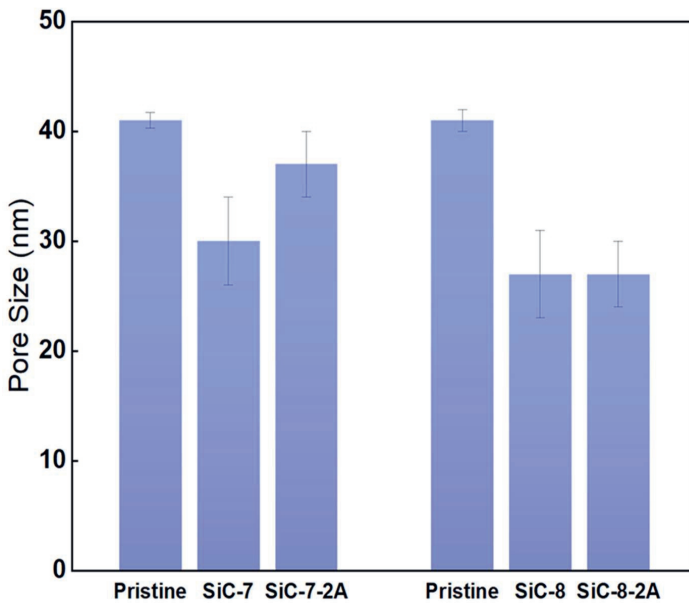


Figure 3.7. Pore size measurements of Pristine; SiC-7; SiC-8; SiC-7-2A; and SiC-8-2A membranes.

### 3.3.3 Morphological and Chemical Post-mortem analysis of NaClO Aged SiC Coated Membranes

The effects of NaClO ageing on the surface and cross-sectional morphology of the SiC coated membranes were also studied by SEM. SEM images of SiC-7-2A and SiC-8-2A membranes are presented in Fig. 3.8a-f. It can be observed from Fig. 3.8a that the SiC nodules on the surface and



random deposits of SiC along the cross-section of SiC-7-2A were removed by the exposure to NaClO. The removal of the SiC coating led to the increase in porosity and pore size of SiC-7-2A (Fig. 3.8b-c). For SiC-8-2A, NaClO exposure had no effect on the SiC coating (Fig. 3.8d-f). These results confirm the stability of SiC coating deposited at a high-temperature (860°C) towards harsh oxidizing treatment of NaClO. We speculate that the coating of SiC on the Al<sub>2</sub>O<sub>3</sub> substrate at high-temperature (860°C) and low-pressure (100mTorr) led to the formation of an adhesive and continuous SiC coating [45]. Therefore, the <sup>-</sup>OCl species could not corrode the SiC coating. Whereas, SiC deposition at low-temperature (750°C) and high-pressure (600mTorr) led to formation of porous and amorphous SiC nodules. Consequentially, the <sup>-</sup>OCl species completely corroded the SiC coating. However, further research is warranted to provide a comprehensive understanding of the mechanisms underlying deterioration.

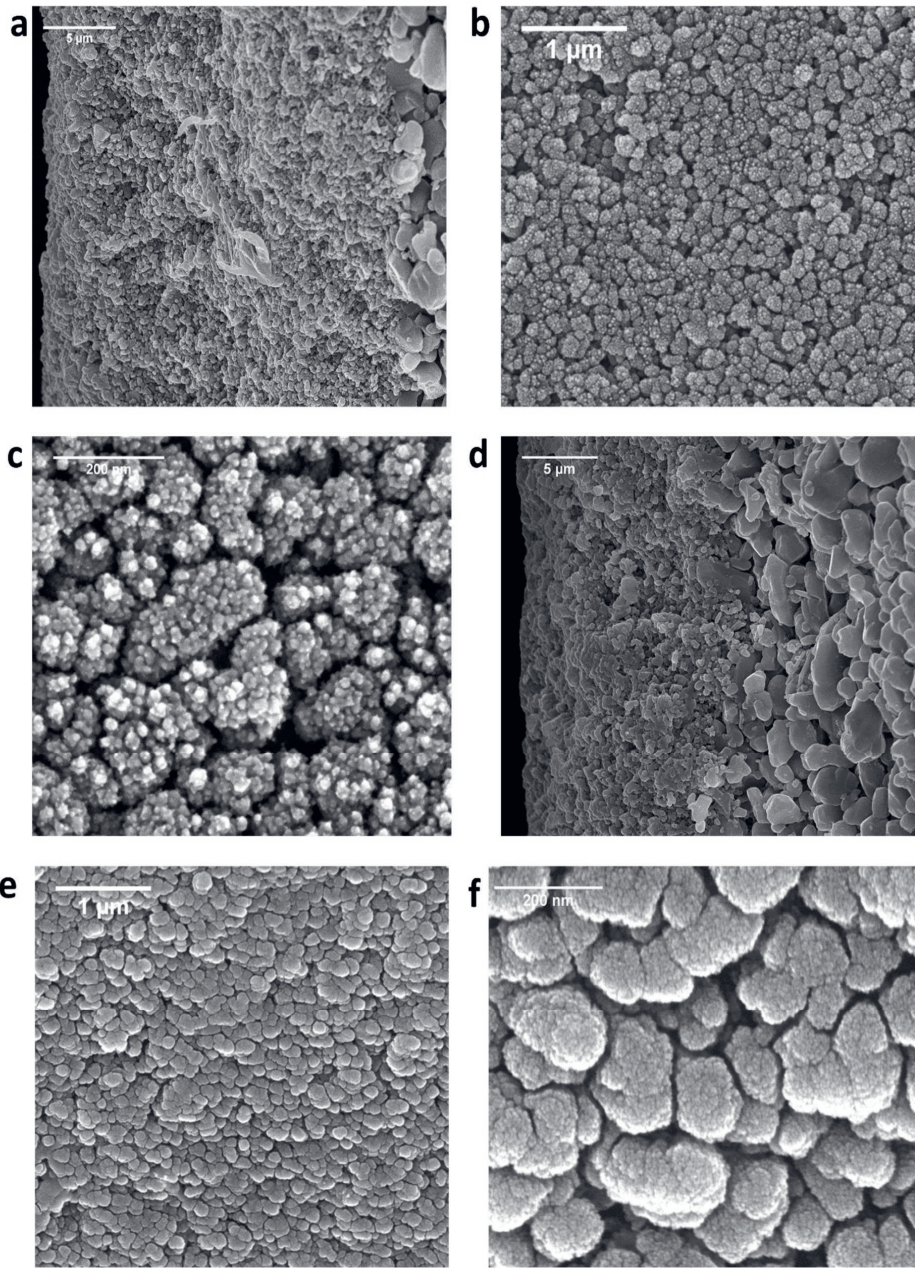


Figure 3.8. SEM cross-sectional images of (a) SiC-7-2A membrane; and (d) SiC-8-2A membrane. SEM surface images of (b-c) SiC-7-2A membrane; and (e-f) SiC-8-2A membrane.

Al  $2p$  spectra of unaged and aged membranes were also analyzed, and the percentage atomic concentration (at.%) of  $\text{Al}^{3+}$  was calculated by the area under the peaks to gain insights about the surface composition of the membranes (Fig. 3.9). For the SiC-7 membrane, the at.% of  $\text{Al}^{3+}$  was 0.79 (Fig. 3.9a). However, after NaClO ageing, the at.% of  $\text{Al}^{3+}$  in SiC-7-2A membrane increased to 17 (Fig 3.9b). This confirms that the SiC coating was removed, and the surface now consisted of  $\text{Al}_2\text{O}_3$  particles. These results are consistent with the SEM results (Fig. 3.8). For the SiC-8 and SiC-8-2A membranes, the at.% of  $\text{Al}^{3+}$  was 2.34 and 1.68 respectively, which shows that the  $\text{Al}_2\text{O}_3$  particles were still shielded by a SiC coating even after ageing in NaClO (Fig. 3.9c-d).

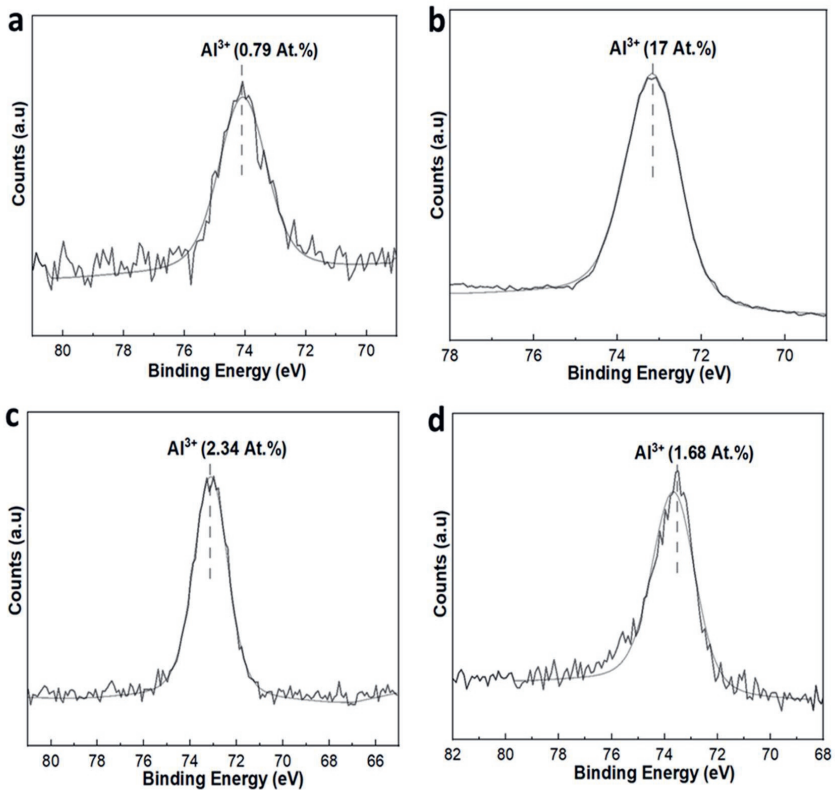


Figure 3.9. XPS spectra of SiC-7 and SiC-7-2A membranes (a-b); SiC-8 and SiC-8-2A membranes (c-d).

### 3.4 Conclusion

SiC coated UF membranes were prepared under two different deposition conditions by LP-CVD. Subsequently, simulated long-term ageing of the SiC membranes was performed in NaClO to elucidate the effect of ageing on the properties and performance of the membranes.

SEM images of pristine and coated membranes show that a SiC coated  $\text{Al}_2\text{O}_3$  selective layer was formed after deposition. Under relatively high-temperature deposition conditions, a continuous and adhesive SiC coating was obtained. Whereas, under relatively low-temperature deposition conditions, SiC deposited in the form of amorphous nodules. PWP and pore size measurements revealed that the SiC deposition at high-temperature led to the formation of a robust SiC coating which was stable in NaClO for 200h. Additionally, XPS results demonstrated that SiC coating performed at low-temperature was removed after 200h of NaClO exposure.

Although further study will be required to elucidate the underlying mechanism on why the high temperature LP-CVD conditions lead to continuous, highly adhesive, and stable SiC coating; it is expected that the findings in this study possess significant implications for preparation of SiC coated UF membranes, and could be an alternative to full SiC UF membranes.

### 3.5 Supplementary information

1. Thickness of SiC coating on Si wafers at different deposition conditions measured by ellipsometry.

---

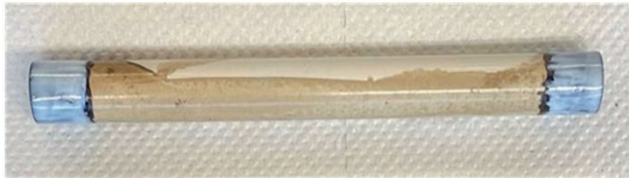
S.No.	Temperature (°C)	Pressure (mTorr)	Time (mins)	SiC Thickness (nm)
1.	750	600	60	16
2.	860	100	30	16

---

Table S3.1. SiC coating thickness as a function of different deposition conditions.

2. SiC-7-2A and SiC-8-2A membranes post-ageing.

#### SiC-7-2A



#### SiC-8-2A



Figure S3.1. SiC coated membranes after ageing in NaClO for 200hrs.

## References

- [1] M.C. Fraga, S. Sanches, J.G. Crespo, V.J. Pereira, Assessment of a New Silicon Carbide Tubular Honeycomb Membrane for Treatment of Olive Mill Wastewaters, *Membranes (Basel)* 7(1) (2017).
- [2] S. Karimzadeh, B. Safaei, T.-C. Jen, P.O. Oviroh, Enhanced removal efficiency of heavy metal ions from wastewater through functionalized silicon carbide membrane: A theoretical study, *Journal of Water Process Engineering* 44 (2021).
- [3] T. Lanjewar, P. Badwaik, M.N. Varma, Removal of water from the spent mixture of nitric-sulfuric acid by using silicon carbide ceramic diffusive membrane, *Separation and Purification Technology* 265 (2021).
- [4] M.C. Fraga, S. Sanches, V.J. Pereira, J.G. Crespo, L. Yuan, J. Marcher, M.V.M. de Yuso, E. Rodríguez-Castellón, J. Benavente, Morphological, chemical surface and filtration characterization of a new silicon carbide membrane, *Journal of the European Ceramic Society* 37(3) (2017) 899-905.
- [5] D. Das, S. Baitalik, B. Haldar, R. Saha, N. Kayal, Preparation and characterization of macroporous SiC ceramic membrane for treatment of waste water, *Journal of Porous Materials* 25(4) (2017) 1183-1193.
- [6] D. Das, N. Kayal, G.A. Marsola, L.A. Damasceno, M.D.d.M. Innocentini, Permeability behavior of silicon carbide-based membrane and performance study for oily wastewater treatment, *International Journal of Applied Ceramic Technology* 17(3) (2020) 893-906.
- [7] S. Nejati, S.A. Mirbagheri, D.M. Warsinger, M. Fazeli, Biofouling in seawater reverse osmosis (SWRO): Impact of module geometry and mitigation with ultrafiltration, *Journal of Water Process Engineering* 29 (2019).
- [8] R. Neufert, M. Moeller, A.K. Bakshi, Dead-End Silicon Carbide Micro-Filters for Liquid Filtration, *Advances in Bioceramics and Porous Ceramics VI2013*, pp. 113-125.
- [9] B. Elyassi, M. Sahimi, T.T. Tsotsis, Silicon carbide membranes for gas separation applications, *Journal of Membrane Science* 288(1) (2007) 290-297.
- [10] E. Eray, V.M. Candelario, V. Boffa, H. Safafar, D.N. Østedgaard-Munck, N. Zahrtmann, H. Kadrispahic, M.K. Jørgensen, A roadmap for the development and applications of silicon carbide membranes for liquid filtration: Recent advancements, challenges, and perspectives, *Chemical Engineering Journal* 414 (2021) 128826.
- [11] D. Hotza, M. Di Luccio, M. Wilhelm, Y. Iwamoto, S. Bernard, J.C. Diniz da Costa, Silicon carbide filters and porous membranes: A review of processing, properties, performance and application, *Journal of Membrane Science* 610 (2020) 118193.
- [12] M.-h. Huang, Y.-m. Li, G.-w. Gu, Chemical composition of organic matters in domestic wastewater, *Desalination* 262(1) (2010) 36-42.
- [13] G. Jungclaus, V. Avila, R. Hites, Organic compounds in an industrial wastewater: a case study of their environmental impact, *Environmental science & technology* 12(1) (1978) 88-96.
- [14] M. Chen, S.G.J. Heijman, M.W.J. Luiten-Olieman, L.C. Rietveld, Oil-in-water emulsion separation: Fouling of alumina membranes with and without a silicon carbide deposition in constant flux filtration mode, *Water Research* 216 (2022) 118267.
- [15] B. Hofs, J. Ogier, D. Vries, E.F. Beerendonk, E.R. Cornelissen, Comparison of ceramic and polymeric membrane permeability and fouling using surface water, *Separation and Purification Technology* 79(3) (2011) 365-374.



- [16] L. Jin, S.L. Ong, H.Y. Ng, Comparison of fouling characteristics in different pore-sized submerged ceramic membrane bioreactors, *Water research* 44(20) (2010) 5907-5918.
- [17] E. Eray, V.M. Candelario, V. Boffa, Ceramic Processing of Silicon Carbide Membranes with the Aid of Aluminum Nitrate Nonahydrate: Preparation, Characterization, and Performance, *Membranes (Basel)* 11(9) (2021).
- [18] F.C. Kramer, R. Shang, S.M. Scherrenberg, L.C. Rietveld, S.J.G. Heijman, Quantifying defects in ceramic tight ultra- and nanofiltration membranes and investigating their robustness, *Separation and Purification Technology* 219 (2019) 159-168.
- [19] B. Malczewska, A. Zak, Structural Changes and Operational Deterioration of the Uf Polyethersulfone (Pes) Membrane Due to Chemical Cleaning, *Sci Rep* 9(1) (2019) 422.
- [20] H. Susanto, M. Ulbricht, Characteristics, performance and stability of polyethersulfone ultrafiltration membranes prepared by phase separation method using different macromolecular additives, *Journal of Membrane Science* 327(1) (2009) 125-135.
- [21] Y. Kourde-Hanafi, P. Loulergue, A. Szymczyk, B. Van der Bruggen, M. Nachtnebel, M. Rabiller-Baudry, J.-L. Audic, P. Pölt, K. Baddari, Influence of PVP content on degradation of PES/PVP membranes: Insights from characterization of membranes with controlled composition, *Journal of Membrane Science* 533 (2017) 261-269.
- [22] R. Prulho, S. Therias, A. Rivaton, J.-L. Gardette, Ageing of polyethersulfone/polyvinylpyrrolidone blends in contact with bleach water, *Polymer Degradation and Stability* 98(6) (2013) 1164-1172.
- [23] K. Li, Q. Su, S. Li, G. Wen, T. Huang, Aging of PVDF and PES ultrafiltration membranes by sodium hypochlorite: Effect of solution pH, *J Environ Sci (China)* 104 (2021) 444-455.
- [24] S. Fukuzaki, Mechanisms of Actions of Sodium Hypochlorite in Cleaning and Disinfection Processes, *Biocontrol Science* 11(4) (2006) 147-157.
- [25] M. Luna-Trujillo, R. Palma-Goyes, J. Vazquez-Arenas, A. Manzo-Robledo, Formation of active chlorine species involving the higher oxide  $\text{MO}_{x+1}$  on active Ti/RuO<sub>2</sub>-IrO<sub>2</sub> anodes: A DEMS analysis, *Journal of Electroanalytical Chemistry* 878 (2020).
- [26] G. Dibrov, G. Kagramanov, V. Sudin, E. Grushevenko, A. Yushkin, A. Volkov, Influence of sodium hypochlorite treatment on pore size distribution of polysulfone/polyvinylpyrrolidone membranes, *Membranes* 10(11) (2020) 356.
- [27] J. Ding, S. Wang, P. Xie, Y. Zou, Y. Wan, Y. Chen, M.R. Wiesner, Chemical cleaning of algae-fouled ultrafiltration (UF) membrane by sodium hypochlorite (NaClO): characterization of membrane and formation of halogenated by-products, *Journal of Membrane Science* 598 (2020) 117662.
- [28] Y. Zhang, J. Wang, F. Gao, H. Tao, Y. Chen, H. Zhang, Impact of sodium hypochlorite (NaClO) on polysulfone (PSF) ultrafiltration membranes: The evolution of membrane performance and fouling behavior, *Separation and Purification Technology* 175 (2017) 238-247.
- [29] M. Chen, R. Shang, P.M. Sberna, M.W.J. Luiten-Olieman, L.C. Rietveld, S.G.J. Heijman, Highly permeable silicon carbide-alumina ultrafiltration membranes for oil-in-water filtration produced with low-pressure chemical vapor deposition, *Separation and Purification Technology* 253 (2020) 117496.
- [30] B. Morana, G. Pandraud, J.F. Creemer, P.M. Sarro, Characterization of LPCVD amorphous silicon carbide (a-SiC) as material for electron transparent windows, *Materials Chemistry and Physics* 139(2) (2013) 654-662.
- [31] R. Shang, F. Vuong, J. Hu, S. Li, A.J.B. Kemperman, K. Nijmeijer, E.R. Cornelissen, S.G.J. Heijman, L.C. Rietveld, Hydraulically irreversible fouling on ceramic MF/UF membranes:

Comparison of fouling indices, foulant composition and irreversible pore narrowing, *Separation and Purification Technology* 147 (2015) 303-310.

[32] A.S. Racz, Z. Kerner, A. Nemeth, P. Panjan, L. Peter, A. Sulyok, G. Vertesy, Z. Zolnai, M. Menyhard, Corrosion Resistance of Nanosized Silicon Carbide-Rich Composite Coatings Produced by Noble Gas Ion Mixing, *ACS Applied Materials & Interfaces* 9(51) (2017) 44892-44899.

[33] J.E. Greene, Chapter 12 - Thin Film Nucleation, Growth, and Microstructural Evolution: An Atomic Scale View, in: P.M. Martin (Ed.), *Handbook of Deposition Technologies for Films and Coatings* (Third Edition), William Andrew Publishing, Boston, 2010, pp. 554-620.

[34] D.W. Pashley, M.J. Stowell, Nucleation and Growth of Thin Films as Observed in the Electron Microscope, *Journal of Vacuum Science and Technology* 3(3) (1966) 156-166.

[35] D.W. Pashley, M.J. Stowell, M.H. Jacobs, T.J. Law, The growth and structure of gold and silver deposits formed by evaporation inside an electron microscope, *Philosophical Magazine* 10(103) (1964) 127-158.

[36] J.-O. Carlsson, P.M. Martin, Chapter 7 - Chemical Vapor Deposition, in: P.M. Martin (Ed.), *Handbook of Deposition Technologies for Films and Coatings* (Third Edition), William Andrew Publishing, Boston, 2010, pp. 314-363.

[37] Q. You, J. Xiong, Z. Guo, J. Liu, T.e. Yang, C. Qin, Microstructure and properties of CVD coated Ti(C, N)-based cermets with varying WC additions, *International Journal of Refractory Metals and Hard Materials* 81 (2019) 299-306.

[38] E. Eray, V. Boffa, M.K. Jørgensen, G. Magnacca, V.M. Candelario, Enhanced fabrication of silicon carbide membranes for wastewater treatment: From laboratory to industrial scale, *Journal of Membrane Science* 606 (2020).

[39] R. Hashimoto, A. Ito, T. Goto, Effect of deposition atmosphere on the phase composition and microstructure of silicon carbide films prepared by laser chemical vapour deposition, *Ceramics International* 41(5) (2015) 6898-6904.

[40] J. Chastain, R.C. King Jr, *Handbook of X-ray photoelectron spectroscopy*, Perkin-Elmer Corporation 40 (1992) 221.

[41] Q. You, Y. Liu, J. Wan, Z. Shen, H. Li, B. Yuan, L. Cheng, G. Wang, Microstructure and properties of porous SiC ceramics by LPCVI technique regulation, *Ceramics International* 43(15) (2017) 11855-11863.

[42] A.I. Labropoulos, C.P. Athanasekou, N.K. Kakizis, A.A. Sapalidis, G.I. Pilatos, G.E. Romanos, N.K. Kanellopoulos, Experimental investigation of the transport mechanism of several gases during the CVD post-treatment of nanoporous membranes, *Chemical Engineering Journal* 255 (2014) 377-393.

[43] C.-F. Wang, D.-S. Tsai, Low pressure chemical vapor deposition of silicon carbide from dichlorosilane and acetylene, *Materials chemistry and physics* 63(3) (2000) 196-201.

[44] J. Alam, M. Alhoshan, L.A. Dass, A.K. Shukla, M. Muthumareeswaran, M. Hussain, A.S. Aldwayyan, Atomic layer deposition of TiO<sub>2</sub> film on a polyethersulfone membrane: separation applications, *Journal of Polymer Research* 23(9) (2016) 1-9.

[45] B.-K. Sea, K. Ando, K. Kusakabe, S. Morooka, Separation of hydrogen from steam using a SiC-based membrane formed by chemical vapor deposition of triisopropylsilane, *Journal of Membrane Science* 146(1) (1998) 73-82.



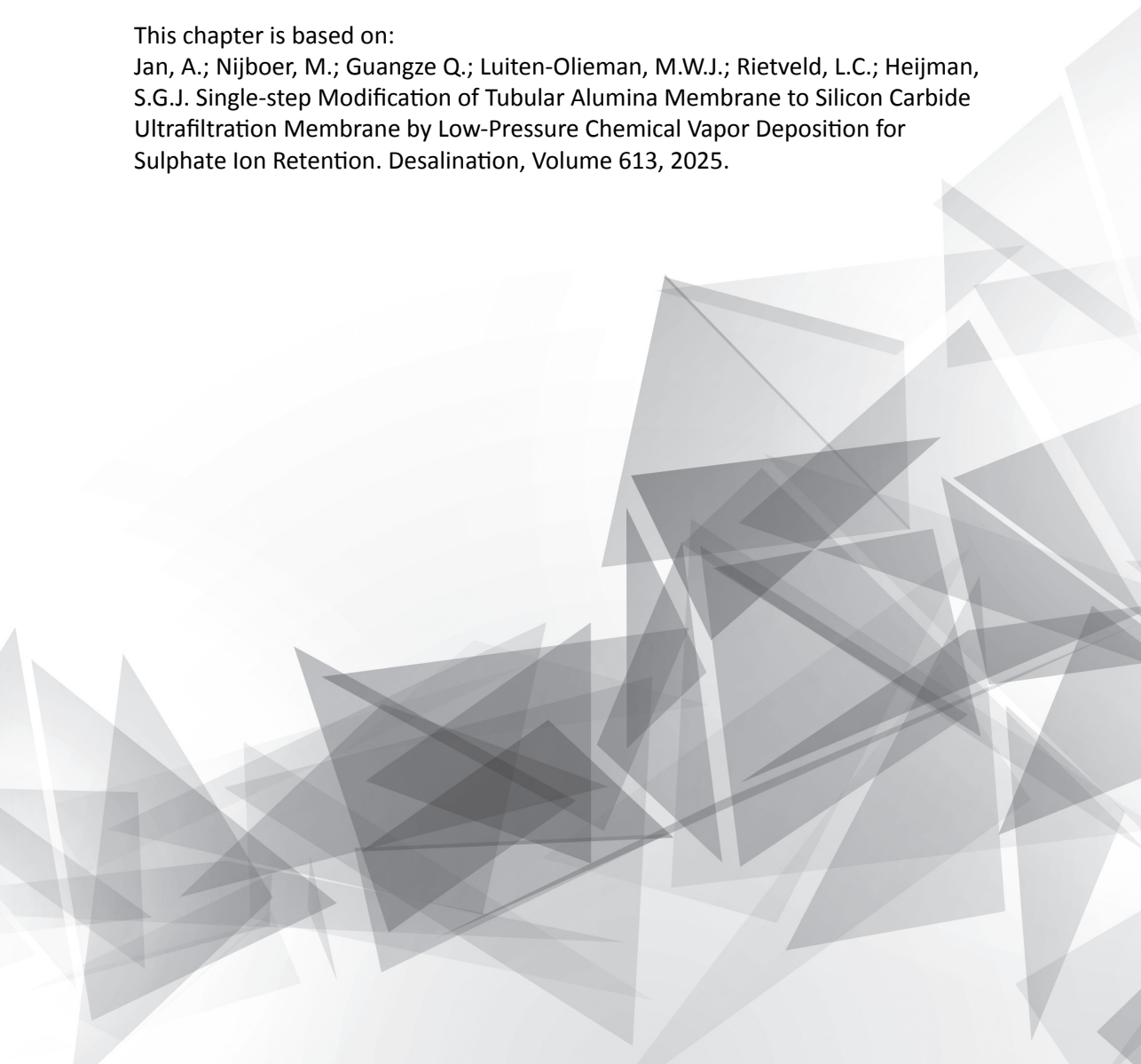


# Chapter 4

Single-step modification of tubular alumina membrane to silicon carbide tight-ultrafiltration membrane by low-pressure chemical vapor deposition for sulphate ion retention

This chapter is based on:

Jan, A.; Nijboer, M.; Guangze Q.; Luiten-Olieman, M.W.J.; Rietveld, L.C.; Heijman, S.G.J. Single-step Modification of Tubular Alumina Membrane to Silicon Carbide Ultrafiltration Membrane by Low-Pressure Chemical Vapor Deposition for Sulphate Ion Retention. *Desalination*, Volume 613, 2025.



## **Chapter 4 Single-step modification of tubular alumina membrane to silicon carbide tight-ultrafiltration membrane by low-pressure chemical vapor deposition for sulphate ion retention**

### **Abstract**

Sulphate ( $\text{SO}_4^{2-}$ ) is a model ion due to its negative charge and multivalent nature. Its rejection behavior serves as an indicator of the separation performance for other analogous ions in modified membranes. In literature the rejection of the  $\text{SO}_4^{2-}$  by negatively charged polymeric NF membranes has been studied extensively with rejection percentages of more than 90%. SiC membranes have gained attention for (waste)water treatment due to their high hydrophilicity and negative charge. However, no negatively charged ceramic UF membranes have been tested yet for  $\text{SO}_4^{2-}$  retention. In this study, a commercial  $\text{Al}_2\text{O}_3$  UF membrane was converted into a highly negatively charged UF membrane by coating it with SiC. This was achieved by depositing a  $5\mu\text{m}$  SiC coating in a single-step via LP-CVD. LP-CVD facilitates preparation of a SiC layer at much lower temperatures ( $700\text{-}900^\circ\text{C}$ ) compared to the sol-gel methods (ca.  $2100^\circ\text{C}$ ), and it does not require multiple coating cycles and sintering steps to achieve the desired pore size. Subsequently, properties and performance of the as-prepared UF membrane coated with SiC were evaluated. The SiC coated membrane had a highly negative charge of  $-70\text{ mV}$  at pH of 6, and a permeance of  $26\text{ L}\cdot\text{m}^{-2}\cdot\text{h}^{-1}\cdot\text{bar}^{-1}$ . Further, the SiC coated membrane demonstrated a  $\text{SO}_4^{2-}$  rejection of 79% despite of having a large pore size of  $7\text{ nm}$ , in comparison with the pore sizes of below  $1\text{ nm}$  of NF membranes. These results highlight the potential of single-step LP-CVD modification of commercial UF ceramic membranes to produce highly negatively charged SiC coated UF membranes with a high  $\text{SO}_4^{2-}$  rejection, and without a large loss of permeance normally associated

with NF membranes. Also backwashing of the ultrafiltration membrane is still possible which is an advantage in dealing with cake layer fouling.

## 4.1 Introduction

Industries, such as mining, and for textiles', steel and pharmaceuticals' manufacturing, produce significant quantities of wastewater [1]. These effluents contain elevated levels of various contaminants, including  $\text{Na}_2\text{SO}_4$  and sodium chloride ( $\text{NaCl}$ ) [2]. The removal of  $\text{SO}_4^{2-}$  ions from these (waste)waters is essential to avoid environmental pollution and health hazards [3].

Membrane technology has emerged as a promising approach for (waste)water treatment, offering the capability to separate pollutants from mixtures, maintain a high-quality permeate, and reduce operational costs [4-6]. While polymeric reverse osmosis (RO) and NF membranes have extensively been studied and offer  $\text{SO}_4^{2-}$  rejection [7, 8], they cannot be backwashed, rendering them particularly prone to fouling. Consequently, feed waters for RO and NF systems require rigorous pretreatment to remove particulates and foulants, thereby preserving membrane performance. Additionally, they are plagued by limitations such as low mechanical strength, temperature sensitivity, low flux, fouling, chemical vulnerability, and susceptibility to degradation upon chemical cleaning [9-13]. Conversely, ceramic membranes offer superior characteristics including high mechanical strength, low fouling, and stability against temperature and chemicals [14, 15] and UF-membranes can be backwashed.

The rejection mechanism of  $\text{SO}_4^{2-}$  by membranes can involve size exclusion (steric exclusion), charge exclusion (Donnan exclusion), or a combination of both [16, 17]. Steric exclusion occurs when the membranes' pore diameter is smaller than that of the hydrated  $\text{SO}_4^{2-}$  ion diameter, whereas Donnan exclusion arises from electrostatic repulsion between the membrane's surface (meaning that the surface is negatively charged) and the negatively charged  $\text{SO}_4^{2-}$  ion.

Wadkar et al. explored the  $\text{SO}_4^{2-}$  rejection mechanisms of commercially available fully-aromatic PA and semi-aromatic poly(piperazine (PP), polymeric NF membranes [18]. Their findings

revealed that  $\text{SO}_4^{2-}$  rejection percentages exceeded 98%, with different mechanisms predominating in the various membrane types. The semi-aromatic PP NF membranes exhibited rejection primarily via steric exclusion, while other membranes performed through a combination of steric and Donnan exclusion mechanisms. Chong et al. modified tubular  $\text{Al}_2\text{O}_3$  MF membranes into positively charged PA NF membranes through interfacial polymerization. In their study, a  $\text{SO}_4^{2-}$  rejection of only 65% was observed, however, a detailed mechanistic explanation was not reported, while steric exclusion was suspected to play a role [19]. The positive charge of the membrane surface may have contributed to the observed low rejection, although further investigation may be required to confirm this.

As an alternative for the above mentioned polymeric membranes, Chen et al. tested the  $\text{SO}_4^{2-}$  rejection of a ceramic multi-channel tubular titania ( $\text{TiO}_2$ ) NF membrane [20]. The pore size of the membrane was reported to be 1.5 nm. The membrane had a low  $\text{SO}_4^{2-}$  ion rejection of 39%, and the rejection was attributed to both steric and Donnan exclusion. In a similar study, Cha et al. measured the  $\text{SO}_4^{2-}$  rejection of a commercially available  $\text{TiO}_2$  NF membrane with a pore size of 0.9 nm, being ca. 60% [21]. Although, the pore size of the membrane was close to the hydrated radius of the  $\text{SO}_4^{2-}$ , it was proposed that the Donnan exclusion was responsible for the  $\text{SO}_4^{2-}$  rejection. Finally, Van Gestel et al. prepared  $\text{TiO}_2$  NF membranes by using the sol-gel dip coating procedure, and observed a  $\text{SO}_4^{2-}$  rejection of only ca. 40% [22].

While oxide ceramics have received considerable attention [23-25], studies on carbide ceramics, such as SiC, for industrial (waste)water treatment remain limited. SiC membranes, prepared using the conventional sol-gel technique, typically require a high-temperature sintering step (ca. 2100°C) and multiple coating and sintering cycles, making the method costly [26, 27]. In addition, with this method it is difficult to precisely control the pore size and selective layers' chemistry. However,

the intrinsic hydrophilicity, the negative charge of SiC [28], and the low susceptibility to irreversible and reversible fouling [29], present promising attributes for  $\text{SO}_4^{2-}$  rejection, even with pore sizes larger than those typical of NF membranes. LP-CVD offers the advantage of depositing SiC onto the membrane surface or within its pores in a single-step. The thickness of the SiC coating can be controlled by varying the deposition time and structural properties can be controlled by the deposition temperature. Additionally, there is no need for a separate sintering step, which leads to significant reduction in costs [30, 31]. Despite these promising characteristics of LP-CVD to produce SiC coated membranes, to the authors' knowledge, research lacks exploration into SiC coated membrane preparation by LP-CVD with ion rejection properties.

In this context, the present study focuses on the modification of commercially available tubular  $\text{Al}_2\text{O}_3$  UF membranes by depositing a coating of SiC by LP-CVD. This process transforms the  $\text{Al}_2\text{O}_3$  UF membrane into a SiC coated tight-UF membrane with different surface properties and a smaller pore size. The surface chemical composition, cross-sectional morphology, zeta potential, and pore size of the SiC coated membrane were studied. Subsequently, the performance of the SiC coated membrane was tested by measuring for the permeance and  $\text{SO}_4^{2-}$  rejection in both pure water and NaCl salt solution.

## **4.2 Materials and Methods**

### **4.2.1 Materials & Chemical Agents**

Commercial single-channel tubular membranes (CoorsTek, the Netherlands) with a support as well as a selective layer of  $\text{Al}_2\text{O}_3$  were used for LP-CVD of SiC. The membranes had an inner diameter of 7 mm, an outer diameter of 10 mm, and were 10 cm long. As per suppliers' specifications, the mean pore size of the selective and support layers were 20 nm and 600 nm respectively. The SiC coated tubular  $\text{Al}_2\text{O}_3$  membranes were used for permeance, pore size, SEM, and  $\text{SO}_4^{2-}$  rejection

measurements. Flat sheet  $\text{Al}_2\text{O}_3$  membranes (Inopor, Germany), coated with SiC under identical LP-CVD conditions, were used for zeta potential and transmission electron microscopy (TEM). The flat sheet  $\text{Al}_2\text{O}_3$  membranes had a nominal pore size of 100 nm, a rectangular geometry of 1 cm x 2 cm, and a thickness of 1 mm.

#### 4.2.2 Low-Pressure Chemical Vapor Deposition

A hot-wall LP-CVD furnace (Tempress Systems BV, The Netherlands) was used for the deposition of SiC coating on the  $\text{Al}_2\text{O}_3$  membrane, as described by Morana et al. [32]. The precursor  $\text{SiH}_2\text{Cl}_2$  was used as the source of Si, and 5% acetylene  $\text{C}_2\text{H}_2$  in hydrogen  $\text{H}_2$  was used as source of C. Ultrapure  $\text{N}_2$  from a liquid  $\text{N}_2$  source was employed as purging gas in the system. SiC deposition was carried out at a temperature of  $860^\circ\text{C}$ , a pressure of 100 mTorr, and a deposition time of 40 mins. During SiC deposition, the membranes were placed longitudinally to the flow of the precursor gases.

#### 4.2.3 Membrane Characterization and Performance Evaluation

The morphology of the  $\text{Al}_2\text{O}_3$  and the SiC coated membranes was observed by SEM (FEI Nova NanoSEM 450, USA). An energy dispersive x-ray (EDX) analyzer coupled with SEM was used to determine the Si atomic percentage. Sample preparation for SEM involved breaking the membranes with a hammer to obtain a relatively flat specimen which was afterwards sputter coated with gold to increase sample conductivity to achieve clear images.

The thickness and chemical composition of the SiC coating was studied by FEI cubed titan Cs-corrected 80-300kV TEM. Elemental mapping in scanning transmission electron microscopy (STEM) mode was performed using the super-X in the ChemiSTEM<sup>TM</sup> configuration. In STEM mode, a small electron beam scans the specimen. For each beam position the diffracted electrons are collected on a ring detector, thus forming an annular dark field (ADF) image after the complete



area is scanned. At the same time, an EDX spectrum is collected for each beam position, and elemental maps are obtained.

Pore size measurements were performed by Micromeritics Mercury Intrusion Porosimetry (MIP). In the standard MIP test, mercury is forced to penetrate into the pore system of a specimen by increasing the applied pressure. Assuming that the pores are cylindrical in shape, the correlation between the applied pressure  $P$  (MPa) and the pore diameter  $d$  ( $\mu\text{m}$ ) can then be described by the Washburn equation [33]:

$$d = (-4. \gamma H g. \cos \theta) / P$$

Where  $\gamma_{\text{Hg}}$  (0.48 N/m) is the surface tension of the mercury [34];  $\theta$  ( $140^\circ$ ) is the contact angle between mercury and the pore wall [35].

The zeta potential was estimated on the SiC coated  $\text{Al}_2\text{O}_3$  flat-sheet membrane using an electrokinetic analyzer (SurPASS, Anton Paar, Graz, Austria). The instrument measures the streaming current coefficient, and the Helmholtz–Smoluchowski equation was then used for the calculation of the zeta potential of the membrane. The isoelectric point (IEP) was measured in a titration system, encompassing a pH range of 3 to 10.

The Debye length for feed solutions of various ionic strengths was calculated using the following equation [36]:

$$k^{-1} = \left( \frac{\epsilon_0 \epsilon_r k_B T}{2000 N_A e^2 I} \right)$$

Where  $\epsilon_0$  = vacuum permittivity ( $8.85 \times 10^{-12}$  C V<sup>-1</sup> m<sup>-1</sup>),  $\epsilon_r$  = relative permittivity of the background solution (80 for water at 20°C),  $k_B$  = Boltzmann constant ( $1.38 \times 10^{-23}$  JK<sup>-1</sup>); T = absolute temperature (K);  $N_A$  = Avogadro number ( $6.0 \times 10^{23}$  mol<sup>-1</sup>); e = elementary charge ( $1.6 \times 10^{-19}$  C); I = ionic strength (mol L<sup>-1</sup>).

For membrane performance evaluation,  $\text{Na}_2\text{SO}_4$  and  $\text{NaCl}$  salts were purchased from Sigma-Aldrich Chemicals (the Netherlands). Feed solutions of various concentrations were prepared with deionized (DI) water. The permeance and  $\text{SO}_4^{2-}$  ion rejection by the SiC coated membrane was measured under constant flux in an in-house built cross-flow filtration setup for tubular membranes, as described by Jan et al. [30], using DI water and  $\text{NaCl}$  salt solution.

## 4.3 Results and Discussion

### 4.3.1 Structural characteristics of the SiC selective layer

#### 4.3.1.1 Morphological evolution

Surface properties of the pristine  $\text{Al}_2\text{O}_3$  membrane, such as defects and inhomogeneities, can influence the properties and performance of any subsequently deposited coating [37]. And, given that commercially available tubular  $\text{Al}_2\text{O}_3$  membranes are not completely defect-free [38], an  $\text{Al}_2\text{O}_3$  membrane with minimal inhomogeneities was selected for the coating of SiC. To identify such a membrane, the PWP of various  $\text{Al}_2\text{O}_3$  membranes were first measured. Membranes exhibiting similar PWP values, indicative of comparable pore structures and minimal defects, were then chosen for subsequent SiC coating to ensure consistency in performance across the selected membranes. Fig. 4.1(a & c) shows the surface and cross-sectional morphologies of the  $\text{Al}_2\text{O}_3$  membrane. In Fig 4.1c, it can be observed that the  $\text{Al}_2\text{O}_3$  membrane had an asymmetric structure comprising of a macroporous support and mesoporous selective layer with a nominal pore size of 20 nm. However, the actual pore size was measured to be 13 nm by MIP (Fig. S4.1). Additionally, non-homogeneous domains in the form of larger grains and pores can also be observed on the membranes' surface (Fig. 4.1a). In comparison, LP-CVD modification of the  $\text{Al}_2\text{O}_3$  membrane resulted in a homogeneous SiC coating on the former  $\text{Al}_2\text{O}_3$  selective layer of the membrane, see

Fig. 4.1b (also Fig. S4.2). Thus, the SiC coated Al<sub>2</sub>O<sub>3</sub> selective layer could function as the new selective layer.

The permeance of a membrane is dependent on the total resistance of the support and selective layers [16]. It has been reported that the experimental hydraulic resistance of support and selective layer can be much larger than the combined theoretical resistances of the two. The increased resistance is due to the presence of transitional boundary layers at the interface of a macroporous support and a mesoporous/microporous selective layer [39]. Therefore, LP-CVD conditions, i.e. temperature and pressure, must be tuned to accurately control the thickness of the coating so that the interface remains unmodified. Moreover, the growth rate of the coating is not uniform along the axial direction of the LP-CVD furnace. The growth rate at the inlet of the furnace is high and decreases along the length of the furnace [40]. This was validated by our observations as well. The SiC deposition on the Al<sub>2</sub>O<sub>3</sub> membrane at the inlet of the furnace resulted in a gradient SiC coating thickness and SiC coating also penetrated beyond the interface of support and selective layer into the bulk of the material (Fig. S4.3). Therefore, the LP-CVD of SiC was carried out further away from the inlet of the furnace and the resultant SiC coating did not penetrate into the bulk of the support and had a constant thickness across the length of the membrane (Fig. 4.1d). Furthermore, in LP-CVD, the growth of the coating has two main aspects: (a) longitudinal growth; and (b) radial growth [41]. These affect both the selectivity and permeance due to change of the pore size of membrane (pore size measurements will be discussed in the subsequent section). Therefore, to measure the thickness of the SiC coating, i.e. growth in longitudinal direction, a line-scan along the cross-section of the membrane was conducted via SEM-EDX (Fig. S4.4). The SiC coating did penetrate about 5 μm into the Al<sub>2</sub>O<sub>3</sub> selective layer of membrane.

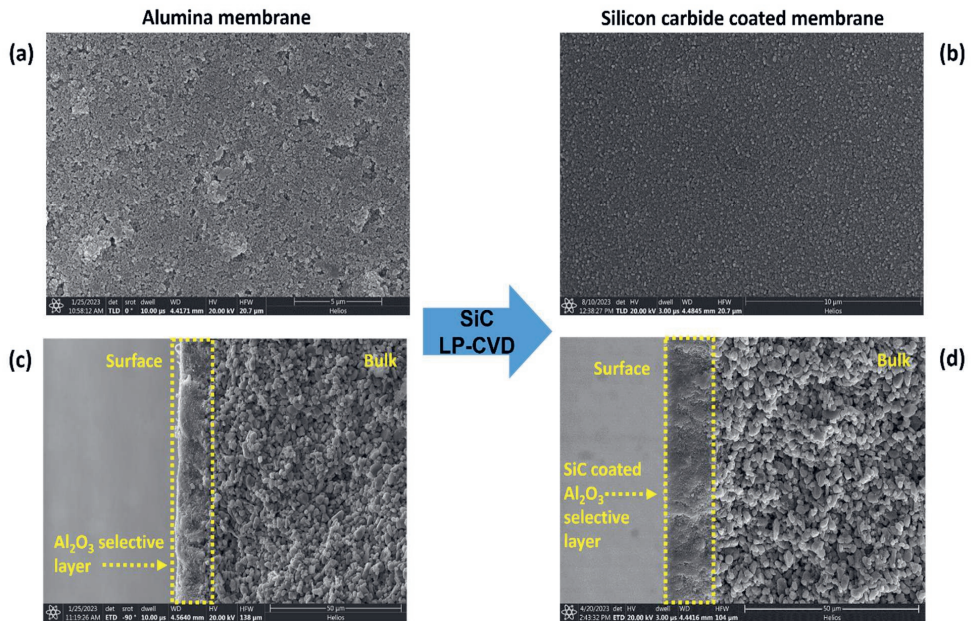


Figure 4.1. Surface morphology of alumina and silicon carbide coated membranes (a-b); cross-sectional morphology of alumina and silicon carbide coated membranes (c-d).

#### 4.3.1.2 Radial growth of SiC coating and effective change in pore size of membrane

The radial growth of the SiC coating was analyzed by TEM and elemental mapping was conducted in the STEM mode to calculate the atomic percentages of Si and C respectively. It can be seen that the  $\text{Al}_2\text{O}_3$  particles were completely shielded by the SiC coating (Fig. 4.2a-d). The radial thickness of the SiC coating was measured to be ca. 12 nm. (Fig. 4.2f). Additionally, the atomic percentages of Si and C were measured at area-1. Area-1 is shown in the marked circle in Fig. 4.2e, and the respective enlarged image is shown in Fig. 4.2f. Both Si and C were present in equal atomic percentages (Fig. 4.2g). Oxygen was also detected in the SiC coating, which can be attributed to the presence of hydroxyl (-OH) groups on the surface. These -OH groups are responsible for the negative charge and hydrophilic properties of SiC coating.

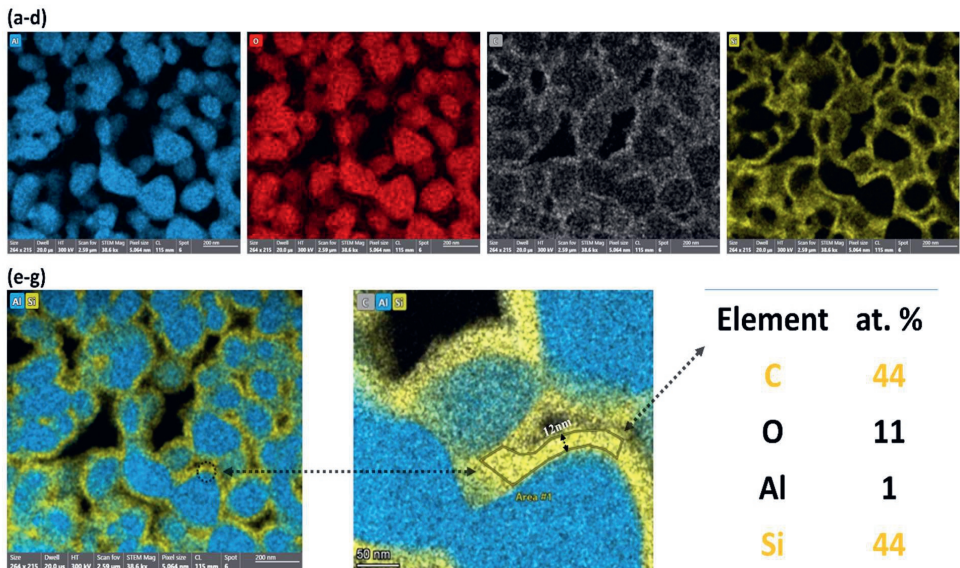


Figure 4.2. STEM elemental mapping of silicon carbide coating (a-f); elemental composition of silicon carbide coating (g).

The pore size of SiC coated membrane, determined via mercury intrusion MIP, is presented in Fig. 4.3. During MIP analysis, mercury initially intrudes the macropores due to the relatively low pressure required for penetration. As shown in Fig. 4.3a, the mean macropore size of the SiC coated membrane was found to be 650 nm. With increasing pressure, mercury progressively intrudes mesopores and micropores until the available pore volume is saturated. However, a limitation of MIP is its reduced sensitivity to the pore size distribution of asymmetric membranes. Specifically, the dominant contribution of the macroporous support layer to the overall intrusion data often masks the influence of the selective layer, which has a significantly lower pore volume [42]. This limitation is evident in the present study, as only a minimal volume of mercury was intruded into the SiC coated  $\text{Al}_2\text{O}_3$  selective layer, resulting in an estimated mean pore size of 7 nm (Fig. 4.3b).

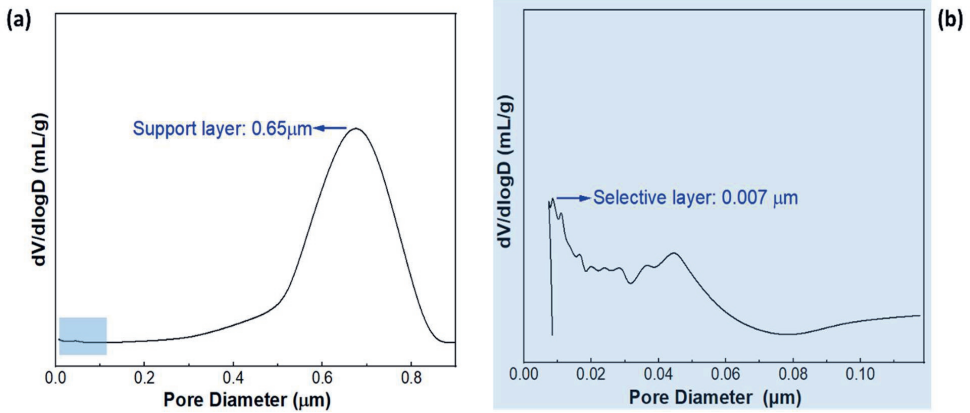


Figure 4.3. Pore size distribution of silicon carbide coated membrane as measured by mercury intrusion porosimetry (a); enlarged view of the selected region (b).

### 4.3.2 SiC coated membrane properties: permeance and zeta potential

#### 4.3.2.1 Pure water permeability

The PWP of the  $\text{Al}_2\text{O}_3$  membrane was ca.  $277 \text{ L}\cdot\text{m}^{-2}\cdot\text{h}^{-1}\cdot\text{bar}^{-1}$ , see Fig. 4.4a. After deposition of SiC for 40 mins, the PWP dropped to  $26 \text{ L}\cdot\text{m}^{-2}\cdot\text{h}^{-1}\cdot\text{bar}^{-1}$ . It can be seen in Table 4.1 that the PWP of SiC coated membrane is high in comparison with other ceramic membranes prepared by sol-gel methods. For instance, sol-gel-based  $\text{TiO}_2$  membranes typically exhibit PWPs ranging from 1.4 to  $7 \text{ L}\cdot\text{m}^{-2}\cdot\text{h}^{-1}\cdot\text{bar}^{-1}$ , depending on their preparation parameters and microstructure. The high PWP of the SiC coated membrane can be attributed to the inherent hydrophilicity of the SiC [29], and LP-CVD process which minimizes additional pore constriction while enhancing surface properties. SiC coated membranes were also prepared with extended deposition times exceeding 40 mins. However, it resulted in complete pore clogging of the  $\text{Al}_2\text{O}_3$  membranes by SiC coating and no PWP was observed.

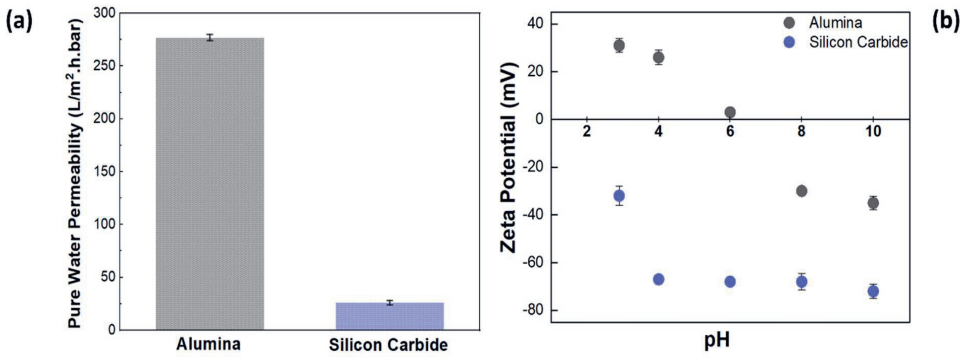


Figure 4.4. Pure water permeability of membranes (a); zeta potential of membranes (b).

Table 4.1. Comparison of sulphate rejection of silicon carbide coated membrane with membranes reported in literature.

Selective layer	Preparation method	PWP (L.m <sup>-2</sup> .h <sup>-1</sup> .bar <sup>-1</sup> )	Na <sub>2</sub> SO <sub>4</sub> feed concentration (mM)	SO <sub>4</sub> <sup>-2</sup> rejection (%)	Reference
Titania	Sol-gel	-	7	39	[20]
Titania	Sol-gel	-	2	60	[21]
Titania	Sol-gel	7	100	36	[43]
Polyethersulfone	-	5	25	55	[44]
Zirconia/alumina*	-	-	10	70	[45]
Titania	Sol-gel	1.4	-	68	[46]
<i>Silicon carbide</i>	<i>LP-CVD</i>	<i>26</i>	<i>2</i>	<i>79</i>	<i>This work</i>

#### 4.3.2.2 Zeta potential

The zeta potential, also known as electrokinetic potential, is the consequential potential difference that is created between different regions of different charge densities in direction perpendicular to the pore wall. It is measured between the imaginary shear/slipping plane of the stagnant water layer in the electrical double layer close to a solid surface [47].



The zeta potential of the SiC coated membrane remained negative across the pH range of 3-10 and became highly negative at pH values above 4 (Fig. 4.4b). This aligns with the observations reported in the literature for other SiC membranes. Studies have shown that SiC coated membranes prepared by LP-CVD consistently display negative zeta potential which reflects the distinct surface chemistry and hydrophilicity of SiC [14, 31]. Full SiC membranes used in water treatment applications have demonstrated zeta potentials of -20 to -40 mV at pH 7 [48], facilitating the rejection of negatively charged solutes and mitigating fouling. In contrast, the uncoated Al<sub>2</sub>O<sub>3</sub> membrane exhibited a positive charge at pH < 6, transitioning to a negative charge at pH > 6. Furthermore, membranes based on Al<sub>2</sub>O<sub>3</sub> and titania typically exhibit an isoelectric point (IEP) between pH 5-7, where the surface charge is zero. This highlights the advantages of SiC in applications requiring treatment of anionic feeds.

### 4.3.3 SiC coated membrane rejection properties

#### 4.3.3.1 Sulphate ion rejection in deionized water

Fig. 4.5a shows the SO<sub>4</sub><sup>2-</sup> rejection of the SiC coated membrane as a function of increasing Na<sub>2</sub>SO<sub>4</sub> feed concentration. It can be seen that the SiC coated membrane exhibited the highest SO<sub>4</sub><sup>2-</sup> rejection of 79% for 2mM Na<sub>2</sub>SO<sub>4</sub> feed solution. Table 4.1 shows that the SO<sub>4</sub><sup>2-</sup> rejection of the SiC coated membrane is high in comparison with other ceramic NF membranes reported in literature [19-21, 43-46]. However, increasing the Na<sub>2</sub>SO<sub>4</sub> feed concentration to 20mM led to a decrease of SO<sub>4</sub><sup>2-</sup> rejection to 34%.

The decrease of the rejection at higher feed concentrations can be attributed to the increased ionic strength of the solution which lowers the membranes' zeta potential [16, 49]. Higher ionic strength increases the counter-ion concentration near the membrane surface, either partially or fully compensating the surface charge of membrane within the slipping plane. This process causes a

reduction in the Debye length, thereby weakening electrostatic interactions [16]. As shown in Table 4.2, the Debye length decreased with increasing feed ionic strength, leading to a lower zeta potential and a diminished electrostatic effect on co-ion transport through the membrane. These findings are consistent with the observed trends in  $\text{SO}_4^{2-}$  rejection for the SiC coated membrane.

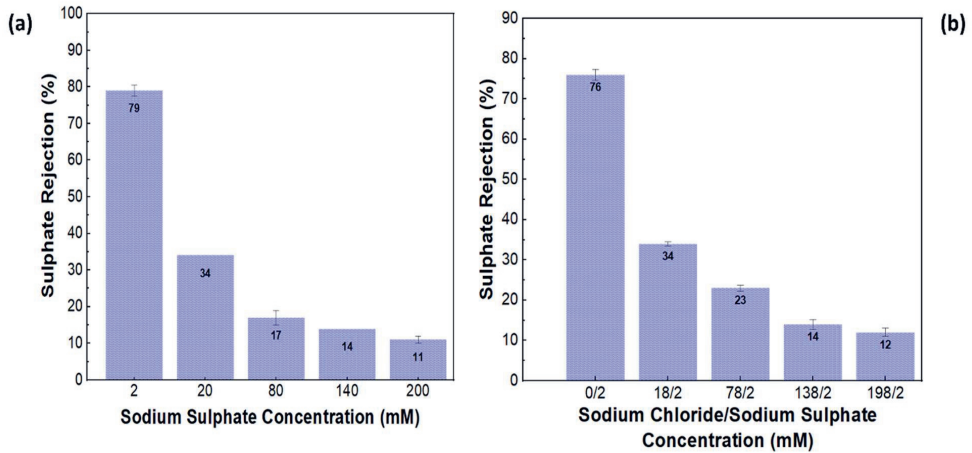


Figure 4.5. Sulphate rejection of silicon carbide coated membrane with increasing  $\text{Na}_2\text{SO}_4$  feed concentration (a); and mixed ( $\text{NaCl}$  and  $\text{Na}_2\text{SO}_4$ ) feed solution (b).

Table 4.2. Debye length calculated for feed solutions of various ionic strengths.

Ionic strength (mM)	Debye length (nm)
2	6.82
20	2.16
80	1.08
140	0.82
200	0.68

#### 4.3.3.2 Influence of mixed Na<sub>2</sub>SO<sub>4</sub> and NaCl feed on sulphate ion rejection

To obtain more insights in the rejection mechanism, SO<sub>4</sub><sup>2-</sup> rejection was also measured by using a mixed feed of NaCl and Na<sub>2</sub>SO<sub>4</sub> (Fig. 4.5b). The Na<sub>2</sub>SO<sub>4</sub> concentration was fixed at 2mM and the NaCl concentration was varied, to correlate change in the electrical double layer with SO<sub>4</sub><sup>2-</sup> rejection by the SiC coated membrane. For 2mM Na<sub>2</sub>SO<sub>4</sub> concentration without any NaCl, a SO<sub>4</sub><sup>2-</sup> rejection of ca. 76% was observed, which is consistent with the previous observations. With increasing NaCl concentration, a decreasing trend in SO<sub>4</sub><sup>2-</sup> rejection was observed (Fig. 4.5b). This stems from the fact that a high concentration of sodium (Na<sup>+</sup>) counter-ions will compress the electrical double layer and the zeta potential of the SiC coated membrane. Nicolini et al. measured the SO<sub>4</sub><sup>2-</sup> rejection of a Na<sub>2</sub>SO<sub>4</sub> solution by a commercially available negatively charged PES (NP010) membrane with an average pore radius of 1.29 nm [44]. The SO<sub>4</sub><sup>2-</sup> rejection was ca. 55%, and it was concluded that the increased concentration of counter-ions at the membranes' surface reduces the SO<sub>4</sub><sup>2-</sup> (co-ion) rejection. Similarly, Caltran et al. observed that the SO<sub>4</sub><sup>2-</sup> rejection of a mixed NaCl/Na<sub>2</sub>SO<sub>4</sub> feed solution by commercially available TiO<sub>2</sub> membrane with a mean pore size of 0.9 nm was only 36% [43]. They concluded that the Donnan effect is responsible for the retention and suspected that the low rejection was due to low negative zeta potential of the membrane. In present study the SO<sub>4</sub><sup>2-</sup> rejection by the SiC coated membrane for a mixed 2mM Na<sub>2</sub>SO<sub>4</sub> and 18mM NaCl feed solution decreased to 34%, and further increasing the NaCl concentration, while keeping Na<sub>2</sub>SO<sub>4</sub> concentration fixed, led to an even more drastic decrease of SO<sub>4</sub><sup>2-</sup> rejection.

According to Donnan exclusion principle, charged ceramic membranes can effectively repel co-ions and attract counter-ions, enabling the exclusion of ionic species whose hydrated species are much smaller than the nominal pore diameter. The strength of this electrostatic exclusion, however,

depends critically on the ratio between the pore radius and the Debye length of the electrical double layer [50]. A schematic of membrane pore size and Debye length as a function of feed ionic strength is shown in Fig. 4.6. At 2mM feed ionic strength, the Debye length is calculated to be 6.82 nm (Table 4.2), leading to an overlap of diffuse double layer within the membrane pores. Under these conditions,  $\text{SO}_4^{2-}$  ions concentration is depleted in the pore interior due to the overlap of the diffuse double layers. Positive ions are in excess in the diffuse double layer and negative ions are decreased in concentration in the diffuse double layer of a negative surface. Conversely, at 20mM feed ionic strength, the Debye length is reduced to 2.16 nm (Table 4.2), which is less than the pore radius (ca. 3.5 nm) and thus preventing diffuse layer overlap within the pores. Consequentially, allowing  $\text{SO}_4^{2-}$  ions to penetrate the pores more freely, thus leading to lower rejection. Remarkably, despite having a relatively large pore size of 7 nm, the highly negatively charged SiC coated membrane effectively rejected  $\text{SO}_4^{2-}$  ions which possess a hydrated diameter of 0.75 nm [51].

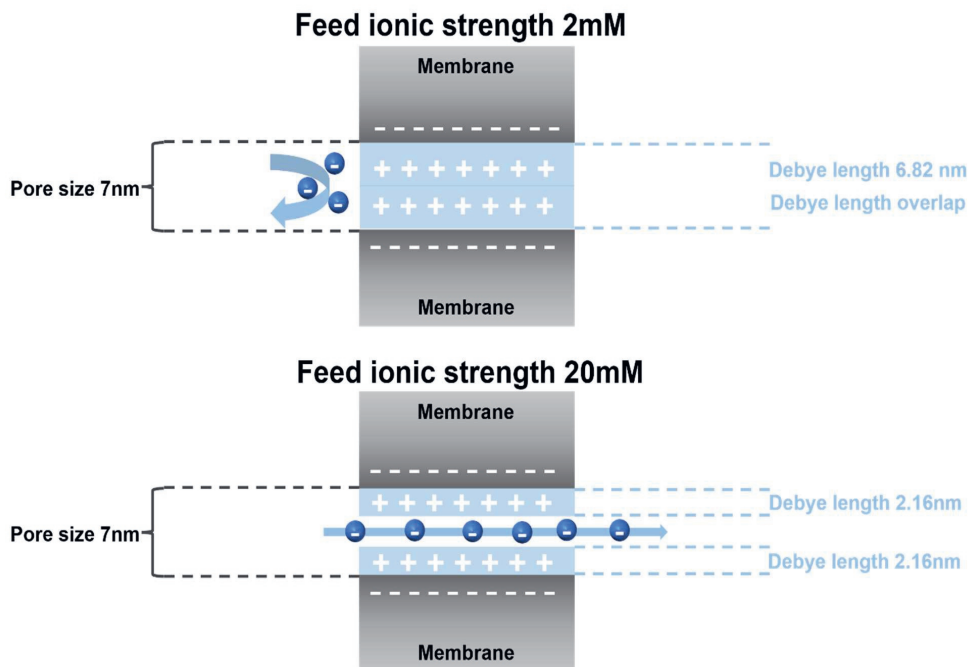


Figure 4.6. Schematic of SiC coated membrane pore size and Debye length as a function of feed ionic strength.

#### 4.4 Conclusions

An  $\text{Al}_2\text{O}_3$  UF membrane was successfully converted into a SiC UF membrane in a single-step via coating with LP-CVD. The deposition conditions were optimized to form a SiC coating encapsulating the  $\text{Al}_2\text{O}_3$  selective layer. Notably, the LP-CVD method eliminated the need for high temperature sintering step (ca. 2100°C) typically required in sol-gel based SiC membrane fabrication, offering a potentially more cost-effective manufacturing route.

SEM analysis revealed that the longitudinal thickness of the SiC coating in the selective layer was 5  $\mu\text{m}$ , while STEM analysis confirmed a radial thickness of only 12 nm. These deposition characteristics resulted in a membrane with a mean pore size of 7 nm. Zeta potential measurements indicated a highly negative surface charge, leading to a  $\text{SO}_4^{2-}$  rejection of 79% at low feed ionic

strengths, despite the membranes' relatively large pore size compared to  $\text{SO}_4^{2-}$  ions (size of the ion only 10% of the pore size). However, increasing the ionic strength of both single and mixed salt solutions led to a decline in  $\text{SO}_4^{2-}$  rejection, highlighting the dominant role of electrostatic interactions in the separation process. These findings confirm that both pore size and Donnan exclusion govern the  $\text{SO}_4^{2-}$  rejection, with higher ionic strengths suppressing the electrostatic repulsion due to double layer compression.

The present study demonstrates the potential of LP-CVD derived SiC membranes for selective ion separation and provides insights into the interplay between membrane charge, pore structure, and feedwater chemistry, which are critical for designing efficient ceramic membranes for water purification applications.

## 4.5 Supplementary information

1. Pore size of pristine  $\text{Al}_2\text{O}_3$  membrane measured by mercury intrusion porosimetry.

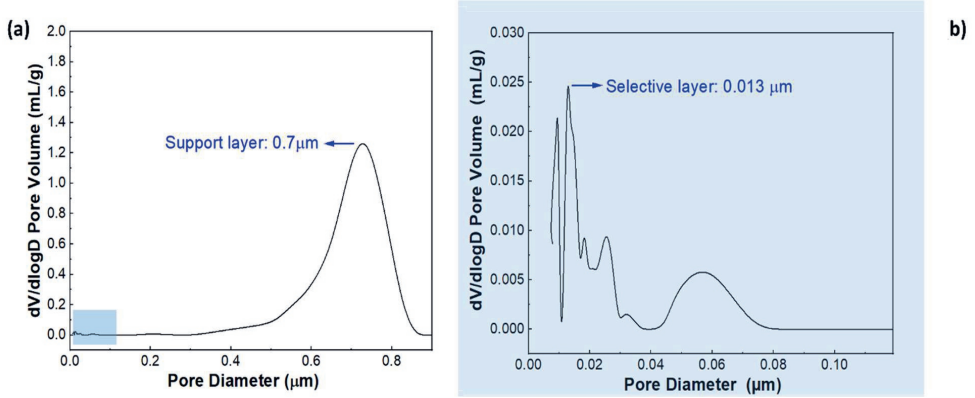


Figure S4.1. Pore size of pristine  $\text{Al}_2\text{O}_3$  membrane measured by mercury intrusion porosimetry (a); enlarged view of the selected region (b).

2. Surface composition of membranes by SEM-EDX.

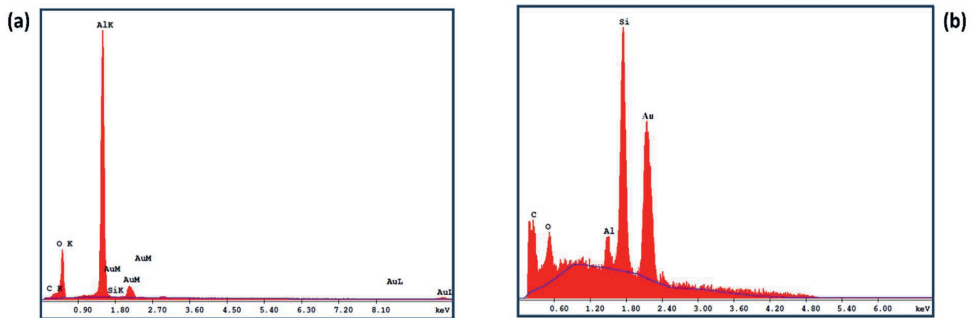


Figure S4.2. Surface composition of alumina (a); and silicon carbide membrane (b) by SEM-EDX.

3. SiC coating deposition at the inlet of the LP-CVD furnace.

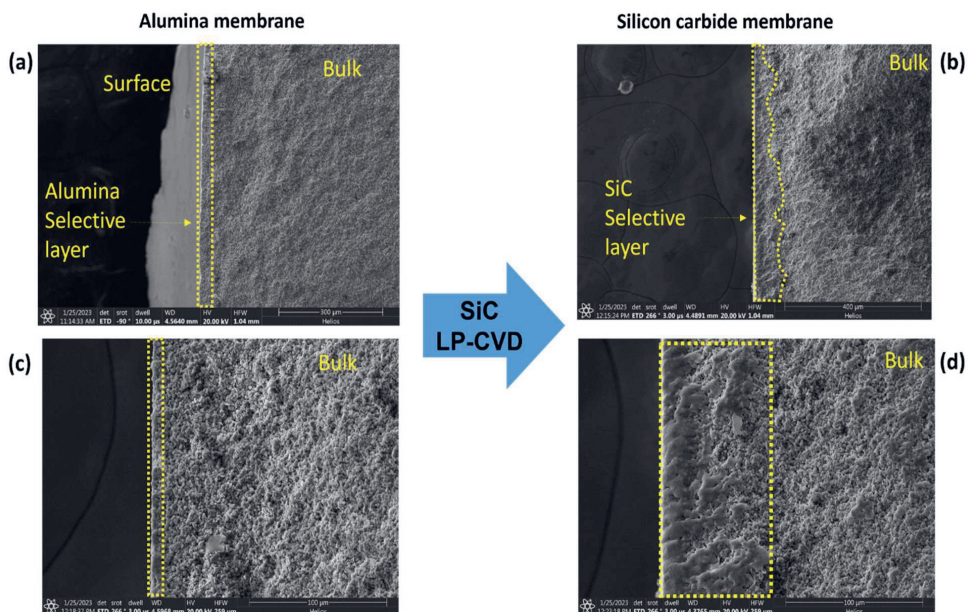


Figure S4.3. Cross-sectional morphology of alumina (a & c); and silicon carbide coated membrane (b & d) modified at the inlet of LP-CVD furnace.

4. Longitudinal growth of SiC coated Al<sub>2</sub>O<sub>3</sub> selective layer.

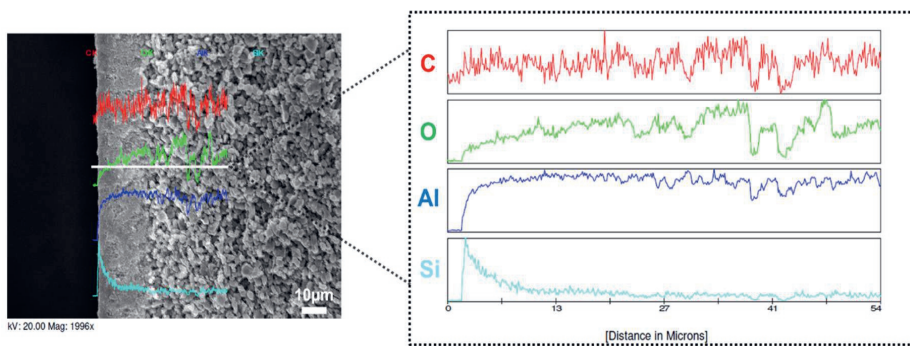


Figure S4.4. Longitudinal thickness of as-prepared SiC coated Al<sub>2</sub>O<sub>3</sub> selective layer estimated by a cross-sectional line-scan by SEM-EDX.



## References

- [1] A. Chatla, I.W. Almanassra, A. Abushawish, T. Laoui, H. Alawadhi, M.A. Atieh, N. Ghaffour, Sulphate removal from aqueous solutions: State-of-the-art technologies and future research trends, *Desalination* 558 (2023) 116615.
- [2] W.A.M. Fernando, I.M.S.K. Ilankoon, T.H. Syed, M. Yellishetty, Challenges and opportunities in the removal of sulphate ions in contaminated mine water: A review, *Minerals Engineering* 117 (2018) 74-90.
- [3] J.R. Werber, C.O. Osuji, M. Elimelech, Materials for next-generation desalination and water purification membranes, *Nature Reviews Materials* 1(5) (2016) 16018.
- [4] E. Eray, V.M. Candelario, V. Boffa, Ceramic Processing of Silicon Carbide Membranes with the Aid of Aluminum Nitrate Nonahydrate: Preparation, Characterization, and Performance, *Membranes (Basel)* 11(9) (2021).
- [5] A. Farsi, S.H. Jensen, P. Roslev, V. Boffa, M.L. Christensen, Inorganic Membranes for the Recovery of Effluent from Municipal Wastewater Treatment Plants, *Industrial & Engineering Chemistry Research* 54(13) (2015) 3462-3472.
- [6] C. Reith, B. Birkenhead, Membranes enabling the affordable and cost effective reuse of wastewater as an alternative water source, *Desalination* 117(1) (1998) 203-209.
- [7] S.S. Wadekar, Y. Wang, O.R. Lokare, R.D. Vidic, Influence of chemical cleaning on physicochemical characteristics and ion rejection by thin film composite nanofiltration membranes, *Environmental Science & Technology* 53(17) (2019) 10166-10176.
- [8] Y. Wang, S. Zhao, Z. Zha, Z. Wang, J. Wang, Host-guest nanofiltration membranes having amino-complexed cucurbituril supramolecular channel for monovalent/divalent salts separation, *Desalination* 527 (2022) 115582.
- [9] G. Dibrov, G. Kagramanov, V. Sudin, E. Grushevenko, A. Yushkin, A. Volkov, Influence of sodium hypochlorite treatment on pore size distribution of polysulfone/polyvinylpyrrolidone membranes, *Membranes* 10(11) (2020) 356.
- [10] J. Ding, S. Wang, P. Xie, Y. Zou, Y. Wan, Y. Chen, M.R. Wiesner, Chemical cleaning of algae-fouled ultrafiltration (UF) membrane by sodium hypochlorite (NaClO): characterization of membrane and formation of halogenated by-products, *Journal of Membrane Science* 598 (2020) 117662.
- [11] Y. Kourde-Hanafi, P. Loulergue, A. Szymczyk, B. Van der Bruggen, M. Nachtnebel, M. Rabiller-Baudry, J.-L. Audic, P. Pölt, K. Baddari, Influence of PVP content on degradation of PES/PVP membranes: Insights from characterization of membranes with controlled composition, *Journal of Membrane Science* 533 (2017) 261-269.
- [12] K. Li, Q. Su, S. Li, G. Wen, T. Huang, Aging of PVDF and PES ultrafiltration membranes by sodium hypochlorite: Effect of solution pH, *J Environ Sci (China)* 104 (2021) 444-455.
- [13] B. Malczewska, A. Zak, Structural Changes and Operational Deterioration of the Uf Polyethersulfone (Pes) Membrane Due to Chemical Cleaning, *Sci Rep* 9(1) (2019) 422.
- [14] M. Chen, R. Shang, P.M. Sberna, M.W.J. Luiten-Olieman, L.C. Rietveld, S.G.J. Heijman, Highly permeable silicon carbide-alumina ultrafiltration membranes for oil-in-water filtration produced with low-pressure chemical vapor deposition, *Separation and Purification Technology* 253 (2020) 117496.
- [15] C. Li, W. Sun, Z. Lu, X. Ao, S. Li, Ceramic nanocomposite membranes and membrane fouling: A review, *Water Research* 175 (2020) 115674.

- [16] C. Guizard, G. Rios, Chapter 12 Transport and fouling phenomena in liquid phase separation with inorganic and hybrid membranes, in: A.J. Burggraaf, L. Cot (Eds.), *Membrane Science and Technology*, Elsevier 1996, pp. 569-618.
- [17] A. Szymczyk, P. Fievet, Ion transport through nanofiltration membranes: the steric, electric and dielectric exclusion model, *Desalination* 200(1-3) (2006) 122-124.
- [18] S.S. Wadekar, R.D. Vidic, Influence of Active Layer on Separation Potentials of Nanofiltration Membranes for Inorganic Ions, *Environmental Science & Technology* 51(10) (2017) 5658-5665.
- [19] J.Y. Chong, R. Wang, From micro to nano: Polyamide thin film on microfiltration ceramic tubular membranes for nanofiltration, *Journal of Membrane Science* 587 (2019) 117161.
- [20] P. Chen, X. Ma, Z. Zhong, F. Zhang, W. Xing, Y. Fan, Performance of ceramic nanofiltration membrane for desalination of dye solutions containing NaCl and Na<sub>2</sub>SO<sub>4</sub>, *Desalination* 404 (2017) 102-111.
- [21] M. Cha, C. Boo, C. Park, Simultaneous retention of organic and inorganic contaminants by a ceramic nanofiltration membrane for the treatment of semiconductor wastewater, *Process Safety and Environmental Protection* 159 (2022) 525-533.
- [22] T. Van Gestel, C. Vandecasteele, A. Buekenhoudt, C. Dotremont, J. Luyten, R. Leysen, B. Van der Bruggen, G. Maes, Salt retention in nanofiltration with multilayer ceramic TiO<sub>2</sub> membranes, *Journal of Membrane Science* 209(2) (2002) 379-389.
- [23] F. Li, Y. Yang, Y. Fan, W. Xing, Y. Wang, Modification of ceramic membranes for pore structure tailoring: The atomic layer deposition route, *Journal of Membrane Science* 397-398 (2012) 17-23.
- [24] R. Shang, A. Goulas, C.Y. Tang, X. de Frias Serra, L.C. Rietveld, S.G.J. Heijman, Atmospheric pressure atomic layer deposition for tight ceramic nanofiltration membranes: Synthesis and application in water purification, *Journal of Membrane Science* 528 (2017) 163-170.
- [25] X. Zhou, Y.-Y. Zhao, S.-R. Kim, M. Elimelech, S. Hu, J.-H. Kim, Controlled TiO<sub>2</sub> Growth on Reverse Osmosis and Nanofiltration Membranes by Atomic Layer Deposition: Mechanisms and Potential Applications, *Environmental Science & Technology* 52(24) (2018) 14311-14320.
- [26] E. Eray, V.M. Candelario, V. Boffa, H. Safafar, D.N. Østedgaard-Munck, N. Zahrtmann, H. Kadrispahic, M.K. Jørgensen, A roadmap for the development and applications of silicon carbide membranes for liquid filtration: Recent advancements, challenges, and perspectives, *Chemical Engineering Journal* 414 (2021) 128826.
- [27] D. Hotza, M. Di Luccio, M. Wilhelm, Y. Iwamoto, S. Bernard, J.C. Diniz da Costa, Silicon carbide filters and porous membranes: A review of processing, properties, performance and application, *Journal of Membrane Science* 610 (2020) 118193.
- [28] M. Chen, S.G.J. Heijman, M.W.J. Luiten-Olieman, L.C. Rietveld, Oil-in-water emulsion separation: Fouling of alumina membranes with and without a silicon carbide deposition in constant flux filtration mode, *Water Research* 216 (2022) 118267.
- [29] B. Hofs, J. Ogier, D. Vries, E.F. Beerendonk, E.R. Cornelissen, Comparison of ceramic and polymeric membrane permeability and fouling using surface water, *Separation and Purification Technology* 79(3) (2011) 365-374.
- [30] A. Jan, M. Chen, M. Nijboer, M.W.J. Luiten-Olieman, L.C. Rietveld, S.G.J. Heijman, Effect of Long-Term Sodium Hypochlorite Cleaning on Silicon Carbide Ultrafiltration Membranes Prepared via Low-Pressure Chemical Vapor Deposition, *Membranes* 14(1) (2024) 22.

- [31] G. Qin, A. Jan, Q. An, H. Zhou, L.C. Rietveld, S.G.J. Heijman, Chemical vapor deposition of silicon carbide on alumina ultrafiltration membranes for filtration of microemulsions, *Desalination* 582 (2024) 117655.
- [32] B. Morana, G. Pandraud, J.F. Creemer, P.M. Sarro, Characterization of LPCVD amorphous silicon carbide (a-SiC) as material for electron transparent windows, *Materials Chemistry and Physics* 139(2) (2013) 654-662.
- [33] E.W. Washburn, The dynamics of capillary flow, *Physical review* 17(3) (1921) 273.
- [34] Y. Zhang, G. Ye, Z. Yang, Pore size dependent connectivity and ionic transport in saturated cementitious materials, *Construction and Building Materials* 238 (2020) 117680.
- [35] C. Hoffmann, B. Reinhardt, D. Enke, S. Kaskel, Inverse silicon carbide replica of porous glasses, *Microporous and Mesoporous Materials* 184 (2014) 1-6.
- [36] R.J. Hunter, *Zeta potential in colloid science: principles and applications*, Academic press 2013.
- [37] P.M. Biesheuvel, H. Verweij, Design of ceramic membrane supports: permeability, tensile strength and stress, *Journal of membrane science* 156(1) (1999) 141-152.
- [38] M. Nijboer, A. Jan, M. Chen, K. Batenburg, J. Peper, T. Aarnink, F. Roozeboom, A. Kovalgin, A. Nijmeijer, M. Luiten-Olieman, Tuning Nanopores in Tubular Ceramic Nanofiltration Membranes with Atmospheric-Pressure Atomic Layer Deposition: Prospects for Pressure-Based In-Line Monitoring of Pore Narrowing, *Separations* 11(1) (2024) 24.
- [39] J. Randon, A. Julbe, P. David, K. Jaafari, S. Elmaleh, Computer simulation of inorganic membrane morphology: 2. Effect of infiltration at the membrane support interface, *Journal of colloid and interface science* 161(2) (1993) 384-388.
- [40] C.-F. Wang, D.-S. Tsai, Low pressure chemical vapor deposition of silicon carbide from dichlorosilane and acetylene, *Materials chemistry and physics* 63(3) (2000) 196-201.
- [41] Y.S. Lin, A theoretical analysis on pore size change of porous ceramic membranes after modification, *Journal of Membrane Science* 79(1) (1993) 55-64.
- [42] M.B. Tanis-Kanbur, R.I. Peinador, J.I. Calvo, A. Hernández, J.W. Chew, Porosimetric membrane characterization techniques: A review, *Journal of Membrane Science* 619 (2021) 118750.
- [43] I. Caltran, L.C. Rietveld, H.L. Shorney-Darby, S.G.J. Heijman, Separating NOM from salts in ion exchange brine with ceramic nanofiltration, *Water Research* 179 (2020) 115894.
- [44] J.V. Nicolini, C.P. Borges, H.C. Ferraz, Selective rejection of ions and correlation with surface properties of nanofiltration membranes, *Separation and Purification Technology* 171 (2016) 238-247.
- [45] J.M. Skluzacek, M.I. Tejedor, M.A. Anderson, Influence of membrane support structure on the efficiency of an iron-modified silica nanofiltration membrane, *Journal of Porous Materials* 15 (2008) 303-309.
- [46] S.S. Wadekar, R.D. Vidic, Comparison of ceramic and polymeric nanofiltration membranes for treatment of abandoned coal mine drainage, *Desalination* 440 (2018) 135-145.
- [47] S. Bhattacharjee, DLS and zeta potential – What they are and what they are not?, *Journal of Controlled Release* 235 (2016) 337-351.
- [48] E. Eray, V. Boffa, M.K. Jørgensen, G. Magnacca, V.M. Candelario, Enhanced fabrication of silicon carbide membranes for wastewater treatment: From laboratory to industrial scale, *Journal of Membrane Science* 606 (2020) 118080.
- [49] R.J. Gross, J. Osterle, Membrane transport characteristics of ultrafine capillaries, *The Journal of chemical physics* 49(1) (1968) 228-234.

[50] H.K. Lonsdale, W. Pusch, A. Walch, Donnan-membrane effects in hyperfiltration of ternary systems, *Journal of the Chemical Society, Faraday Transactions 1: Physical Chemistry in Condensed Phases* 71 (1975) 501-514.

[51] E.R. Nightingale, Jr., Phenomenological Theory of Ion Solvation. Effective Radii of Hydrated Ions, *The Journal of Physical Chemistry* 63(9) (1959) 1381-1387.



# Chapter 5

## A review on atomically modified materials by atomic layer deposition for wastewater treatment

This chapter is based on:

Jan, A.; Tanis-Kanbur M.B.; Rietveld, L.C.; Heijman, S.G.J. A Review on Atomically Modified Materials by Atomic Layer Deposition for Wastewater Treatment, Open Ceramics, 2025, 100780, ISSN 2666-5395.



## **Chapter 5 A review on atomically modified materials by atomic layer deposition for wastewater treatment**

### **Abstract**

The growing global water crisis necessitates advanced wastewater treatment technologies capable of addressing complex contaminants. Adsorbents and membrane technologies provide viable solutions for wastewater treatment, and their performance can be significantly enhanced through surface modification by ALD. ALD enables nanoscale engineering of materials, offering unprecedented control over surface chemistry, pore structure, and functional properties for improved wastewater treatment efficiency. This review critically examines the advancements in ALD-modified membranes and adsorbents for industrial wastewater treatment, highlighting how ALD enhances adsorption kinetics and selectivity in adsorbents, improves hydrophilicity and antifouling behavior in polymeric membranes, and enhances chemical and mechanical stability in ceramic membranes. Despite these advantages, challenges remain in adoption of ALD in wastewater treatment. Future research should focus on optimizing ALD process parameters and exploring synergies with emerging water purification strategies. The continued development of ALD presents a promising pathway towards more efficient and sustainable wastewater treatment solutions.

## 5.1 Introduction

Over the past century, global water demand has surged sixfold, driven by population growth, economic development, and evolving consumption patterns [1, 2]. The escalating demand coupled with a relatively stagnant water supply, has exacerbated water stress, posing a significant challenge to modern society. Anthropogenic activities contribute to this issue by generating vast quantities of wastewater, which contains suspended, colloidal, and dissolved solids [3]. However, wastewater represents a largely untapped resource for water recycling, with potential to mitigate water stress and contribute to a circular economy [4].

Wastewater treatment methods, such as chemical coagulation, flocculation, distillation, and ion exchange, suffer from high energy consumption and suboptimal efficiency [5, 6]. In contrast, membrane- and adsorption-based technologies have emerged as promising alternatives due to their higher filtration efficiency and lower energy consumption [7, 8]. However, the transition to these technologies hinges on innovation in the precise engineering of surface properties at the atomic level [9]. Key surface characteristics critical for efficient filtration are pore size, surface charge, catalytic functionality, and material durability [10, 11].

Current approaches to modifying surface properties, such as sol-gel techniques, chemical grafting, and plasma or UV treatments, are limited by high energy demands, substrate compatibility challenges, limited atomic-scale control, and significant capital costs [5]. Furthermore, the porous nature of membranes and adsorbents makes it challenging for conventional methods to uniformly coat surfaces with functional and thin selective layers [12]. Therefore, innovative fabrication techniques are required to develop robust materials tailored for wastewater treatment applications. Thin films are essential in various technologies, including magnetic storage devices, optoelectronic components, catalysts, and membranes [13]. Vapor deposition techniques, specifically chemical



CVD and ALD, offer promising solutions for engineering thin films on a wide range of substrates [14]. CVD is a versatile process that enables the deposition of thin films via chemical reactions of gaseous precursors on or near the substrate surface [15]. The fundamental step in preparing CVD is to identify the chemical reaction responsible for the deposition of the desired product. Subsequently, the thermodynamics and kinetics of the reaction should be studied to determine the reaction's feasibility. On the basis of the chemical reaction, gaseous precursors are chosen, which are simultaneously flown into the reaction chamber at a particular temperature and pressure to form the desired film on the substrate, whereas the by-product gases are vented. As a result, by choosing the appropriate precursors and deposition parameters, thin films of most metals, non-metallic elements, and a large number of compounds, including carbides, nitrides, and oxides, can be produced [16]. The following are the advantages of CVD:

- Ability to produce dense and uniform films with good reproducibility and adhesion.
- Control over crystal structure and surface morphology by controlling the process parameters.
- Flexibility to deposit a wide range of materials (e.g., metals, carbides, nitrides, oxides, sulfides) due to the wide availability of precursors (halides, hydrides, and organometallics).

There are, however, some disadvantages with CVD as well, which restrict the widespread applicability of CVD. In particular, the inherent limitation of CVD restricts its applicability for modifying pores smaller than approximately 10 nm [17, 18]. Moreover, the following limitations are identified:

- Not all CVD reactions yield conformal films.
- Controlling the thickness of grown layers can be challenging due to island-type nucleation

mechanisms [19].

- CVD requires high temperatures (typically above 600°C), limiting its use on substrates that cannot withstand such conditions [20].

ALD, a subset of CVD, facilitates conformal thin film deposition with atomic scale precision through sequential and self-limiting chemical reactions of gaseous precursors [21]. The self-limiting nature of ALD reactions ensures that a monolayer is deposited per cycle of ALD [22], even on porous substrates [23]. The unique capabilities of ALD make it particularly advantageous for wastewater treatment applications, as it allows for:

- Precise tuning of pore sizes to nanofiltration and reverse osmosis range ( $< 2$  nm) [24].
- Altering surface charge by depositing a thin layer of targeted material [25].
- Transformation of adsorbent and membrane material's surface areas from hydrophobic to hydrophilic, and vice versa [26].
- Imparting photocatalytic properties to enhance contaminant degradation [27].
- Mitigate fouling in membrane separation [28].
- Convenient separation of adsorbents from the aqueous phase by deposition of magnetic materials.
- ALD operates in a lower temperature range (80-400°C), enabling thin film deposition on a wide range of substrates, even on polymeric materials [29].

Despite widespread applicability of ALD for membrane modification, functionalization, and fabrication, existing reviews remain segmented in focus. They primarily focus on membrane applications for gas/water separation, ALD-based interfacial engineering, or broader functional materials without a dedicated emphasis on wastewater treatment. While some studies have

explored ALD's potential for enhancing membrane antifouling or tuning pore size [30-33], and others have reviewed multifunctional materials for aquatic remediation [34, 35], a comprehensive review that highlights ALD's role in modifying both adsorbents and membranes for complex wastewater streams is lacking. This review bridges this gap by providing a comprehensive analysis of ALD's role in wastewater treatment, with particular emphasis on its advantages in enhancing adsorption kinetics and selectivity of adsorbents, improving the hydrophilicity and antifouling properties of polymeric membranes, and enabling advanced fabrication routes for robust ceramic membranes. It begins with an overview of ALD's historical development and fundamental chemistry, highlighting key processing parameters and their influence on thin film properties. While several extensive reviews discuss ALD's mechanisms and broader applications [12, 21, 35], this manuscript integrates materials science and water process engineering to offer a holistic perspective specifically tailored to wastewater purification, which has not yet been adequately addressed. Key studies from the last decade are examined to showcase ALD's potential in modifying wastewater treatment materials, followed by a discussion of the current challenges and future research directions in the field.

## **5.2 Historical perspective and fundamentals of ALD**

### **5.2.1 Brief history of ALD**

ALD evolved from CVD, a well-established thin film deposition technique in use since the 1880s. Early applications of CVD included the enhancement of incandescent lamp filaments through carbon or metal coatings [20]. The conceptual foundation of ALD was first laid in the 1950s in the former USSR, where researchers explored sequential surface reactions for controlled film growth [36, 37]. However, its industrial relevance emerged, independently, in Finland in 1970s, when Suntola et al. established the technique under the name of atomic layer epitaxy (ALE) for

fabricating thin films in electroluminescent displays [38]. The first Finnish patent for ALE was filed in November 1974, followed by a U.S. patent granted in 1977. Initially, ALE was primarily associated with epitaxial film growth. However, as the technique gained broader applicability beyond epitaxial systems, extending to polycrystalline and amorphous films, the term ALD became widely adopted in the early 2000s.

### 5.2.2 Working principle of ALD: The ALD cycle

Thin film formation in ALD results from chemical reactions between the precursor molecules and reactive functional groups on the substrate's surface. To achieve complete surface saturation, the injected dose of the precursors must be sufficient to react with all the available functional groups. Once saturation is reached, further exposure to precursor does not contribute to additional growth, leading to a self-limiting deposition process.

To illustrate the fundamental mechanism, the ALD of  $\text{Al}_2\text{O}_3$  using trimethylaluminium TMA ( $\text{Al}(\text{CH}_3)_3$ ) and steam ( $\text{H}_2\text{O}$ ) is presented as a model system [39]. The deposition cycle consists of four distinct steps (see also Fig. 5.1):

- **Precursor exposure:** The substrate is first exposed to TMA, which selectively reacts with the surface -OH groups, forming a  $-\text{CH}_3$  terminated surface and releasing methane ( $\text{CH}_4$ ) as a reaction byproduct. The reaction proceeds until all accessible -OH sites are consumed.
- **Purge step:** An inert gas (e.g., nitrogen or argon) is introduced to remove the unreacted precursor molecules and gaseous byproducts, preventing unwanted gas-phase reactions.
- **Co-reactant exposure:** The second precursor  $\text{H}_2\text{O}$  is introduced, which reacts with  $-\text{CH}_3$  terminated surface to regenerate -OH groups while forming a monolayer of  $\text{Al}_2\text{O}_3$ .  $\text{CH}_4$  is again released as a byproduct in this step. This reaction also follows a self-limiting mechanism and it ceases once all available  $-\text{CH}_3$  sites have reacted.

- **Final purge:** A second inert gas purge is applied to remove any H<sub>2</sub>O and reaction byproducts, preparing the surface for the next ALD cycle.

Each ALD cycle deposits a thin layer, with growth per cycle (GPC) typically ranging from 0.4 – 2.5 Å [21], depending on precursor chemistry and the targeted material. The final thickness is a function of the total number of ALD cycles performed. This GPC deposition ensures precise thickness control and conformal coating of complex structures.

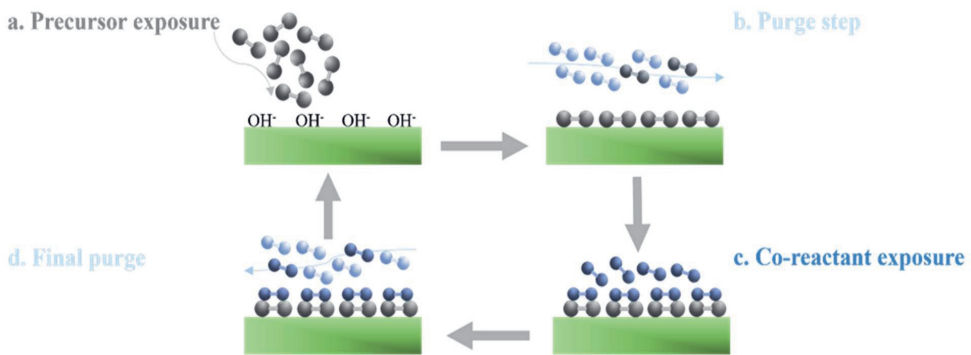


Figure 5.1. Schematic representation of ALD process.

### 5.2.3 ALD precursors

The selection of appropriate precursors is fundamental to achieving controlled and reproducible ALD. Given that ALD typically operates within a deposition temperature range of 80-400°C [21], precursors must exhibit adequate volatility at the operating conditions while maintaining thermal stability over extended periods.

For an optimal ALD process, precursors must meet the following criteria [9, 21, 40-42]:

- **Volatility:** The precursor must be sufficiently volatile at the deposition temperature and pressure to ensure transport to the reaction site.
- **Thermal stability:** The precursor should remain chemically stable without decomposition

or self-reaction at the deposition temperature.

- **Reactivity:** It must exhibit high reactivity towards the surface functional groups.
- **Inertness to film:** The precursor should not etch or degrade the substrate or the growing film.
- **Safe handling:** Non-toxic and non-corrosive precursors are preferred for safer handling and process reliability.

A practical strategy for identifying suitable ALD precursors involves adapting reactants from a well-established CVD process [41, 43]. In this approach, a binary reaction scheme used in CVD is modified to an ABAB... cycle, where reactants are introduced sequentially to achieve self-limiting growth. A key distinction between ALD and CVD lies in GPC, verifying the layer thickness increment per cycle ensures that the deposition follows ALD kinetics rather than CVD-like continuous growth.

#### 5.2.4 ALD variants: thermal and plasma/radical assisted ALD

Once a chemical reaction has been identified for deposition, the next step is to determine the appropriate variant of ALD. The two primary variants of ALD are thermal-assisted ALD (TALD) and plasma/radical-assisted ALD (PALD), each distinguished by the energy source used to drive the surface reactions.

In TALD, heat energy provides the activation energy for precursor-surface reactions. Common materials deposited using TALD include binary metal oxides ( $\text{Al}_2\text{O}_3$ ,  $\text{TiO}_2$ ,  $\text{ZnO}$ ,  $\text{ZrO}_2$ ,  $\text{HfO}_2$ ,  $\text{Ta}_2\text{O}_5$ ), binary metal nitrides ( $\text{TiN}$ ,  $\text{TaN}$ ,  $\text{W}_2\text{N}$ ), and certain metal sulfides ( $\text{ZnS}$ ,  $\text{CdS}$ ) [44, 45].

In contrast, PALD relies on radicals generated in plasma to facilitate chemical reactions that may not be energetically favored under thermal conditions alone. The radicals enhance surface reactivity, allowing for deposition of materials such as metals (e.g., Ta, Pt, Ru) and semiconductors

(e.g., Si, Ge) that are challenging to achieve using TALD. PALD is particularly advantageous for depositing films at lower temperatures, making it suitable for coating thermally sensitive substrates. However, the high recombination affinity of radicals in PALD may limit penetration into porous structures, challenging its applicability to membrane and adsorbent structures [46].

### **5.2.5 Deposition temperature of ALD: The ALD window**

Deposition temperature is a key parameter in ALD. The GPC is influenced by temperature, and within a specific temperature range, the deposition process exhibits a stable and self-limiting behavior. This temperature range, known as the ALD window, represents the optimal conditions for achieving consistent and reproducible film growth [47, 48].

As illustrated in Fig. 5.2, at temperatures below the ALD window, precursor condensation or incomplete surface reactions may occur due to insufficient activation energy, leading to non-uniform or inhibited film growth. Conversely, at temperatures above the ALD window, precursor decomposition can result in CVD-like growth, i.e. deposition is not self-limiting [21, 42]. Maintaining deposition within the ALD window is crucial for ensuring uniformity, reproducibility, and the desired film properties.

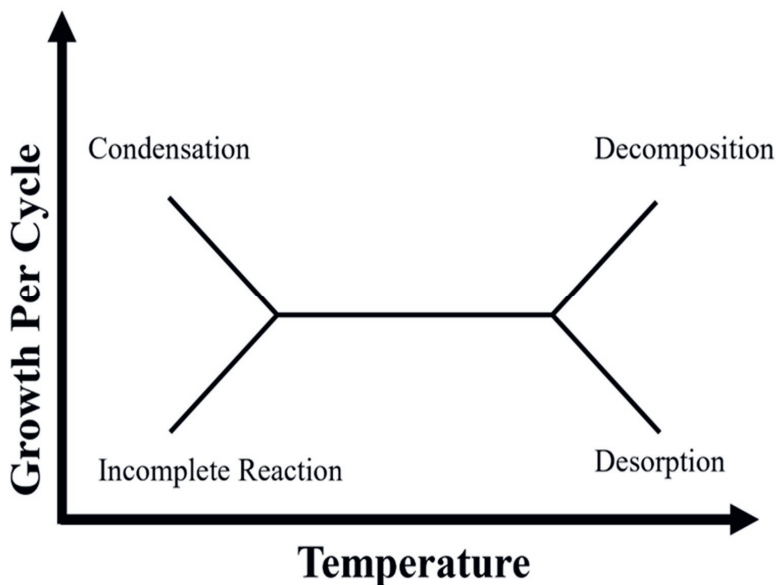


Figure 5.2. Schematic representation of growth per cycle as a function of process temperature, i.e. the ALD window.

### 5.3 Atomically Engineered Materials by ALD for Wastewater Treatment

#### 5.3.1 Characteristics of Wastewater and treatment technologies

Industrial wastewater contains a complex mixture of various organic and inorganic micropollutants, necessitating efficient and selective treatment technologies. Conventional treatment methods often fail to completely remove contaminants. As a result, advanced techniques, such as adsorption and membrane filtration, have emerged as promising alternatives for efficient wastewater treatment.

Adsorption-based treatment relies on high-surface area materials to capture contaminants, while membrane filtration enables selective separation based on size exclusion and surface interactions. The performance of adsorbents and membranes is largely dictated by their surface properties,



which govern adsorption affinity, permeability, and selectivity. ALD had been extensively explored as a post-modification strategy to enhance these properties, enabling precise atomic-level control over surface characteristics (Fig. 5.3).

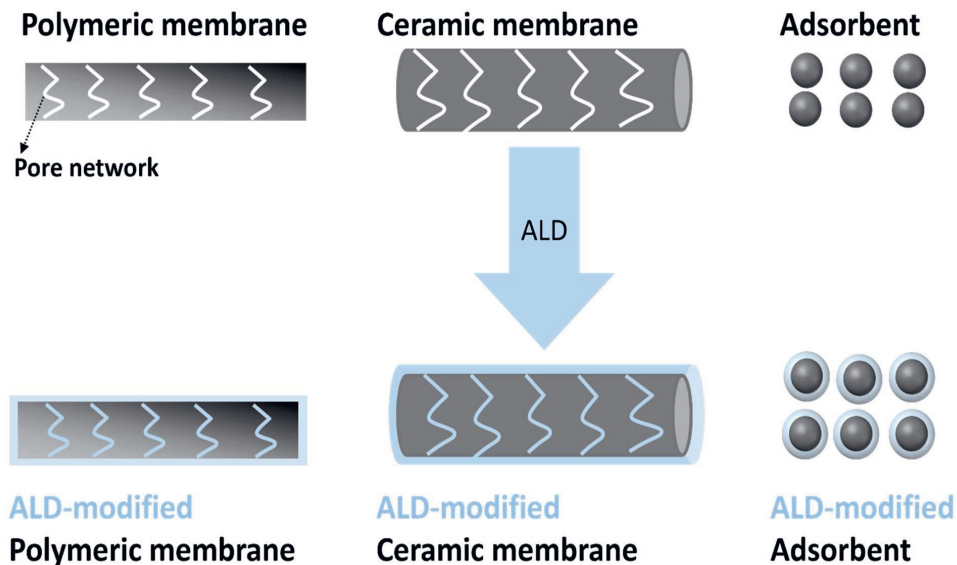


Figure 5.3. A schematic of atomic-scale modification of polymeric, ceramic membranes, and adsorbents by ALD.

The post-modification by ALD involves the deposition of thin films to coat adsorbents and membranes, thereby tailoring their surface chemistry, pore size, and hydrophilicity/hydrophobicity. This single-step modification approach offers significant advantages over conventional methods, such as sol-gel processing, which often require multiple preparation steps and are associated with high material and processing costs. Moreover, ALD allows for the deposition of a wide range of function materials, including metal oxides, nitrides, and sulfides, onto both organic and inorganic substrates.

In this section, we systematically summarize the applications of ALD-modified adsorbents and membranes for wastewater treatment, emphasizing their improved performance in contaminant removal, selectivity, and long-term stability.

### 5.3.2 ALD-modified adsorbents

#### 5.3.2.1 ALD-modified inorganic adsorbents with single photo-catalysts

A variety of ALD-modified adsorbents have been reported in the literature for removal of (i) dyes (methylene blue, phenols); (ii) toxic, heavy metal ions (Arsenic, Chromium, Copper, Lead); (iii) antibiotics (ciprofloxacin); and (iv) oil from water (Fig. 5.4) [34]. The primary research focus has been ALD of photo-catalytically active materials, such as  $\text{TiO}_2$  and zinc oxide ( $\text{ZnO}$ ), onto adsorbents to facilitate their in-situ regeneration via UV irradiation. This approach enhances the long-term stability and reusability of the adsorbents, thereby improving their service life and operational efficiency in wastewater applications. However, Dey et al. concluded that, after growing thin films of  $\text{TiO}_2$  on carbon fibers by ALD [49] and compared to both  $\text{TiO}_2$  and bare carbon fibers, the  $\text{TiO}_2$  films on carbon fibers also improved methylene blue (MB) adsorption on the surface, thus facilitating higher removal from water (Fig. 5.4a). Additionally, due to the photocatalytic properties of the deposited  $\text{TiO}_2$  films, the exposure to the UV-light photocatalytically degraded the adsorbed MB, thus regenerating the adsorption sites for the next cleaning cycle. Seo et al. have conducted a similar study in which they deposited  $\text{TiO}_2$  films on a porous silicon dioxide ( $\text{SiO}_2$ ) by ALD [50]. Although  $\text{TiO}_2$  deposition results in a decrease of the total surface area, compared to bare  $\text{SiO}_2$ , it shows the same MB adsorption capacity as that of bare  $\text{SiO}_2$ . However because after saturation, the active adsorption sites of the  $\text{TiO}_2$  deposited  $\text{SiO}_2$  could be regenerated by annealing at  $500^\circ\text{C}$ , the overall performance of the ALD modified surface improves (Fig. 5.4b & c). Wang et al. coated  $\text{SiO}_2$  particles with  $\text{TiO}_2$  to compare the adsorption

of metal and metalloid ions on as-deposited TiO<sub>2</sub> and annealed TiO<sub>2</sub> [51]. It has been concluded that the, as-deposited TiO<sub>2</sub> removes metal and metalloid ions more effectively than the annealed TiO<sub>2</sub>, which has been attributed to the larger surface area. Furthermore, the TiO<sub>2</sub>/SiO<sub>2</sub> particles have a high sedimentation rate compared to the commercial TiO<sub>2</sub> nanoparticles, facilitating the separation of the adsorbent from the wastewater. Jeong et al. deposited another photocatalytic material, ZnO thin films, on mesoporous SiO<sub>2</sub> particles by ALD. ZnO/SiO<sub>2</sub> particles have a lower surface area than SiO<sub>2</sub> particles, but they show a higher adsorption capacity for MB compared to the bare SiO<sub>2</sub> particles [52]. The photocatalytic properties of ZnO also degrade and desorb the adsorbed MB upon exposure to UV light, thus regenerating ZnO/SiO<sub>2</sub>.

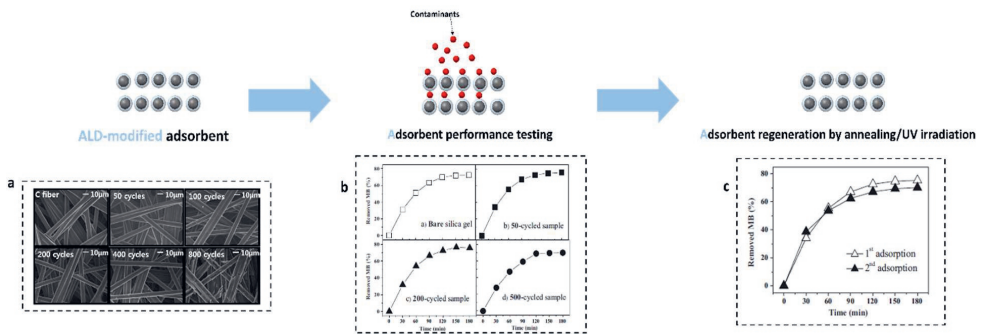


Figure 5.4. Enhanced performance and regeneration of ALD-modified adsorbents for contaminant removal.

(a) SEM images showing conformal TiO<sub>2</sub> coatings deposited on carbon fibres by ALD. Adapted with permission from [49].

(b) MB adsorption capacity of TiO<sub>2</sub>-coated SiO<sub>2</sub> adsorbents as a function of ALD cycle number, illustrating the tunability of surface properties. Adapted with permission from [50].

(c) Regeneration of TiO<sub>2</sub>-coated SiO<sub>2</sub> adsorbents through annealing at 500°C, demonstrating sustained adsorption performance. Adapted with permission from [50].

### 5.3.2.2 ALD modification in organic adsorbents with composite catalysts

An adsorbent that possesses a high density of functional adsorption sites for pollutants may not also possess photocatalytic activity to degrade the adsorbed species and regenerate the adsorbent for the next cleaning cycle, and vice versa. Therefore, Li et al. have come up with a composite catalyst ( $\text{Mn}_3\text{O}_4@\text{ZnO}/\text{Mn}_3\text{O}_4$ ), which consists of a  $\text{Mn}_3\text{O}_4@\text{ZnO}$  photocatalyst and a  $\text{Mn}_3\text{O}_4$  adsorbent [53].  $\text{Mn}_3\text{O}_4$  nanoparticles have been prepared using a hydrothermal method, and subsequently, the nanoparticles were coated with ZnO by ALD. The photocatalyst shows a high activity towards the reduction of Cr (VI) species under sunlight irradiation, and the adsorbent facilitates the migration of the reduced species away from the active sites of the photocatalyst, finally resulting in a Cr (VI) reduction efficiency of 94% and total Cr removal of 92% in 70 minutes under simulated sunlight irradiation. By employing the same preparation method, Li et al. have prepared a magnetic  $\text{Fe}_2\text{O}_3@\text{ZnO}$  composite photocatalyst for ciprofloxacin degradation [54]. The  $\text{Fe}_2\text{O}_3@\text{ZnO}$  composite photocatalyst exhibit a high adsorption and degradation efficiency, i.e. 92.5%, towards ciprofloxacin as compared to bare iron oxide ( $\text{Fe}_2\text{O}_3$ ) and ZnO nanoparticles, stemming from the enhanced surface area and zeta potential. A challenge in water purification by adsorbent powders is the complete separation of the powder from the liquid phase, e.g. to reuse it for further purification cycles. However, the  $\text{Fe}_2\text{O}_3@\text{ZnO}$  composite photocatalyst has magnetic properties, and, after each filtration cycle, the photocatalyst could be collected by applying a magnetic field, while retaining the photocatalytic degradation efficiency after six cycles.

### 5.3.2.3 ALD modification of organic adsorbents

Recently, ALD has also been utilized to modify organic adsorbents and carbon nanotubes for metal ions removal and oil-water separation. Mauro et al. have deposited ZnO on polyethylene

naphthalene (PEN) by ALD [55]. They have elucidated the properties of the ZnO films, deposited at different temperatures, and have observed that ZnO films can be grown even at a low deposition temperature of 40°C. Their results show that ZnO-modified PEN have a larger affinity towards MB and phenol degradation than pristine PEN. Short et al. ameliorated the oil sorption capacity of cellulose by ALD of Al<sub>2</sub>O<sub>3</sub> [56]. Compared to the untreated cellulose, modified cellulose exhibits a 35 times larger oil sorption capacity. Xiong et al. have deposited ZnO on melamine foams by ALD for oil adsorption [57]. They have observed that the deposited ZnO film also incorporates organic components. As a result, the film becomes hydrophobic (water contact angle: 86°), whereas, smooth wurtzite ZnO films are typically hydrophilic with a water contact angle of less than 20°. Therefore, they have subsequently carried out a calcination step at 600°C, changing the surface properties to hydrophilic (water contact angle of 16°). However, they have used the organic moieties-induced hydrophobicity to their advantage and have produced oil adsorbents of high stability and capacity. You et al. have modified multiwalled carbon nanotubes (MWCNTs) firstly by ALD of Fe<sub>2</sub>O<sub>3</sub>, in order to introduce magnetic properties, and then subsequently by polyethyleneimine (PEI) [58]. PEI provides a high density of amine groups for adsorption of Cr(VI). The adsorption capacity of the modified MWCNTs has been reported to be 42.8% higher than MWCNTs modified with Fe<sub>2</sub>O<sub>3</sub> nanoparticles alone.

#### **5.3.2.4 ALD modified adsorbents from waste materials**

ALD has also been employed to modify industrial waste materials to use them as adsorbents for wastewater treatment. Iakovleva et al. compared the arsenic (III) and (V) removal efficiencies of two solid waste materials, i.e. industrial sand and sulfate tailings, by modifying them with two different techniques: (i) NaOH modification; and (ii) ALD. TiO<sub>2</sub> and Al<sub>2</sub>O<sub>3</sub> deposited on industrial waste materials by ALD show a two-times higher arsenic removal efficiency than the materials

modified with NaOH to activate iron compounds and generate -OH functional groups [59]. Wang et al. have deposited Al<sub>2</sub>O<sub>3</sub> on biochar by ALD to improve its surface hydrophilicity [60]. Although the results demonstrate that the Al<sub>2</sub>O<sub>3</sub> coating result in an increase in adsorption sites at the expense of surface area, the Al<sub>2</sub>O<sub>3</sub>-modified biochar show a higher removal efficiency for MB than the pristine biochar. In this study, the effect of the surface charge of modified biochar on the interaction of MB has also been analyzed with the conclusion that at a low pH of 5, the high concentration of H<sub>3</sub>O<sup>+</sup> ions competitively saturates the adsorption sites, resulting in a decrease of MB adsorption, whereas at a high pH of 9, the concentration of H<sub>3</sub>O<sup>+</sup> ions decreases, and the adsorption of MB is relatively high, i.e. ca. 90%. Iakovleva et al. have also employed ALD to modify the surface of metallurgical solid waste materials, i.e. sulfate tailings, but this time with Al<sub>2</sub>O<sub>3</sub> [61], with the conclusion that the modified adsorbent selectively removes 97% of cyanide compounds from synthetic acidic wastewater.

The aforementioned applications highlight the importance of ALD for modification of both organic and inorganic adsorbents. Table 5.1 presents a comparison of these adsorbents.

Table 5.1. ALD-modified adsorbents and their properties for degradation of various water contaminants.

Adsorbent	Material Deposited by ALD	Contaminant Targeted	Contaminant Removal in Dark (%)	Contaminant Removal Time in Dark (min)	Contaminant Removal in UV/Normal light (%)	Contaminant Removal Time in Light (min)	Adsorbent Regeneration Method	Adsorbent Regeneration time (min)	Reference
Carbon Paper	TiO <sub>2</sub>	Methylene Blue	-	-	-	-	UV light	60	[45]
Silica	TiO <sub>2</sub>	Methylene Blue	ca. 70	180	ca. 80	180	Annealing 500°C	120	[46]
Silica	ZnO	Methylene Blue	-	-	-	-	UV light	420	[48]
Silica Gel	TiO <sub>2</sub>	Arsenic	-	-	92	-	-	-	-
		Selenium	-	-	85	-	-	-	-
		Molybdenum	-	-	99	-	-	-	-
		Lead	-	-	94	-	-	-	-
Polyethylene Naphthalate	ZnO	Phenols	-	-	30	240	-	-	[51]
Type 1: Industrial Sand Type 2: Sulphate Tailings	TiO <sub>2</sub> & Al <sub>2</sub> O <sub>3</sub> TiO <sub>2</sub> & Al <sub>2</sub> O <sub>3</sub>	Arsenic (III)	-	-	97 & 99 92 & 95	-	-	-	[55]
		Methylene Blue	-	-	60	1440	-	-	[56]
Manganese Oxide	ZnO	Chromium	-	-	92	70	UV light	-	[49]
Iron (III) Oxide	ZnO	Ciprofloxacin	18.3	30	92.5	60	UV light	30	[50]
Sulfate Tailings Type 1: caFe-Cake Type 2: SuFe	Al <sub>2</sub> O <sub>3</sub>	Cyanide	-	-	99 99	210 210	-	-	[57]
		Oil	-	-	-	-	-	-	[52]
Melamine Foams	ZnO	Oil	-	-	-	-	-	-	[53]
Multi-walled Carbon Nanotubes	Fe <sub>2</sub> O <sub>3</sub>	Chromium	-	-	ca. 90	-	-	-	[54]

### 5.3.3 ALD-modified Organic membranes

Because ALD can be performed at low-deposition temperatures, typically in the range of 50-400°C [29], the modification of materials with low thermal stability such as polymeric materials is enabled (Fig. 5.5). In membrane technology, polymeric membranes have the highest market share in the industrial wastewater treatment industry. Numerous research groups have attempted to ameliorate the surface properties of the polymeric membranes by ALD post-treatment [62]. ALD on/in polymeric membranes was found to: (i) enhance hydrophilicity [27], (ii) reduce pore size [63], (iii) modify surface charge [26], (iv) improve fouling resistance [64], and (v) improve mechanical properties. As a consequence, ALD-modified polymeric membranes offer higher contaminant rejection than unmodified membranes.

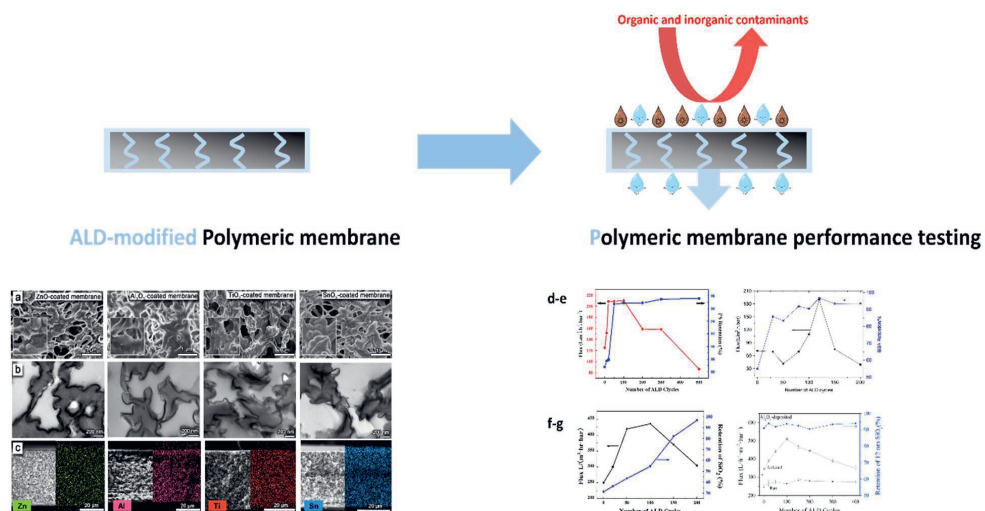


Figure 5.5. Performance enhancement of polymeric membranes via ALD for contaminant removal.

(a-c) SEM, TEM, and EDS images of ALD coated membranes with ZnO, Al<sub>2</sub>O<sub>3</sub>, TiO<sub>2</sub>, and SnO<sub>2</sub>.

Adapted with permission from [65].

(d) Pure water flux and PS retention of Al<sub>2</sub>O<sub>3</sub>-coated PTFE membranes as a function of ALD cycle

number. Adapted with permission from [26].



(e) Pure water flux and BSA retention of TiO<sub>2</sub>-coated PVDF membranes as a function of ALD cycle number. Adapted with permission from [66].

(f) Pure water flux and SiO<sub>2</sub> retention of TiO<sub>2</sub>-coated PP membranes as a function of ALD cycle number. Adapted with permission from [67].

(g) Pure water flux and SiO<sub>2</sub> retention of Al<sub>2</sub>O<sub>3</sub>-coated PP membranes as a function of ALD cycle number. Adapted with permission from [68].

### 5.3.3.1 Enhanced permeability: ALD of Al<sub>2</sub>O<sub>3</sub>

To the best of our knowledge, Li et al. have published the first report on the ALD of Al<sub>2</sub>O<sub>3</sub> on polymeric substrates for wastewater treatment [63]. They have utilized track-etched polycarbonate membranes of a nominal pore size of ca. 30 nm. After 100 cycles of ALD of Al<sub>2</sub>O<sub>3</sub>, the pore size has been reduced to ca. 20 nm with an enhancement in surface hydrophilicity. The reported growth rate of 0.8 Å per cycle confirms that the deposition process proceeds in a self-limiting manner, characteristic of ALD. This study has further shown that the membranes modified with less ALD cycles (<50) results in an around 20% increase in bovine serum albumin (BSA) retention compared to unmodified membrane, and at only a slight expense of pure water permeability (PWP). However, further increase in the number of ALD cycles results in a gradual increase in BSA retention at the cost of a larger decline in PWP. However, after 100 ALD cycles, the PWP was reduced only to 5 L·h<sup>-1</sup>·m<sup>-2</sup>·bar<sup>-1</sup>, compared to ca. 12 L·h<sup>-1</sup>·m<sup>-2</sup>·bar<sup>-1</sup> for unmodified membranes. Xu et al. have attempted to explore this phenomena further by depositing Al<sub>2</sub>O<sub>3</sub> on polytetrafluoroethylene (PTFE) membranes with a pore size of 200 nm [26]. They have found that during the initial 10-50 ALD cycles, Al<sub>2</sub>O<sub>3</sub> nucleation and growth occurs predominantly within the pores; while at 50-200 cycles, nucleation shifted to the surface. After just 20 cycles, the PWP increases, by 67.7% compared to the pristine membrane, due to improved hydrophilicity from

Al<sub>2</sub>O<sub>3</sub> growth on the pore walls. When increasing the ALD cycles to 50 the modified membrane still maintains the PWP but the retention of polystyrene nanospheres (kinetic diameter: 190 nm) is enhanced to 96.7%; whereas, increasing the ALD cycles beyond 100 drastically reduced the PWP (Fig. 5.5d). This study highlights the importance of choosing ALD parameters carefully to optimize the properties of membranes. Attempts have also been made to convert hydrophilic surfaces to hydrophobic ones; Kong et al. have converted the surface of a filter paper sheet (pore size: 20-25 μm) from hydrophilic to hydrophobic in two steps [69]. First, they have performed ALD of Al<sub>2</sub>O<sub>3</sub>, and secondly coupled silane molecules onto the pre-coated Al<sub>2</sub>O<sub>3</sub> layer. After 90 ALD cycles, the modified filter paper then shows a lower PWP but a higher permeability to various oils than the unmodified filter paper.

### 5.3.3.2 Enhanced selectivity: ALD of TiO<sub>2</sub>

In another study, Alam et al. have deposited TiO<sub>2</sub> exclusively on the surface of the PES membranes [70]. The deposition has resulted in a smoother membrane surface, with NaCl rejection improving more than fourfold to over 90%, albeit with ca. 30% reduction in pure water flux. PTFE is highly inert and hydrophobic without the presence of functional groups, which can result in island-type growth during ALD. To circumvent this problem, Xu et al. have, therefore, introduced an intermediate plasma treatment step to activate the PTFE membrane before ALD of TiO<sub>2</sub> [64]. They have used the same PTFE membrane of pore size of 200 nm as used by Xu et al. [26]. Compared with the untreated PTFE membrane, the 150 cycles of ALD deposition on the activated membrane has resulted in a continuous thin film of TiO<sub>2</sub> with an increase in PWP by 154% compared to the pristine membrane. Additionally, the retention of monodispersed SiO<sub>2</sub> nanospheres (kinetic diameter: 142 nm) has increased to ca. 33%. In a similar study, Xu et al. have also deposited TiO<sub>2</sub> in the form of conformal thin layers on polypropylene (PP) membranes (pore size: 45 nm) by ALD

[67]. This was achieved by the aforementioned plasma pre-treatment to activate the surface of the pristine PP membranes by the formation of active groups on the pore walls. As a result, the film growth was highly conformal and the plasma-treated ALD membranes had a higher hydrophilicity than the non-treated ALD membranes (Fig. 5.5f). Wang et al. have deposited  $\text{TiO}_2$  on polyvinylidene fluoride (PVF) UF membranes via ALD [66]. They observed that upon increasing the number of ALD cycles, the PWP first decreased, followed by a sharp increase, which peaked at 120 cycles, and then finally decreased (Fig. 5.5e). They thus concluded that the optimum number of ALD cycles for obtaining a membrane with the best PWP and BSA retention is 120 cycles. They also elucidated the effect of exposure time on the formation of the  $\text{TiO}_2$  film. Their results have shown that even a very short exposure time of 0.5 seconds facilitates greater diffusion of the precursors into the substrate membrane, which results in a thicker film deposition but at the expense of PWP.

The aforementioned plasma activation of the inert porous substrates is an energy-intensive process. Therefore, Chen et al. have invented an alternative activation step for PP membranes (pore size: 43 nm) by using a nitric acid bath [68], which enriches the surface with oxygen and nitrogen-containing active groups that can readily react with the precursors of the ALD process to produce conformal thin films on inert surfaces. Compared to the bare membrane, the modified membranes have shown a higher PWP and a higher retention of  $\text{SiO}_2$  nanospheres (kinetic diameter: 12nm).

### **5.3.3.3 Enhanced separation performance: ALD of ZnO**

In a different pre-treatment approach, Li et al. have deposited ZnO on PVF membranes (pore size: 200 nm) by employing a pre-treatment step in the ALD chamber [71]. In the first case, a ZnO-like layer has been deposited on the surface of the PVF membrane by employing 10 cycles of nitrogen dioxide and diethyl zinc precursors prior to the actual deposition of ZnO by diethyl zinc and  $\text{H}_2\text{O}$

precursors. In the second case, the ALD has been carried out without the deposition of the ZnO-like layer beforehand on the surface. Results show that the activation step prior to the ALD results in the formation of uniform films with a high PWP and BSA retention compared to the membranes that were modified by ALD without pre-treatment.

Juholin et al. have treated mine wastewater by modifying commercial NF membranes, NF90 (polyamide) and NF270 (polypiperzine), with ALD to deposit a ZnO thin film [72]. The modified membranes is less susceptible to reversible fouling; however, the ZnO thin film has not any effect on irreversible fouling. ALD modified membranes are also used for oil/water separation. Yang et al. have prepared oil-repellant membranes by ALD of several oxides (ZnO, Al<sub>2</sub>O<sub>3</sub>, TiO<sub>2</sub>, and SnO<sub>2</sub>) on PVF membranes (pore size: 200 nm) [65]. They have found that, among all the oxides, TiO<sub>2</sub> and SnO<sub>2</sub> surfaces have higher water molecule densities near the surface and thus stronger interactions with water (Fig. 5.5a-c). Consequently, a hydration layer is formed, which acts as a crude oil-repellant, hence limiting fouling by restricting direct contact between oil and surface. Zhou et al. have deposited TiO<sub>2</sub> on commercial RO and NF membranes [25]. The ALD cycles have been kept low to minimize the loss of PWP while maximizing the selectivity towards salts such as NaCl, CaCl<sub>2</sub>, and Na<sub>2</sub>SO<sub>4</sub>. Their results have demonstrated that high ALD cycles result in the formation of a nonporous dense layer, which greatly reduces the PWP. However, low ALD cycles (< 5) result in a high PWP and a high salt rejection. Huang et al. have used ALD in conjunction with the hydrothermal method to prepare ZnO nanowires on copper mesh for oil/water separation [73]. Under gravity-driven oil/water separation, a ZnO modified copper mesh have achieved a high separation efficiency of 97% coupled with a good stability in acidic, salty, and alkaline solutions.

#### 5.3.3.4 ALD integration with computational fluid dynamics

Most of the ALD studies have aimed to find the optimum ALD condition (precursor dose time, exposure time, etc.) via the trial-and-error method. Xiong et al. have taken a systematic approach and have employed computational fluid dynamics to find the optimum conditions for ALD of  $\text{Al}_2\text{O}_3$  on PTFE membranes [74]. After 100 cycles of ALD, hydrophobic membranes have been converted into hydrophilic membranes. By keeping the ALD cycles to a minimum, the trade-off between permeability and selectivity has been reduced, and the modified membranes have had both improved permeability and selectivity. Itzhak et al. have deposited alumina on two polymeric UF membranes, namely polyacrylonitrile and polyetherimide [75]. They have examined the effect of precursor exposure time on membrane performance. With short exposure times, a substantial layer of  $\text{Al}_2\text{O}_3$  is formed primarily at the membrane surface, leading to pore blockage and a corresponding reduction in PWP. In contrast, longer exposure times allows the  $\text{Al}_2\text{O}_3$  to distribute more uniformly across the membrane cross-section, preventing pore blockage and resulting in improved PWP. Membranes, modified with a low number of ALD cycles (10-30) and longer exposure times (10 seconds), exhibit a reduced oil coverage during oil/water emulsion separation and demonstrate effective fouling removal during crossflow cleaning.

The aforementioned applications and Table 5.2 highlight the usefulness of ALD for modifying the properties of polymeric membranes. Depending on the application, hydrophilic, hydrophobic, highly permeable, or highly selective membranes can be tailored. However, care must be taken to keep the ALD cycles to a minimum and allow the precursors to diffuse through the porous membrane to achieve both a high permeability and selectivity.

Table 5.2. ALD-modified organic membranes and their water filtration characteristics.

Substrate	Substrate Pore Size (nm)	Material Deposited by ALD	ALD Exposure Mode Included	Optimum ALD cycles*	Pore Size After ALD (nm)	Pure Water Flux L/(m <sup>2</sup> ·hr·bar)	Contaminant Targeted	Rejection (%)	Reference
Polycarbonate	30	Al <sub>2</sub> O <sub>3</sub>	No	100	ca. 19	5	Bovine serum albumin	ca. 77	[59]
PTFE	200	Al <sub>2</sub> O <sub>3</sub>	Yes	100	NR	210	Polystyrene	97	[26]
PTFE	200	TiO <sub>2</sub>	Yes	150	NR	ca. 4000	Silica nanospheres	35	[60]
PVDF	NR	TiO <sub>2</sub>	Yes	125	NR	ca. 190	Bovine serum albumin	97	[64]
PP	43	TiO <sub>2</sub>	Yes	100	NR	430	Silica nanospheres	55	[63]
Filter Paper (cotton fibers)	20k	Al <sub>2</sub> O <sub>3</sub>	Yes	90	NR	ca. 10	Diesel Oil	90	[61]
PP	43	Type 1: Al <sub>2</sub> O <sub>3</sub> Type 2: TiO <sub>2</sub>	Yes	100	NR	Type 1: ca. 600 Type 2: ca. 570	Silica nanospheres	Type 1: 95 Type 2: 92	[65]
PVDF	220	ZnO	Yes	100	NR	ca. 5000	Bovine serum albumin	96	[66]
polyethersulfone	NR	TiO <sub>2</sub>	No	100	NR	ca. 47	Sodium Chloride	90	[62]
NF90 (polyamide) NF270 (polyperazine)	NR	ZnO	No	-	-	-	-	-	[67]
PVDF	200	ZnO, Al <sub>2</sub> O <sub>3</sub> , TiO <sub>2</sub> , SnO <sub>2</sub>	No	-	-	-	-	-	[68]
Type 1: SW30 XLE Type 2: NF270	NR	TiO <sub>2</sub>	Yes	5	NR	(normalized permeability reported)	Sodium Chloride Calcium Chloride Sodium Sulfate	ca. 70 ca. 60 ca. 95 (reported for NF270 only)	[25]
Copper Mesh	NR	ZnO	Yes	100	NR	NR	Mineral Oil	99.7	[69]
PTFE	200	Al <sub>2</sub> O <sub>3</sub>	No	100	NR	185 (reported as PWP, LMH/bar)	Silica microspheres	ca. 93	[70]
Type 1: Polyacrylonitrile Type 2: Polyetherimide	16 21	Al <sub>2</sub> O <sub>3</sub>	Yes	50	10.6 14.1	ca. 120 ca. 100	-	-	[71]

### 5.3.4 ALD-modified Inorganic Membranes

The application of ALD for the modification of ceramic membranes is in its early stages of development (Fig. 5.6). From a wastewater treatment applications' perspective, ceramic membranes have gained attention due to their stability across temperature, pH, and pressure gradients [10]. Additionally, they offer a high PWP in comparison to organic membranes, which is highly desirable for large-scale industrial applications [11].

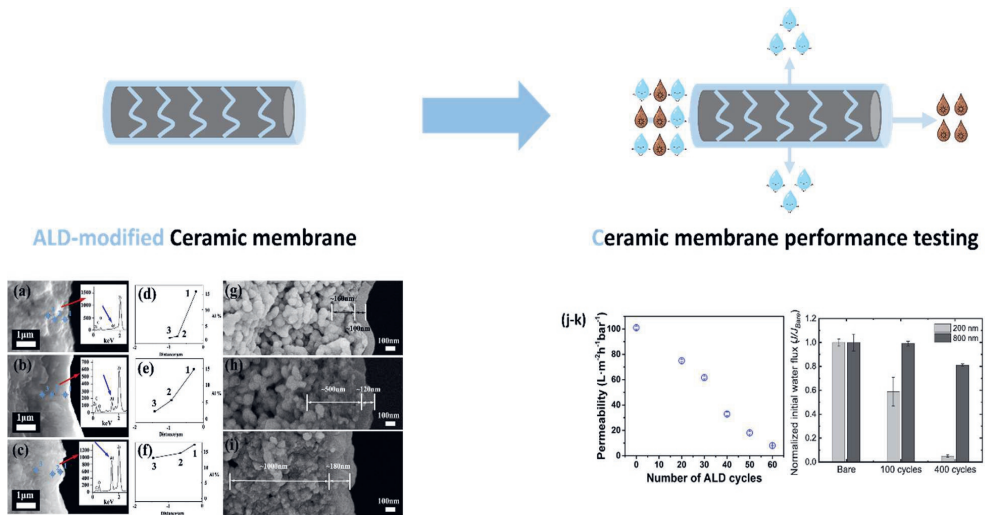


Figure 5.6. Performance enhancement of ceramic membranes via ALD.

(a-i) Cross-sectional SEM images and corresponding EDS spectra of  $\text{Al}_2\text{O}_3$ -coated  $\text{ZrO}_2\text{-Al}_2\text{O}_3$  membranes deposited with 600 ALD cycles at varying precursor exposure times: (a, d, and g) 0s; (b, e, and h) 10s; (c, f, and i) 40s. Adapted with permission from [76].

(j) Water permeability of  $\text{TiO}_2$ -coated  $\text{TiO}_2\text{-Al}_2\text{O}_3$  membranes as a function of ALD cycle number. Adapted with permission from [77].

(k) Pure water flux of  $\text{ZnO}$ -coated  $\text{ZrO}_2\text{-TiO}_2$  membranes of different nominal pore sizes as a function of ALD cycles. Adapted with permission from [78].

#### 5.3.4.1 Tailoring pore structure and selectivity: ALD of Al<sub>2</sub>O<sub>3</sub>

In comparison with the sol-gel technique, the application of a selective layer on ceramic membranes by ALD can result in (i) processing costs reduction, (ii) precise structural control of the selective layer, and (iii) precise pore size reduction of the ceramic membranes [42]. To the best of our knowledge, the pioneering work on the modification of commercially available ceramic membranes for wastewater treatment has been performed by Li et al. in 2012 [76]. They have utilized a commercially available Al<sub>2</sub>O<sub>3</sub> MF membrane with a zirconia (ZrO<sub>2</sub>) selective layer (pore size: 50 nm), produced by JIUWU HI-TECH China, and have modified its pore size by the ALD of Al<sub>2</sub>O<sub>3</sub>. They have coated the membranes with different ALD cycles and have observed that upon 600 cycles, an ultrathin layer of Al<sub>2</sub>O<sub>3</sub> is formed adjacent to the surface of the ZrO<sub>2</sub> layer. SEM analysis has revealed that the new layer consists of a dense sublayer in tandem with a transition sublayer, forming a selective layer in the form of a thin film coating around the ZrO<sub>2</sub> particles. Additionally, they have discovered that allowing the precursors to stay in the chamber after dosing allows the precursors to diffuse into longer depths in the pores (Fig. 5.6a-i). Membrane performance tests show that the modified membrane has a PWP of 118 L·h<sup>-1</sup>·m<sup>-2</sup>·bar<sup>-1</sup> and a BSA retention of 97%, thus proving the presence of small pores in the newly formed selective layer. Consistent with previous studies, trade-off between selectivity and permeability has been observed, because the membranes, modified at a lower number of ALD cycles, i.e., 100, 200, 300, and 400, have a comparatively high PWP but a lower BSA retention.

#### 5.3.4.2 Engineering nanoporous selective layers: ALD of TiO<sub>2</sub>

If the kinetic diameter of the precursors is larger than the pore size of the substrate, then precursors do not diffuse into the membrane pores. Similarly, if the pore size is slightly larger than the kinetic diameter of precursor molecules, then once a thin film is formed in the pores of the support



membrane, after the first few ALD cycles, further diffusion of the precursor molecules is hindered due to narrowing of the pore aperture [12]. The subsequent thin film layer, deposited on the surface of the membrane, then leads to pore blocking, adversely affecting the PWP. Thus, either the thin film is only formed in the pores of the membrane or the newly formed surface layer must be sufficiently porous to avoid huge reduction of the PWP of the membrane. Chen et al. have developed a strategy to convert the dense surface layer into a microporous layer [79]. They have utilized a modified ALD process that relies on alcohols rather than water as the oxidizing precursor and have deposited a thin film of titanium alkoxide in the pores and also on surface of the  $\alpha$ - $\text{Al}_2\text{O}_3$  ultrafiltration membrane, having a  $\text{TiO}_2$  selective layer (pore size: 5 nm). In a subsequent calcination process, they have burned off the organic moieties, thus generating a microporous  $\text{TiO}_2$  layer. They have observed that after 300 cycles of ALD and a calcination step at  $400^\circ\text{C}$  for 2 h, the initial ultrafiltration membrane is converted into a nanofiltration membrane having a pore size of 1.3 nm, water permeability of  $30 \text{ L}\cdot\text{h}^{-1}\cdot\text{m}^{-2}\cdot\text{bar}^{-1}$ , and polyethylene glycol molecular weight cut-off of 680 Da. Shang et al. have modified the active pore size of the commercial  $\text{Al}_2\text{O}_3$  NF membranes having a  $\text{TiO}_2$  selective layer (pore size: 0.7 nm) by AP-ALD [24]. They have reported that after 1-3 cycles of AP-ALD of  $\text{TiO}_2$ , the size of the active pores, present on the surface of the membrane, decreases from 0.7 nm to 0.5 nm. Consequently, after 3 cycles, the PWP reduces from  $26 \text{ L}\cdot\text{h}^{-1}\cdot\text{m}^{-2}\cdot\text{bar}^{-1}$  to  $11 \text{ L}\cdot\text{h}^{-1}\cdot\text{m}^{-2}\cdot\text{bar}^{-1}$ , and the polyethylene glycol molecular weight cut-off reduces from 490 Da to 277 Da. The reported PWP values are higher than the commercial polymeric NF90 and NF270 NF membranes and sol-gel-made tight ceramic nanofiltration membranes, thus proving the effectiveness of ALD for ceramic membrane modification.

ALD has also been used to impart photocatalytic properties to ceramic membranes for degradation of organic dyes. Berger et al. have coated commercially available anodized  $\text{Al}_2\text{O}_3$  MF (pore size:

200 nm) and UF (pore size: 20 nm) membranes with TiO<sub>2</sub> by ALD for photocatalytic degradation of MB [80]. The PWP of the MF membrane decreases from 3800 L·h<sup>-1</sup>·m<sup>-2</sup>·bar<sup>-1</sup> to 2300 L·h<sup>-1</sup>·m<sup>-2</sup>·bar<sup>-1</sup> upon coating a TiO<sub>2</sub> layer of 6 nm in thickness, and that of UF membrane from 1100 L·h<sup>-1</sup>·m<sup>-2</sup>·bar<sup>-1</sup> to 400 L·h<sup>-1</sup>·m<sup>-2</sup>·bar<sup>-1</sup> upon coating a layer of 15 nm in thickness, respectively. Subsequently, they have observed that the removal of the MB from the feed increases with increasing thickness of the coating layer up to a certain extent. For the UF membrane, the removal efficiency increases up to a coating thickness of 6 nm, but beyond that point, the layer thickness is no longer the limiting factor. In another report, published by Chen et al., TiO<sub>2</sub> has been deposited on a commercial  $\alpha$ -Al<sub>2</sub>O<sub>3</sub> UF membrane having a TiO<sub>2</sub> selective layer (pore size 5 nm) [77]. They have operated ALD in the non-exposure mode, avoiding the diffusion of the precursors in the pores of the membrane, allowing the deposition to take place in the near-surface region only, and avoiding pore narrowing and the resultant decrease of the PWP. After 40 cycles of ALD, the polyethylene glycol MWCO decreases from 7200 Da to 890 Da, and the PWP decreases from 100 L·h<sup>-1</sup>·m<sup>-2</sup>·bar<sup>-1</sup> to 32 L·h<sup>-1</sup>·m<sup>-2</sup>·bar<sup>-1</sup>, respectively (Fig. 5.6j). Furthermore, they have observed that if the membrane and target molecules have the same charge, it results in a higher retention of the molecules due to electrostatic repulsion. After 40 cycles of ALD, the membrane exhibit a rejection of ca. 93% for negatively charged dyes (Rose Bengal and Reactive Black 5), whereas, the rejection for positively charged dye (Cationic Yellow X-2RL) is only 42%, respectively.

#### 5.3.4.3 Emerging applications in photocatalysis: ALD of ZnO

The studies on ALD of ZnO are scarce. Recently, Park et al. have deposited a photocatalytically active ZnO film on the Sterlitech USA ZrO<sub>2</sub>-TiO<sub>2</sub> membrane (pore size: 200 nm, 800 nm), and have tested it for the degradation of the 4-cholorobenzoic acid [78]. They have observed a decrease

of the PWP of the membranes after the ZnO deposition (Fig. 5.6k). However, the deposited ZnO has shown a higher degradation activity compared to the bare membrane. In addition, the accumulation of the 4-cholorobenzoic acid on the bare membrane has resulted in the formation of a biofilm, which greatly reduces the PWP of the bare membrane. In contrast, the ZnO deposited membrane alleviates the formation of biofilm, consequently maintaining the intrinsic PWP.

The aforementioned studies highlight the importance of ceramic membrane modification by ALD. The current research focus has been on oxide ceramic materials. Furthermore, a comparison of these membranes is presented in Table 5.3.

Table 5.3. ALD-modified ceramic membranes and their water filtration characteristics.

Substrate	Substrate Pore Size (nm)	Material Deposited by ALD	ALD Exposure Mode Included	Optimum ALD cycles*	Pore Size after ALD Modification (nm)	Contaminant Targeted	MWCO (Da)	Rejection (%)	Pure Water Flux L/(m <sup>2</sup> .h.bar)	Reference
Al <sub>2</sub> O <sub>3</sub> with ZrO <sub>2</sub> selective layer	50	Al <sub>2</sub> O <sub>3</sub>	Yes	600	NR	bovine serum albumin	NR	97	118	[72]
Al <sub>2</sub> O <sub>3</sub> with TiO <sub>2</sub> selective layer	5	Titanitcone	No	300	1.3	polyethylene glycol	680	97 (for PEG of 1000 Da)	30	[73]
Al <sub>2</sub> O <sub>3</sub> with TiO <sub>2</sub> selective layer	0.7	TiO <sub>2</sub>	Yes	3	0.5	polyethylene glycol	277	95	11	[24]
Al <sub>2</sub> O <sub>3</sub> with TiO <sub>2</sub> selective layer	5	TiO <sub>2</sub>	No	40	1.5	polyethylene glycol	890	90 (for PEG) 93 (for Rose Bengal & Reactive Black-5) 42 (for Cationic Yellow X-2RL)	32	[74]
Al <sub>2</sub> O <sub>3</sub>	Type 1: 200 Type 2: 20	TiO <sub>2</sub>	No	NR	-	-	-	-	Type 1: 2300 Type 2: 400	[75]
ZrO <sub>2</sub> -TiO <sub>2</sub>	Type 1: 200 Type 2: 800	ZnO	No	NR	-	4-chlorobenzoic acid	-	Type 2: 85% (for light intensity 10 mw/cm <sup>2</sup> ) 30% (for light intensity 10 mw/cm <sup>2</sup> )	(reported as normalized flux)	[76]

## **5.4 Challenges and Opportunities**

The applications, highlighted in this review, depict that atomically engineered materials for wastewater treatment can be realized with the help of ALD. Highly conformal coatings ranging in thickness from several angstroms to nanometres can impart desirable properties to materials without changing the fundamental chemistry of the materials [81]. Based on the literature review, the following sub-sections serve as a guide for interested researchers highlighting potential research areas.

### **5.4.1 Structural considerations**

The ALD on/in porous structures comes with its own challenges. Unlike flat non-porous substrates used in the semiconductor industry, porous substrates are characterized by having: (i) high aspect ratios [82-84]; (ii) varying pore size distribution [85]; (iii) different geometry of pores on the surface and in the bulk of the material [86]; and (v) accessible/inaccessible (open/closed) pores [87]. Therefore, before proceeding to ALD, the aforementioned characteristics of the material must be studied with available characterization techniques. Once a proper understanding has been established, then precursors with adequate kinetic diameter (smaller than pore aperture) should be selected to ensure sufficient diffusion of the precursors [88, 89]. To facilitate greater diffusion of precursors, ALD must be operated in exposure mode [90]. In principle, this would result in the formation of a conformal thin film on/in the substrate. The deposition cycles should be set to a minimum so that there is not a high loss of PWP, and an optimum between permeability and selectivity can be achieved.

### **5.4.2 Pre-treatment of substrate**

The precursors in ALD half-cycles react with functional groups of the surface. If a material's surface has a high density of functional groups, then the deposition will proceed in the form of a

continuous thin film. However, the absence of functional groups will lead to the growth of material in the form of distinct islands, which will subsequently coalesce to form a film, mainly when the material-to-be-deposited differs from the substrate [19] [91].

We found only a few studies that reported the adhesion strength of the film on the substrate [92-94]. This element should not be ignored while designing experiments and should be tested and reported.

ALD can be carried out at low-deposition temperatures, so various materials can be modified. If the substrate material is inert, e.g. polymeric material, then a pre-treatment step should be included to render the material reactive. Several strategies could be utilized for this purpose, namely, plasma pre-treatment step, chemical activation, or even an activation step in the ALD chamber utilizing different precursors.

### **5.4.3 ALD materials of focus**

Critical analysis of the ALD literature for wastewater treatment applications shows that the main focus of the majority of research groups is on oxide materials ( $\text{Al}_2\text{O}_3$ ,  $\text{TiO}_2$ ,  $\text{ZnO}$ ,  $\text{ZrO}_2$ ) [95]. However, expanding the list of deposition materials to carbides and nitrides could have the advantage of preparing adsorbents and membranes with improved hydrophilicity, highly negative charge, and low fouling [41, 96].

### **5.4.4 Simulation studies**

Most of the conducted studies try to find the optimum deposition conditions via the trial-and-error method. This is a time-consuming process and often results in suboptimal deposition conditions. Therefore, we propose that simulation studies should precede ALD experimental studies. The simulation studies, e.g. through computational fluid dynamics and density functional theory, would give insights about: (i) suitable precursors; (ii) the behavior of the precursors in the reaction

chamber; (iii) reaction kinetics; and (iv) confirm self-limiting nature of reactions [40, 43]. This allows to select the best precursors and deposition conditions for the particular application.

#### **5.4.5 In-situ characterizations of thin films**

The porosity and pore size of the porous materials decreases as a function of the deposition cycles in the ALD furnace/chamber. However, currently, in situ measurements of pore size are not available. Usually, a Si wafer is placed next to the substrate in the ALD chamber, and the thickness of the film as a function of deposition cycles is measured on the silicon wafer via ellipsometry [97, 98]. The growth behavior on a Si wafer will be different than a porous material due to different: (i) coefficient of thermal expansion; (ii) functional groups; and (iii) lattice mismatch. We therefore propose that ALD chambers must be manufactured with in-situ techniques that can measure the change in porosity, pore size, or stoichiometry of the film.

#### **5.4.6 Scalability for mass production**

ALD has already been commercialized for the production of wafers. However, the commercialization of ALD for manufacturing membranes or sorbents will still need considerable efforts. In our opinion, atmospheric pressure-ALD has the highest potential to be scaled-up to mass production for wastewater treatment applications [24, 99].

### **5.5 Conclusions**

Urban and industrial sectors produce millions of cubic meters of wastewater per annum, which frequently undergoes minor or no treatment before it is discharged. This, in conjunction with water scarcity, leads to water stress which, is a major societal concern. This problem can be tackled by nanoscale engineering of wastewater treatment materials (membranes and adsorbents). Recent breakthroughs in manufacturing methods have paved the way to coat porous materials with

ultrathin films to alter their surface properties and pore size. Consequently, rationalizing the design of porous materials with exceptional filtration capabilities.

ALD can deposit a thin film of variety of materials on a substrate of any geometry, for instance porous materials. The technique is, therefore, being currently explored for modification of membranes and adsorbents. ALD is employed as a post-modification step to coat wastewater treatment materials with a functional thin film of a desired material. The material to be coated is chosen on the basis of the properties required for a particular application, for example hydrophilicity, pore size, and surface charge. This opens up new routes for preparing wastewater treatment materials with precise pore size, surface charge, permeability, and selectivity.

All the advances reported in this review illustrate the potential of ALD to obtain porous materials with high filtration efficiency. Results of various studies demonstrate that ALD-modified materials possess superior wastewater filtration characteristics than unmodified materials. The interest of wastewater treatment research groups all over the world in ALD has pushed forth the boundary of knowledge. However, there are challenges and opportunities to be addressed for commercialization of ALD processes for modifying membranes and adsorbents.



## References

- [1] S. United Nations Educational, C. Organization, The United Nations World Water Development Report 2021, United Nations2021.
- [2] U. Water, Sustainable Development Goal 6 synthesis report on water and sanitation, Published by the United Nations New York, New York 10017 (2018).
- [3] G. Crini, E. Lichtfouse, Wastewater treatment: an overview, Green adsorbents for pollutant removal: fundamentals and design (2018) 1-21.
- [4] W.W.A.P. UNESCO, The United Nations world water development report, 2017: Wastewater: the untapped resource, UNESCO, 2017.
- [5] E. Eray, V.M. Candelario, V. Boffa, H. Safafar, D.N. Østedgaard-Munck, N. Zahrtmann, H. Kadrispahic, M.K. Jørgensen, A roadmap for the development and applications of silicon carbide membranes for liquid filtration: Recent advancements, challenges, and perspectives, Chemical Engineering Journal 414 (2021).
- [6] O.R.N. Laboratory, Materials for Separation Technologies. Energy and Emission Reduction Opportunities, United States, 2005, p. Medium: ED; Size: 118 p.
- [7] M.M. Pendergast, E.M. Hoek, A review of water treatment membrane nanotechnologies, Energy & Environmental Science 4(6) (2011) 1946-1971.
- [8] Z. He, Z. Lyu, Q. Gu, L. Zhang, J. Wang, Ceramic-based membranes for water and wastewater treatment, Colloids and Surfaces A: Physicochemical and Engineering Aspects 578 (2019) 123513.
- [9] C. Detavernier, J. Dendooven, S.P. Sree, K.F. Ludwig, J.A. Martens, Tailoring nanoporous materials by atomic layer deposition, Chem Soc Rev 40(11) (2011) 5242-53.
- [10] Z. He, Z. Lyu, Q. Gu, L. Zhang, J. Wang, Ceramic-based membranes for water and wastewater treatment, Colloids and Surfaces A: Physicochemical and Engineering Aspects 578 (2019).
- [11] C. Li, W. Sun, Z. Lu, X. Ao, S. Li, Ceramic nanocomposite membranes and membrane fouling: A review, Water Res 175 (2020) 115674.
- [12] M. Weber, A. Julbe, A. Ayril, P. Miele, M. Bechelany, Atomic Layer Deposition for Membranes: Basics, Challenges, and Opportunities, Chemistry of Materials 30(21) (2018) 7368-7390.
- [13] P.M. Martin, Handbook of deposition technologies for films and coatings : science, applications and technology, (2009).
- [14] W. Kern, K.K. Schuegraf, Deposition technologies and applications: Introduction and overview, Handbook of Thin Film Deposition Processes and Techniques, Elsevier2001, pp. 11-43.
- [15] H.O. Pierson, 2 - Fundamentals of Chemical Vapor Deposition, in: H.O. Pierson (Ed.), Handbook of Chemical Vapor Deposition (CVD) (Second Edition), William Andrew Publishing, Norwich, NY, 1999, pp. 36-67.
- [16] J. Creighton, P. Ho, Introduction to Chemical Vapor Deposition (CVD), ASM International (2001).
- [17] J.-O. Carlsson, P.M. Martin, Chemical vapor deposition, Handbook of Deposition Technologies for films and coatings, Elsevier2010, pp. 314-363.
- [18] M. Miao, T. Liu, J. Bai, Y. Wang, Engineering the wetting behavior of ceramic membrane by carbon nanotubes via a chemical vapor deposition technique, Journal of Membrane Science 648 (2022) 120357.
- [19] J. Greene, Thin film nucleation, growth, and microstructural evolution: an atomic scale view, Handbook of Deposition Technologies for Films and Coatings, Elsevier2010, pp. 554-620.

- [20] H.O. Pierson, Handbook of chemical vapor deposition: principles, technology and applications, William Andrew 1999.
- [21] S.M. George, Atomic Layer Deposition: An Overview, Chemical Reviews 110(1) (2010) 111-131.
- [22] A. Pakkala, M. Putkonen, Atomic layer deposition, Handbook of deposition technologies for films and coatings, Elsevier 2010, pp. 364-391.
- [23] Y. Hu, J. Lu, H. Feng, Surface modification and functionalization of powder materials by atomic layer deposition: a review, RSC Adv 11(20) (2021) 11918-11942.
- [24] R. Shang, A. Goulas, C.Y. Tang, X. de Frias Serra, L.C. Rietveld, S.G.J. Heijman, Atmospheric pressure atomic layer deposition for tight ceramic nanofiltration membranes: Synthesis and application in water purification, Journal of Membrane Science 528 (2017) 163-170.
- [25] X. Zhou, Y.Y. Zhao, S.R. Kim, M. Elimelech, S. Hu, J.H. Kim, Controlled TiO<sub>2</sub> Growth on Reverse Osmosis and Nanofiltration Membranes by Atomic Layer Deposition: Mechanisms and Potential Applications, Environ Sci Technol 52(24) (2018) 14311-14320.
- [26] Q. Xu, Y. Yang, X. Wang, Z. Wang, W. Jin, J. Huang, Y. Wang, Atomic layer deposition of alumina on porous polytetrafluoroethylene membranes for enhanced hydrophilicity and separation performances, Journal of Membrane Science 415-416 (2012) 435-443.
- [27] N. Li, Y. Tian, J. Zhang, Z. Sun, J. Zhao, J. Zhang, W. Zuo, Precisely-controlled modification of PVDF membranes with 3D TiO<sub>2</sub>/ZnO nanolayer: enhanced anti-fouling performance by changing hydrophilicity and photocatalysis under visible light irradiation, Journal of Membrane Science 528 (2017) 359-368.
- [28] G. Mahmodi, A. Ronte, S. Dangwal, P. Wagle, E. Echeverria, B. Sengupta, V. Vatanpour, D.N. McIlroy, J.D. Ramsey, S.-J. Kim, Improving antifouling property of alumina microfiltration membranes by using atomic layer deposition technique for produced water treatment, Desalination 523 (2022) 115400.
- [29] R.W. Johnson, A. Hultqvist, S.F. Bent, A brief review of atomic layer deposition: from fundamentals to applications, Materials today 17(5) (2014) 236-246.
- [30] A.H. Behroozi, V. Vatanpour, L. Meunier, M. Mehrabi, E.H. Koupaie, Membrane Fabrication and Modification by Atomic Layer Deposition: Processes and Applications in Water Treatment and Gas Separation, ACS Applied Materials & Interfaces 15(11) (2023) 13825-13843.
- [31] J. Lee, I.S. Kim, M.-H. Hwang, K.-J. Chae, Atomic layer deposition and electrospinning as membrane surface engineering methods for water treatment: a short review, Environmental Science: Water Research & Technology 6(7) (2020) 1765-1785.
- [32] S. Xiong, X. Qian, Z. Zhong, Y. Wang, Atomic layer deposition for membrane modification, functionalization and preparation: A review, Journal of Membrane Science 658 (2022) 120740.
- [33] H.C. Yang, R.Z. Waldman, Z. Chen, S.B. Darling, Atomic layer deposition for membrane interface engineering, Nanoscale 10(44) (2018) 20505-20513.
- [34] R. Li, N. Li, J. Hou, Y. Yu, L. Liang, B. Yan, G. Chen, Aquatic environment remediation by atomic layer deposition-based multi-functional materials: A review, J Hazard Mater 402 (2021) 123513.
- [35] X. Yang, A.B. Martinson, J.W. Elam, L. Shao, S.B. Darling, Water treatment based on atomically engineered materials: Atomic layer deposition and beyond, Matter 4(11) (2021) 3515-3548.

- [36] A.A. Malygin, V.E. Drozd, A.A. Malkov, V.M. Smirnov, From V. B. Aleskovskii's "Framework" Hypothesis to the Method of Molecular Layering/Atomic Layer Deposition Chemical Vapor Deposition 21(10-11-12) (2015) 216-240.
- [37] R.L. Puurunen, A Short History of Atomic Layer Deposition: Tuomo Suntola's Atomic Layer Epitaxy, Chemical Vapor Deposition 20(10-11-12) (2014) 332-344.
- [38] N. Pinna, M. Knez, Atomic layer deposition of nanostructured materials, John Wiley & Sons 2012.
- [39] R.L. Puurunen, Surface chemistry of atomic layer deposition: A case study for the trimethylaluminum/water process, Journal of applied physics 97(12) (2005).
- [40] E.A. Filatova, D. Hausmann, S.D. Elliott, Investigating routes toward atomic layer deposition of silicon carbide: Ab initio screening of potential silicon and carbon precursors, Journal of Vacuum Science & Technology A: Vacuum, Surfaces, and Films 35(1) (2017).
- [41] M. Fraga, R. Pessoa, Progresses in Synthesis and Application of SiC Films: From CVD to ALD and from MEMS to NEMS, Micromachines (Basel) 11(9) (2020).
- [42] M. Weber, A. Julbe, S.S. Kim, M. Bechelany, Atomic layer deposition (ALD) on inorganic or polymeric membranes, Journal of Applied Physics 126(4) (2019).
- [43] E.A. Filatova, D. Hausmann, S.D. Elliott, Understanding the Mechanism of SiC Plasma-Enhanced Chemical Vapor Deposition (PECVD) and Developing Routes toward SiC Atomic Layer Deposition (ALD) with Density Functional Theory, ACS Applied Materials & Interfaces 10(17) (2018) 15216-15225.
- [44] M. Leskelä, M. Ritala, Atomic layer deposition (ALD): from precursors to thin film structures, Thin solid films 409(1) (2002) 138-146.
- [45] M. Ritala, M. Leskelä, Atomic layer deposition, Handbook of Thin Films, Elsevier 2002, pp. 103-159.
- [46] R. Grubbs, S. George, Attenuation of hydrogen radicals traveling under flowing gas conditions through tubes of different materials, Journal of Vacuum Science & Technology A: Vacuum, Surfaces, and Films 24(3) (2006) 486-496.
- [47] L. Niinistö, M. Nieminen, J. Päiväsäari, J. Niinistö, M. Putkonen, M. Nieminen, Advanced electronic and optoelectronic materials by Atomic Layer Deposition: An overview with special emphasis on recent progress in processing of high-k dielectrics and other oxide materials, physica status solidi (a) 201(7) (2004) 1443-1452.
- [48] T. Suntola, Surface chemistry of materials deposition at atomic layer level, Applied Surface Science 100 (1996) 391-398.
- [49] N.K. Dey, M.J. Kim, K.-D. Kim, H.O. Seo, D. Kim, Y.D. Kim, D.C. Lim, K.H. Lee, Adsorption and photocatalytic degradation of methylene blue over TiO<sub>2</sub> films on carbon fiber prepared by atomic layer deposition, Journal of Molecular Catalysis A: Chemical 337(1-2) (2011) 33-38.
- [50] H.O. Seo, C.W. Sim, K.-D. Kim, Y.D. Kim, D.C. Lim, Nanoporous TiO<sub>2</sub>/SiO<sub>2</sub> prepared by atomic layer deposition as adsorbents of methylene blue in aqueous solutions, Chemical Engineering Journal 183 (2012) 381-386.
- [51] X. Wang, A.R. Donovan, R.L. Patel, H. Shi, X. Liang, Adsorption of metal and metalloid ions onto nanoporous microparticles functionalized by atomic layer deposition, Journal of Environmental Chemical Engineering 4(4) (2016) 3767-3774.
- [52] B. Jeong, D.H. Kim, E.J. Park, M.-G. Jeong, K.-D. Kim, H.O. Seo, Y.D. Kim, S. Uhm, ZnO shell on mesoporous silica by atomic layer deposition: Removal of organic dye in water by an adsorbent and its photocatalytic regeneration, Applied Surface Science 307 (2014) 468-474.

- [53] N. Li, Y. Tian, J. Zhao, J. Zhang, J. Zhang, W. Zuo, Y. Ding, Efficient removal of chromium from water by Mn<sub>3</sub>O<sub>4</sub>@ZnO/Mn<sub>3</sub>O<sub>4</sub> composite under simulated sunlight irradiation: Synergy of photocatalytic reduction and adsorption, *Applied Catalysis B: Environmental* 214 (2017) 126-136.
- [54] N. Li, J. Zhang, Y. Tian, J. Zhao, J. Zhang, W. Zuo, Precisely controlled fabrication of magnetic 3D  $\gamma$ -Fe<sub>2</sub>O<sub>3</sub>@ZnO core-shell photocatalyst with enhanced activity: Ciprofloxacin degradation and mechanism insight, *Chemical Engineering Journal* 308 (2017) 377-385.
- [55] A. Di Mauro, M. Cantarella, G. Nicotra, V. Privitera, G. Impellizzeri, Low temperature atomic layer deposition of ZnO: Applications in photocatalysis, *Applied Catalysis B: Environmental* 196 (2016) 68-76.
- [56] A.E. Short, S.V. Pamidi, Z.E. Bloomberg, Y. Li, M.D. Losego, Atomic layer deposition (ALD) of subnanometer inorganic layers on natural cotton to enhance oil sorption performance in marine environments, *Journal of Materials Research* 34(4) (2019) 563-570.
- [57] S. Xiong, Y. Yang, Z. Zhong, Y. Wang, One-Step Synthesis of Carbon-Hybridized ZnO on Polymeric Foams by Atomic Layer Deposition for Efficient Absorption of Oils from Water, *Industrial & Engineering Chemistry Research* 57(4) (2018) 1269-1276.
- [58] J. You, Y. Zhao, L. Wang, W. Bao, Y. He, Atomic layer deposition of  $\gamma$ -Fe<sub>2</sub>O<sub>3</sub> nanoparticles on modified MWCNT for efficient adsorption of Cr(VI) ions from aqueous solution, *Journal of Physics and Chemistry of Solids* 142 (2020).
- [59] E. Iakovleva, P. Maydannik, T.V. Ivanova, M. Sillanpää, W.Z. Tang, E. Mäkilä, J. Salonen, A. Gubal, A.A. Ganeev, K. Kamwilaisak, S. Wang, Modified and unmodified low-cost iron-containing solid wastes as adsorbents for efficient removal of As(III) and As(V) from mine water, *Journal of Cleaner Production* 133 (2016) 1095-1104.
- [60] X. Wang, M.R. Bayan, M. Yu, D.K. Ludlow, X. Liang, Atomic layer deposition surface functionalized biochar for adsorption of organic pollutants: improved hydrophilia and adsorption capacity, *International Journal of Environmental Science and Technology* 14(9) (2017) 1825-1834.
- [61] E. Iakovleva, M. Sillanpää, C. Mangwandi, A.B. Albadarin, P. Maydannik, S. Khan, V. Srivastava, K. Kamwilaisak, S. Wang, Application of Al<sub>2</sub>O<sub>3</sub> modified sulfate tailings (CaFe-Cake and SuFe) for efficient removal of cyanide ions from mine process water, *Minerals Engineering* 118 (2018) 24-32.
- [62] M.O. Mavukkandy, S.A. McBride, D.M. Warsinger, N. Dizge, S.W. Hasan, H.A. Arafat, Thin film deposition techniques for polymeric membranes– A review, *Journal of Membrane Science* 610 (2020) 118258.
- [63] F. Li, L. Li, X. Liao, Y. Wang, Precise pore size tuning and surface modifications of polymeric membranes using the atomic layer deposition technique, *Journal of Membrane Science* 385-386 (2011) 1-9.
- [64] Q. Xu, Y. Yang, J. Yang, X. Wang, Z. Wang, Y. Wang, Plasma activation of porous polytetrafluoroethylene membranes for superior hydrophilicity and separation performances via atomic layer deposition of TiO<sub>2</sub>, *Journal of Membrane Science* 443 (2013) 62-68.
- [65] H.C. Yang, Y. Xie, H. Chan, B. Narayanan, L. Chen, R.Z. Waldman, S. Sankaranarayanan, J.W. Elam, S.B. Darling, Crude-Oil-Repellent Membranes by Atomic Layer Deposition: Oxide Interface Engineering, *ACS Nano* 12(8) (2018) 8678-8685.
- [66] Q. Wang, X. Wang, Z. Wang, J. Huang, Y. Wang, PVDF membranes with simultaneously enhanced permeability and selectivity by breaking the tradeoff effect via atomic layer deposition of TiO<sub>2</sub>, *Journal of Membrane Science* 442 (2013) 57-64.

- [67] Q. Xu, J. Yang, J. Dai, Y. Yang, X. Chen, Y. Wang, Hydrophilization of porous polypropylene membranes by atomic layer deposition of TiO<sub>2</sub> for simultaneously improved permeability and selectivity, *Journal of Membrane Science* 448 (2013) 215-222.
- [68] H. Chen, L. Kong, Y. Wang, Enhancing the hydrophilicity and water permeability of polypropylene membranes by nitric acid activation and metal oxide deposition, *Journal of Membrane Science* 487 (2015) 109-116.
- [69] L. Kong, Q. Wang, S. Xiong, Y. Wang, Turning Low-Cost Filter Papers to Highly Efficient Membranes for Oil/Water Separation by Atomic-Layer-Deposition-Enabled Hydrophobization, *Industrial & Engineering Chemistry Research* 53(42) (2014) 16516-16522.
- [70] J. Alam, M. Alhoshan, L.A. Dass, A.K. Shukla, M.R. Muthumareeswaran, M. Hussain, A.S. Aldwayyan, Atomic layer deposition of TiO<sub>2</sub> film on a polyethersulfone membrane: separation applications, *Journal of Polymer Research* 23(9) (2016).
- [71] N. Li, J. Zhang, Y. Tian, J. Zhang, W. Zhan, J. Zhao, Y. Ding, W. Zuo, Hydrophilic modification of polyvinylidene fluoride membranes by ZnO atomic layer deposition using nitrogen dioxide/diethylzinc functionalization, *Journal of Membrane Science* 514 (2016) 241-249.
- [72] P. Juholin, M.-L. Kääriäinen, M. Riihimäki, R. Sliz, J.L. Aguirre, M. Pirilä, T. Fabritius, D. Cameron, R.L. Keiski, Comparison of ALD coated nanofiltration membranes to unmodified commercial membranes in mine wastewater treatment, *Separation and Purification Technology* 192 (2018) 69-77.
- [73] A. Huang, C.-C. Kan, S.-C. Lo, L.-H. Chen, D.-Y. Su, J.F. Soesanto, C.-C. Hsu, F.-Y. Tsai, K.-L. Tung, Nanoarchitected design of porous ZnO@copper membranes enabled by atomic-layer-deposition for oil/water separation, *Journal of Membrane Science* 582 (2019) 120-131.
- [74] S. Xiong, X. Jia, K. Mi, Y. Wang, Upgrading polytetrafluoroethylene hollow-fiber membranes by CFD-optimized atomic layer deposition, *Journal of Membrane Science* 617 (2021).
- [75] T. Itzhak, N. Segev-Mark, A. Simon, V. Abetz, G.Z. Ramon, T. Segal-Peretz, Atomic Layer Deposition for Gradient Surface Modification and Controlled Hydrophilization of Ultrafiltration Polymer Membranes, *ACS Appl Mater Interfaces* 13(13) (2021) 15591-15600.
- [76] F. Li, Y. Yang, Y. Fan, W. Xing, Y. Wang, Modification of ceramic membranes for pore structure tailoring: The atomic layer deposition route, *Journal of Membrane Science* 397-398 (2012) 17-23.
- [77] H. Chen, S. Wu, X. Jia, S. Xiong, Y. Wang, Atomic layer deposition fabricating of ceramic nanofiltration membranes for efficient separation of dyes from water, *AIChE Journal* 64(7) (2018) 2670-2678.
- [78] K.-H. Park, P.-F. Sun, E.H. Kang, G.D. Han, B.J. Kim, Y. Jang, S.-H. Lee, J.H. Shim, H.-D. Park, Photocatalytic anti-biofouling performance of nanoporous ceramic membranes treated by atomic layer deposited ZnO, *Separation and Purification Technology* 272 (2021).
- [79] H. Chen, X. Jia, M. Wei, Y. Wang, Ceramic tubular nanofiltration membranes with tunable performances by atomic layer deposition and calcination, *Journal of Membrane Science* 528 (2017) 95-102.
- [80] T.E. Berger, C. Regmi, A.I. Schäfer, B.S. Richards, Photocatalytic degradation of organic dye via atomic layer deposited TiO<sub>2</sub> on ceramic membranes in single-pass flow-through operation, *Journal of Membrane Science* 604 (2020).
- [81] P. Chen, T. Mitsui, D.B. Farmer, J. Golovchenko, R.G. Gordon, D. Branton, Atomic layer deposition to fine-tune the surface properties and diameters of fabricated nanopores, *Nano letters* 4(7) (2004) 1333-1337.

- [82] J. Dendooven, K. Devloo-Casier, E. Levrau, R. Van Hove, S. Pulinthanathu Sree, M.R. Baklanov, J.A. Martens, C. Detavernier, In situ monitoring of atomic layer deposition in nanoporous thin films using ellipsometric porosimetry, *Langmuir* 28(8) (2012) 3852-3859.
- [83] R.G. Gordon, D. Hausmann, E. Kim, J. Shepard, A kinetic model for step coverage by atomic layer deposition in narrow holes or trenches, *Chemical Vapor Deposition* 9(2) (2003) 73-78.
- [84] T. Keuter, N.H. Menzler, G. Mauer, F. Vondahlen, R. Vaßen, H.P. Buchkremer, Modeling precursor diffusion and reaction of atomic layer deposition in porous structures, *Journal of Vacuum Science & Technology A: Vacuum, Surfaces, and Films* 33(1) (2015) 01A104.
- [85] D. Hotza, M. Di Luccio, M. Wilhelm, Y. Iwamoto, S. Bernard, J.C. Diniz da Costa, Silicon carbide filters and porous membranes: A review of processing, properties, performance and application, *Journal of Membrane Science* 610 (2020).
- [86] Q. You, Y. Liu, J. Wan, Z. Shen, H. Li, B. Yuan, L. Cheng, G. Wang, Microstructure and properties of porous SiC ceramics by LPCVI technique regulation, *Ceramics International* 43(15) (2017) 11855-11863.
- [87] B.K. Sea, K. Ando, K. Kusakabe, S. Morooka, Separation of hydrogen from steam using a SiC-based membrane formed by chemical vapor deposition of triisopropylsilane, *Journal of Membrane Science* 146(1) (1998) 73-82.
- [88] L.-S. Hong, Gas-to-Particle Conversion Mechanism in Chemical Vapor Deposition of Silicon Carbide by SiH<sub>4</sub> and C<sub>2</sub>H<sub>2</sub>, *Industrial & Engineering Chemistry Research* (1998) 3602-3609.
- [89] A.I. Labropoulos, C.P. Athanasekou, N.K. Kakizis, A.A. Sapalidis, G.I. Pilatos, G.E. Romanos, N.K. Kanellopoulos, Experimental investigation of the transport mechanism of several gases during the CVD post-treatment of nanoporous membranes, *Chemical Engineering Journal* 255 (2014) 377-393.
- [90] J. Dendooven, D. Deduytsche, J. Musschoot, R.L. Vanmeirhaeghe, C. Detavernier, Modeling the Conformality of Atomic Layer Deposition: The Effect of Sticking Probability, *Journal of The Electrochemical Society* 156(4) (2009).
- [91] S. Nishino, Y. Hazuki, H. Matsunami, T. Tanaka, Chemical vapor deposition of single crystalline  $\beta$ -SiC films on silicon substrate with sputtered SiC intermediate layer, *Journal of the Electrochemical Society* 127(12) (1980) 2674.
- [92] J.W. Clancey, A.S. Cavanagh, R.S. Kukreja, A. Kongkanand, S.M. George, Atomic layer deposition of ultrathin platinum films on tungsten atomic layer deposition adhesion layers: Application to high surface area substrates, *Journal of Vacuum Science & Technology A: Vacuum, Surfaces, and Films* 33(1) (2015) 01A130.
- [93] B.A. Latella, G. Triani, Z. Zhang, K.T. Short, J.R. Bartlett, M. Ignat, Enhanced adhesion of atomic layer deposited titania on polycarbonate substrates, *Thin Solid Films* 515(5) (2007) 3138-3145.
- [94] O.M.E. Ylivaara, X. Liu, L. Kilpi, J. Lyytinen, D. Schneider, M. Laitinen, J. Julin, S. Ali, S. Sintonen, M. Berdova, E. Haimi, T. Sajavaara, H. Ronkainen, H. Lipsanen, J. Koskinen, S.-P. Hannula, R.L. Puurunen, Aluminum oxide from trimethylaluminum and water by atomic layer deposition: The temperature dependence of residual stress, elastic modulus, hardness and adhesion, *Thin Solid Films* 552 (2014) 124-135.
- [95] X. Yang, A.B.F. Martinson, J.W. Elam, L. Shao, S.B. Darling, Water treatment based on atomically engineered materials: Atomic layer deposition and beyond, *Matter* 4(11) (2021) 3515-3548.

- [96] X. Meng, Y.C. Byun, H.S. Kim, J.S. Lee, A.T. Lucero, L. Cheng, J. Kim, Atomic Layer Deposition of Silicon Nitride Thin Films: A Review of Recent Progress, Challenges, and Outlooks, *Materials (Basel)* 9(12) (2016).
- [97] D.R. Baer, S. Thevuthasan, Characterization of thin films and coatings, *Handbook of Deposition Technologies for Films and Coatings*, Elsevier 2010, pp. 749-864.
- [98] P. Whiteside, J. Chininis, H. Hunt, Techniques and Challenges for Characterizing Metal Thin Films with Applications in Photonics, *Coatings* 6(3) (2016).
- [99] M.B.M. Mousa, C.J. Oldham, G.N. Parsons, Atmospheric Pressure Atomic Layer Deposition of Al<sub>2</sub>O<sub>3</sub> Using Trimethyl Aluminum and Ozone, *Langmuir* 30(13) (2014) 3741-3748.







# Chapter 6

Conclusions and future research directions



## Chapter 6 Conclusions and future research directions

### 6.1 Conclusions

In this thesis, LP-CVD to fabricate SiC coated Al<sub>2</sub>O<sub>3</sub> membranes has been explored. Al<sub>2</sub>O<sub>3</sub> supports were used and the deposition conditions were systematically varied to reduce pore size and achieve robust SiC coated Al<sub>2</sub>O<sub>3</sub> membranes. Finally, the SiC coated Al<sub>2</sub>O<sub>3</sub> membranes were evaluated for their stability in a membrane cleaning solution (NaClO) and their SO<sub>4</sub><sup>2-</sup> ion retention performance. Building upon prior research within the Water Management department at Delft University of Technology, particularly the works of Shang [1] and Chen [2], in this thesis the following key research questions have been addressed:

1. What are key findings in literature regarding LP-CVD modification of ceramic membranes for wastewater treatment?
2. How to prepare chemically robust SiC coated Al<sub>2</sub>O<sub>3</sub> membranes using the available LP-CVD setup?
3. What is the smallest pore size achievable for SiC coated Al<sub>2</sub>O<sub>3</sub> membranes by LP-CVD, and what is the SO<sub>4</sub><sup>2-</sup> retention?
4. How can the limitations of LP-CVD in preparing ceramic nanofiltration membranes be overcome by ALD?

Overall, our findings demonstrate that LP-CVD is a promising technique for ceramic membrane modification, offering single-step SiC coating that enables pore size control and surface charge modification. Unlike sol-gel methods, LP-CVD circumvents the need for high temperature sintering (ca. 2100°C) [3]. However, LP-CVD inherently struggles to deliver angstrom-level thickness precision required to coat and modify RO and NF membranes. By contrast, ALD employs sequential and self-limiting surface reactions that deposit one monolayer per cycle.

Consequentially, offering atomic-scale control over coating thickness and exceptional conformality even within complex pore networks. As a result, ALD has the potential for post-treating RO and NF membranes to tune pore size, enhance chemical and mechanical stability, and impart antifouling functionality without loss in permeance.

In the following sections, specific conclusions corresponding to the research questions are outlined.

### **6.1.1 Influence of LP-CVD parameters**

In chapter 3 LP-CVD conditions that affect the chemical robustness of SiC coatings have been evaluated by comparing two Al<sub>2</sub>O<sub>3</sub> supported membranes bearing SiC coatings of equal thickness (ca. 9 μm): (i) SiC-7 (low-temperature) with a SiC coating carried out at a temperature of 750°C, a pressure of 600 mTorr, and a deposition time of 60 min; (ii) SiC-8 (high-temperature) with a SiC coating carried out at a temperature of 860°C, a pressure of 100 mTorr, and a deposition time of 30 min.

Both SiC coated membranes were subsequently aged in NaClO solution for 200 hours to simulate oxidative cleaning. From these experiments it can be concluded that at the SiC-8 was robust with strong bonding to the Al<sub>2</sub>O<sub>3</sub> support. After NaClO exposure, this membrane retained its permeance and original pore structure, demonstrating excellent chemical stability. The SiC-7 had a poor bonding to the Al<sub>2</sub>O<sub>3</sub> support. Under the same ageing conditions, this coating delaminated and lost permeance, indicating poor durability.

These results underscore that high temperature LP-CVD is essential for obtaining chemically stable SiC coatings capable of undergoing multiple NaClO cleaning cycles, thereby extending the service life of the SiC coated ceramic membrane.

### **6.1.2 Limits of LP-CVD for pore size reduction**

Chapter 4 reports on the intrinsic limits of LP-CVD in modifying ceramic membrane pore sizes into the NF and RO regime. Using a commercial 20 nm nominal pore size Al<sub>2</sub>O<sub>3</sub> support (measured pore size 13 nm), a 38 min SiC deposition reduced the mean pore diameter to approximately 7 nm. Increasing the deposition time beyond this threshold even led to complete pore clogging. This behavior reflects the lack of atomic-scale control over coating thickness and a fundamental limitation of LP-CVD in fabricating NF and RO membranes.

### 6.1.3 Sulphate ion rejection of SiC coated membranes

In chapter 4 also the SO<sub>4</sub><sup>2-</sup> ion rejection of the SiC coated membrane in both deionized water and with a NaCl salt solution has been evaluated. Despite a large average pore size of 7 nm, the membrane's strongly negative surface charge (zeta potential ca. -67 mV at pH 7) enabled high SO<sub>4</sub><sup>2-</sup> rejection of ca. 79% at low feed ionic strengths, e.g. 2 mM Na<sub>2</sub>SO<sub>4</sub>. The high rejection was attributed to Donnan exclusion, where overlapping electric double layers within the pores repel co-ions. However, as feed ionic strength increased to 20mM, the Debye length contracted, thus preventing double layer overlap within the pores and SO<sub>4</sub><sup>2-</sup> rejection decreased to 34%.

### 6.1.4 Transition from CVD to ALD

In CVD, growth rate of a material is temperature and time dependent. Varying deposition time allows control over growth rate to a certain degree. However, the growth rate cannot be monitored and controlled on atomic level. Consequentially, it remains a challenge to tailor pore size to the NF range due to pore clogging [4]. In contrast, the growth of a material per cycle in ALD is one atomic layer thick. The deposition is carried out at even lower temperatures than CVD, and a range of materials can be deposited on porous substrates [5]. ALD therefore presents a viable alternative,

offering precise atomic-level growth in a self-limiting manner to avoid excessive porosity loss and tune down pore size to the nanofiltration range [6, 7].

## **6.2 Future research directions**

Based on the research findings of this thesis, the following research directions have been proposed to advance the technology and commercialization of ceramic membranes.

### **6.2.1 Improved ceramic membrane supports**

Achieving consistent pore narrowing into the UF or NF regime requires membrane supports with: (i) an intrinsically narrow pore size distribution; and (ii) a defect free architecture [8]. Broad pore size distributions can lead to unintended increase in the average pore size post LP-CVD modification due to selective clogging of the smaller pores [9]. Therefore, membrane supports must be improved by precise controls, such as controlled sintering protocols, or template-assisted synthesis, to produce high quality defect free substrates.

Another or complementary strategy to circumvent the problem could be to operate LP-CVD under homogeneous deposition conditions, whereby the local deposition rate is proportional to pore volume. In this regime, larger pores accumulate proportionally more material and smaller pores less, effectively transforming a broad initial pore size distribution into a narrow and uniform pore size distribution [10]. This volume proportional growth, therefore, ensures that all pores are simultaneously reduced toward the same target diameter.

### **6.2.2 Novel ceramic coating materials**

In the literature, membrane-coating research has centered on oxide ceramic coatings, such as alumina, or titania, due to well-established reaction mechanisms and precursor availability [11]. However, in the interest of the membrane community, expanding studies to non-oxide ceramics,

such as carbides or nitrides ceramics can offer new combinations of chemical resistance, mechanical durability, and tailored surface charge for specialized separation applications. As demonstrated in this thesis with SiC coatings on Al<sub>2</sub>O<sub>3</sub> supports, carbide ceramic coatings can be deposited via LP-CVD to produce robust coated ceramic membranes. Similar strategies could be adapted to other carbide and nitride systems by studying their reaction chemistry and identifying novel precursors. This will, consequentially, enable membranes with tailored pore size and surface charge for demanding separations, such as organic solvent nanofiltration and gas-liquid catalysis. Additionally, conductive ceramic coatings can function as ion-selective interfaces, thus expanding membrane roles in energy storage systems.

### **6.2.3 In-situ characterization techniques**

It is difficult to estimate the pore size of the membrane during the coating deposition process. However, the pore size is an important control parameter as it determines the steric properties of the membrane. Currently, the thickness of the coating is measured on Si wafers after the process has been completed [12], limiting real-time control. Developing in-situ monitoring techniques, such as spectroscopic ellipsometry, quartz crystal microbalance, or optical interferometry, would permit monitoring pore size evolution during the deposition process and enhance reproducibility and optimization of LP-CVD and ALD processes.

### **6.2.4 Optimized deposition furnaces**

Vapor deposition techniques are predominantly optimized for semiconductor applications [13], whereas their adaptation for ceramic membranes remains underdeveloped. Existing furnaces are designed for Si wafers, lacking configurations suitable for tubular and flat-sheet membranes. Future research should focus on designing furnaces with uniform thermal profile, controlled gas flow dynamics, geometry adaptability and in-situ diagnostics for efficient membrane coating. By

integrating these requirements, next-generation furnaces can deliver high quality ceramic coatings to accelerate the translation of LP-CVD and ALD into commercial wastewater treatment technologies.

### **6.2.5 Advanced pore size measurement techniques**

Accurate pore size characterization is important for evaluating ceramic membrane performance. Conventional membrane pore size characterization techniques, such as gas adsorption/desorption isotherms, permoporometry, mercury intrusion porosimetry and liquid displacement methods exhibit significant drawbacks. Gas adsorption methods take into account both open and closed pores, thus leading to overestimation of permeable pore volume. Permoporometry's reliance on liquid wetting agents can introduce errors if the liquid evaporates or fails to fully infiltrate the pore network. Mercury intrusion porosimetry not only poses various health and environmental hazards but may also damage brittle ceramic structures under high pressures. Capillary flow porometry, while non-destructive, requires rigorous pore wetting and cannot detect dead-end or highly tortuous pores accurately. Additionally, the hardness and brittleness of ceramic membranes complicate sample preparation, contributing to inter-method variability and undermining comparability of results [14]. No single technique currently spans the full range of all three filtration regimes (MF, UF and NF). Future efforts should be directed toward studying standardized and non-destructive protocols, such as positron annihilation lifetime spectroscopy and synchrotron radiation, for reliable and comprehensive understanding of pore structures.



## References

- [1] R. Shang, Ceramic ultra-and nanofiltration for municipal wastewater reuse, (2014).
- [2] M. Chen, SiC-deposited ceramic membranes for treatment of oil-in-water emulsions, (2023).
- [3] G. Qin, A. Jan, Q. An, H. Zhou, L.C. Rietveld, S.G.J. Heijman, Chemical vapor deposition of silicon carbide on alumina ultrafiltration membranes for filtration of microemulsions, *Desalination* 582 (2024) 117655.
- [4] S.J. Khatib, S.T. Oyama, Silica membranes for hydrogen separation prepared by chemical vapor deposition (CVD), *Separation and Purification Technology* 111 (2013) 20-42.
- [5] S.M. George, Atomic Layer Deposition: An Overview, *Chemical Reviews* 110(1) (2010) 111-131.
- [6] M. Weber, A. Julbe, A. Ayrál, P. Miele, M. Bechelany, Atomic layer deposition for membranes: basics, challenges, and opportunities, *Chemistry of Materials* 30(21) (2018) 7368-7390.
- [7] M. Weber, A. Julbe, S.S. Kim, M. Bechelany, Atomic layer deposition (ALD) on inorganic or polymeric membranes, *Journal of Applied Physics* 126(4) (2019).
- [8] F.C. Kramer, R. Shang, S.M. Scherrenberg, L.C. Rietveld, S.J.G. Heijman, Quantifying defects in ceramic tight ultra- and nanofiltration membranes and investigating their robustness, *Separation and Purification Technology* 219 (2019) 159-168.
- [9] Y. Lin, A theoretical analysis on pore size change of porous ceramic membranes after modification, *Journal of membrane science* 79(1) (1993) 55-64.
- [10] Y. Lin, A. Burggraaf, Experimental studies on pore size change of porous ceramic membranes after modification, *Journal of membrane science* 79(1) (1993) 65-82.
- [11] X. Yang, A.B. Martinson, J.W. Elam, L. Shao, S.B. Darling, Water treatment based on atomically engineered materials: Atomic layer deposition and beyond, *Matter* 4(11) (2021) 3515-3548.
- [12] M. Chen, R. Shang, P.M. Sberna, M.W.J. Luiten-Olieman, L.C. Rietveld, S.G.J. Heijman, Highly permeable silicon carbide-alumina ultrafiltration membranes for oil-in-water filtration produced with low-pressure chemical vapor deposition, *Separation and Purification Technology* 253 (2020) 117496.
- [13] Z. Cai, B. Liu, X. Zou, H.-M. Cheng, Chemical vapor deposition growth and applications of two-dimensional materials and their heterostructures, *Chemical reviews* 118(13) (2018) 6091-6133.
- [14] M.B. Tanis-Kanbur, R.I. Peinador, J.I. Calvo, A. Hernández, J.W. Chew, Porosimetric membrane characterization techniques: A review, *Journal of Membrane Science* 619 (2021) 118750.



## Acknowledgements

As I look out of my window on a rare bright spring afternoon in the Netherlands, I see deciduous trees and lifeless buildings coexisting in harmony under the sun. Gazing at the horizon, I cannot help but recollect the last four springs as a series of vivid episodes, each colored by the full spectrum of human emotions. And, to bring this thesis to a close, I wish to revisit few of those episodes and the lessons they left behind.

My PhD journey in Delft quite literally began on a bicycle. Amidst the unpredictable rain and persistent wind, I found myself navigating both the city and Dutch academia. Thankfully, the impeccable Dutch biking infrastructure - and the no-nonsense workplace directness – guided me like a reliable map. I am deeply grateful to my promoters, Luuk Rietveld and Bas Heijman, for molding me into a capable scientist through their valuable guidance. Bas, thank you for standing beside me in the Water Lab as I tried to fix what must have been the hundredth water leak in my experimental setup. Your practical wisdom also sharpened the engineer in me - thank you for that as well. I would like to thank Luuk for helping me to see the broader picture and impact of my research, and, more importantly, for teaching me to write with confidence and brevity. It is a remarkably difficult task to master, and I am grateful for the path of continuous improvement you helped me set foot on. The lesson here: **whether it is a hypothesis or a headwind, keep pedaling.** An electron does not orbit the nucleus in tidy circles. Instead, it dances unpredictably governed by probability. Imagine taking thousands of snapshots of an electron's position, each a tiny dot. Stitching those together you get a fuzzy two-dimensional map. Extend that into three dimensions, and you get a probability cloud – the orbital – where you are likely to find the electron 90% of the time. Similarly, if you tried to map a PhD candidate with an experimental background, you would find him/her in the lab 90% of the time. And, the rest 10% is spent in the office where social

connections are forged. Perhaps that's why people say a PhD is a solitary journey. But, I was lucky! My 10% in the office made me forget the 90% hardships of the lab.

I am grateful to Ali for patiently listening to my lab (and life) rants, and offering thoughtful advice. Thank you to Iosif for helping me navigate social life abroad, and to Diana for installing a basketball hoop in the office – a surprisingly effective stress relief tool. Anurag, your “instruction manual” for life in the Netherlands was invaluable. Diego, your wisdom and humor, and the occasional reminder that “it’s okay to skip the gym for a beer sometimes” kept me balanced. Thank you to Greg for sharing your football wisdom and sharing your workout regime that nudged me toward the gym more often. Thank you to Qin and Shuo for your support in the lab and the thoughtful conversations during our coffee breaks. Thank you to Zhauxu for proving that with enough will, even the tightest schedule can accommodate a European exploration. To Ibrahim, my fellow countryman, thank you for shared nostalgia of home. Jing, thank you for all the delicious deserts you brought to the office to fuel us. And Bilal, your Desi-on-Dutch observations and deadpan one liners still make me laugh every time I remember them. The lesson here: **even in a probabilistic orbit, the right people bring joy and stability.**

Beyond the office, I found community in the Absolutely Halal group and the Orange Cricket Club where, cricket matches, late-night chai, pizzas and card games became rituals of camaraderie. I would also like to thank the VolleyBolley group for welcoming a complete volleyball novice. The three hour long volleyball sessions with bachelor's and master's students made me feel young, though my lower back occasionally filed a formal complaint. Thank you to Mehtab for being my hometown bridge to Delft; chatting in our native Burushashki while munching on your delicious lamb karahi was always a delight. The lesson here: **community, food, and a questionable volleyball serve go a long way.**

Michiel, a fellow PhD in the SUSSIC project, deserves a special mention. I am so grateful for your valuable insights on my work, and for the solidarity we found in sharing our failed experiments. It is through these shared failures that we both managed to produce research of genuine scientific value. It makes me happy that what began with formal emails and scientific discussions gradually evolved into a friendship powered by memes on Instagram.

To my best friend Shaur who, by fate's charming sense of timing also found himself in the Netherlands and completed his PhD here: thank you for being my built-in therapist. I can speak my mind freely when I am around you, and even the silences that we share feel full of fun. I am also grateful to his wife, Hira, and the little champ, Isa, for always welcoming me with open arms whenever I visited (and I am sure they will keep doing so ^\_^). Hira's delicious food and time spent with the trio always felt like home away from home.

Finally, I must thank my nuclear family. No collection of words could ever fully express my gratitude for your unwavering and unconditional support. The baseline of life is already challenging, and living in a foreign culture adds to it. At times, I questioned whether chasing opportunities was worth leaving the safety and familiarity of home. My mother Nasreen, father Ali, younger brother Waqas, and younger sister Mashal have always respected my sacrifices, stood by me through thick and thin, and reminded me that purpose often lies beyond comfort. I am deeply grateful to my parents for giving me the greatest gift: education. Without you both, I would not be who or where I am today. To my brother Waqas, thank you for sharing your insights on economics and finances, they have made me smarter with my money. To my sister Mashal, thank you for encouraging me to eat healthy and keep up with regular health checkups. To both of you, thank you for the constant check-ins, memes and emotional support across time zones. Also, a heartfelt

thank you to Khala Shahi for always checking in on me with the warmth and care of a motherly figure.

I close this chapter by thanking the person I was when I started this journey. And, I thank the person I have become.

## Curriculum Vitae

Asif Jan

Date of birth: 19-03-1993

Place of birth: Gilgit, Pakistan

Nationality: Pakistani



## Education

Degree	Major	Grade	Uni.	Research Focus	Completion	Country
M.Eng.	Materials Eng.	A	University of Science and Technology	Ceramic materials	Aug. 2019	South Korea
B. Eng.	Materials Eng.	A	NED University of Engineering and Technology	-	Dec. 2015	Pakistan

## Work Experience

Position	Employer	Duration	Key Responsibilities
Research & Development	TU Delft, Netherlands	Apr. 2021 – Mar. 2025	<ul style="list-style-type: none"><li>Membrane technology development</li><li>Membrane technology testing</li><li>Technical report writing</li></ul>
Research & Development	Uni. Stuttgart, Germany	Sep. 2020 – Mar. 2021	<ul style="list-style-type: none"><li>Conversion of carbon dioxide to green fuels</li></ul>
Research & Development	KIST, South Korea	Feb. 2017 – Aug. 2020	<ul style="list-style-type: none"><li>Fuel cells performance optimization</li></ul>

<b>Quality Control</b>	Toyota, Pakistan	Mar. 2016 – Jul. 2016	<ul style="list-style-type: none"> <li>• Implementation of Toyota Production System</li> </ul>
<b>Product Development</b>	Toyota, Pakistan	Mar. 2016 – Jul. 2016	<ul style="list-style-type: none"> <li>• Automotive parts localization</li> </ul>

## Journal Publications

	Journal	Research Focus	Year of Publication	Source
1	RSC Advances	Fuel Cells	2019	<a href="#">(Link)</a>
2	Energy Environ. Sci.	Fuel cells	2020	<a href="#">(Link)</a>
3	Nano Micro Small	Ammonia production	2023	<a href="#">(Link)</a>
4	Separations	Membrane technology	2024	<a href="#">(Link)</a>
5	Membranes	Membrane technology	2024	<a href="#">(Link)</a>
6	Desalination	Membrane technology	2024	<a href="#">(Link)</a>
7	Open Ceramics	Membrane technology	2025	<a href="#">(Link)</a>
8	Desalination	Membrane technology	2025	<a href="#">(Link)</a>

## Patents

- Patent NL2034161B1; WO2024172653A1. **A. Jan & S. Heijman.** Chemically robust silicon carbide ultrafiltration membranes prepared by low-pressure chemical vapor deposition.

[\(Link\)](#)



